

Impact Factor:	ISRA (India) = 6.317	SIS (USA) = 0.912	ICV (Poland) = 6.630
	ISI (Dubai, UAE) = 1.582	РИНЦ (Russia) = 3.939	PIF (India) = 1.940
	GIF (Australia) = 0.564	ESJI (KZ) = 9.035	IBI (India) = 4.260
	JIF = 1.500	SJIF (Morocco) = 7.184	OAJI (USA) = 0.350

SOI: [1.1/TAS](#) DOI: [10.15863/TAS](#)

**International Scientific Journal
Theoretical & Applied Science**

p-ISSN: 2308-4944 (print) e-ISSN: 2409-0085 (online)

Year: 2022 Issue: 01 Volume: 105

Published: 27.01.2022 <http://T-Science.org>

QR – Issue



QR – Article



Denis Chemezov

Vladimir Industrial College

M.Sc.Eng., Corresponding Member of International Academy of Theoretical and Applied Sciences, Lecturer,
Russian Federation

<https://orcid.org/0000-0002-2747-552X>

vic-science@yandex.ru

Vladimir Serov

Vladimir Industrial College
Student, Russian Federation

Maksim Glukhov

Vladimir Industrial College
Student, Russian Federation

Yuriy Mironov

Vladimir Industrial College
Student, Russian Federation

Mikhail Aleksandrov

Vladimir Industrial College
Student, Russian Federation

Konstantin Nefyodov

Vladimir Industrial College
Student, Russian Federation

Andrey Korovkin

Vladimir Industrial College
Student, Russian Federation

REFERENCE DATA OF PRESSURE DISTRIBUTION ON THE SURFACES OF AIRFOILS (HYDROFOILS) HAVING THE NAMES BEGINNING WITH THE LETTER E (THE FIRST PART)

Abstract: The results of the computer calculation of air (water) flow around the airfoils (hydrofoils) having the names beginning with the letter E are presented in the article. The contours of pressure distribution on the surfaces of the airfoils (hydrofoils) at the angles of attack of 0, 15 and -15 degrees in conditions of the subsonic airplane flight speed were obtained.

Key words: the airfoil, hydrofoil, the angle of attack, pressure, the surface.

Language: English

Citation: Chemezov, D., et al. (2022). Reference data of pressure distribution on the surfaces of airfoils (hydrofoils) having the names beginning with the letter E (the first part). *ISJ Theoretical & Applied Science*, 01 (105), 501-569.

Soi: <http://s-o-i.org/1.1/TAS-01-105-40> **Doi:** <https://dx.doi.org/10.15863/TAS.2022.01.105.40>

Scopus ASCC: 1507.

Impact Factor:	ISRA (India) = 6.317	SIS (USA) = 0.912	ICV (Poland) = 6.630
	ISI (Dubai, UAE) = 1.582	РИНЦ (Russia) = 3.939	PIF (India) = 1.940
	GIF (Australia) = 0.564	ESJI (KZ) = 9.035	IBI (India) = 4.260
	JIF = 1.500	SJIF (Morocco) = 7.184	OAJI (USA) = 0.350

Introduction

Creating reference materials that determine the most accurate pressure distribution on the airfoils (hydrofoils) surfaces is an actual task of the airplane aerodynamics.

Materials and methods

The study of air (water) flow around the airfoils (hydrofoils) was carried out in a two-dimensional formulation by means of the computer calculation in the *Comsol Multiphysics* program. The airfoils (hydrofoils) in the cross section were taken as objects

of research [1-16]. In this work, the airfoils (hydrofoils) having the names beginning with the letter *E* were adopted. Air (water) flow around the airfoils (hydrofoils) was carried out at the angles of attack (α) of 0, 15 and -15 degrees. The flight speed of the airplane in each case was subsonic. The airplane flight in the atmosphere was carried out under normal weather conditions. The geometric characteristics of the studied airfoils (hydrofoils) are presented in the Table 1. The geometric shapes of the airfoils (hydrofoils) in the cross section are presented in the Table 2.

Table 1. The geometric characteristics of the airfoils (hydrofoils).

Airfoil (hydrofoil) name	Max. thickness	Max. camber	Leading edge radius	Trailing edge thickness
<i>E10(08%)</i>	10.06% at 27.9% of the chord	0.27% at 27.9% of the chord	0.707%	0.0%
<i>E168 (12,45%)</i>	12.44% at 26.7% of the chord	0.0% at 0.0% of the chord	1.027%	0.0%
<i>E169 (14,4%)</i>	14.4% at 26.5% of the chord	0.0% at 0.0% of the chord	1.245%	0.0%
<i>E171</i>	12.25% at 32.4% of the chord	0.0% at 0.0% of the chord	0.7631%	0.0%
<i>E174 (Dicke 8,92%)</i>	8.88% at 28.8% of the chord	3.83% at 39.2% of the chord	0.6574%	0.0%
<i>E176 (8,83%)</i>	8.81% at 29.7% of the chord	3.31% at 40.1% of the chord	0.6147%	0.0%
<i>E178 (8,69%)</i>	8.68% at 30.6% of the chord	2.77% at 40.9% of the chord	0.574%	0.0%
<i>E178P</i>	8.68% at 30.6% of the chord	2.77% at 40.9% of the chord	0.4617%	0.019%
<i>E180 (8,59%)</i>	8.57% at 31.5% of the chord	2.23% at 36.6% of the chord	0.5788%	0.0%
<i>E182 (8,47%)</i>	8.46% at 32.4% of the chord	1.72% at 37.5% of the chord	0.5848%	0.0%
<i>E184 (8,33%)</i>	8.31% at 33.3% of the chord	1.2% at 33.3% of the chord	0.5556%	0.0%
<i>E186 (10,27%)</i>	10.23% at 29.0% of the chord	1.3% at 29.0% of the chord	0.6676%	0.0%
<i>E193 (10,22%)</i>	10.2% at 34.0% of the chord	3.57% at 39.3% of the chord	0.7407%	0.0%
<i>E193-12</i>	12.0% at 30.9% of the chord	3.6% at 40.2% of the chord	0.8629%	0.0%
<i>E195 (11,82%)</i>	11.81% at 34.1% of the chord	3.19% at 44.5% of the chord	0.8291%	0.0%
<i>E197 (13,49%)</i>	13.48% at 34.2% of the chord	2.8% at 44.4% of the chord	0.9373%	0.0%
<i>E201 (11,88%)</i>	11.86% at 33.8% of the chord	3.1% at 44.1% of the chord	0.8305%	0.0%
<i>E203 (13,64%)</i>	13.63% at 33.4% of the chord	2.67% at 48.6% of the chord	0.9472%	0.0%
<i>E205 (10,48%)</i>	10.47% at 30.1% of the chord	3.01% at 35.1% of the chord	0.7673%	0.0%
<i>E2052595</i>	9.5% at 30.1% of the chord	2.5% at 35.1% of the chord	0.461%	0.0%
<i>E207 (12,04%)</i>	12.02% at 30.0% of the chord	2.49% at 39.9% of the chord	0.8618%	0.0%
<i>E209 (13,72%)</i>	13.68% at 29.8% of the chord	1.97% at 44.5% of the chord	0.9792%	0.0%
<i>E210 (13,64%)</i>	13.63% at 31.4% of the chord	4.01% at 46.8% of the chord	1.0214%	0.0%
<i>E211 (10,96%)</i>	10.95% at 33.2% of the chord	2.57% at 59.1% of the chord	0.7569%	0.0%
<i>E212 (10,55%)</i>	10.55% at 27.3% of the chord	2.93% at 58.4% of the chord	0.8043%	0.0%
<i>E214 (11,1%)</i>	11.08% at 31.4% of the chord	4.03% at 52.4% of the chord	0.7962%	0.0%
<i>E216 (10,4%)</i>	10.42% at 28.6% of the chord	5.17% at 55.6% of the chord	0.9126%	0.0%
<i>E220 (11,48%)</i>	11.46% at 36.9% of the chord	2.45% at 36.9% of the chord	0.7408%	0.0%
<i>E221 (9,39%)</i>	9.36% at 27.1% of the chord	1.83% at 32.0% of the chord	0.681%	0.0%
<i>E222 (10,17%)</i>	10.16% at 28.7% of the chord	2.51% at 49.2% of the chord	0.7428%	0.0%
<i>E224 (10,17%)</i>	10.17% at 30.0% of the chord	1.74% at 50.4% of the chord	0.7223%	0.0%
<i>E226 (10,19%)</i>	10.17% at 31.3% of the chord	0.98% at 41.3% of the chord	0.7132%	0.0%
<i>E228</i>	10.2% at 28.3% of the chord	0.28% at 28.3% of the chord	0.2679%	0.168%
<i>E230 (9,96%)</i>	9.96% at 29.3% of the chord	0.0% at 0.0% of the chord	0.8194%	0.0%
<i>E231</i>	12.32% at 41.4% of the chord	2.45% at 41.4% of the chord	0.4968%	0.0%
<i>E374</i>	10.92% at 37.1% of the chord	2.21% at 40.2% of the chord	0.6022%	0.0%
<i>E385 (8,41%)</i>	8.41% at 30.5% of the chord	5.73% at 47.1% of the chord	0.6856%	0.0%
<i>E387</i>	8.88% at 28.8% of the chord	3.83% at 39.2% of the chord	0.6454%	0.179%
<i>E392 (10,15%)</i>	10.13% at 33.1% of the chord	3.83% at 43.6% of the chord	0.6635%	0.0%
<i>E393</i>	11.56% at 32.2% of the chord	4.01% at 47.8% of the chord	0.599%	0.307%
<i>E423</i>	12.51% at 23.7% of the chord	10.03% at 41.4% of the chord	2.6584%	0.0%
<i>E471 (6,25%)</i>	6.25% at 26.1% of the chord	4.73% at 53.3% of the chord	0.4745%	0.0%
<i>E474 (14,09%)</i>	14.08% at 21.5% of the chord	0.0% at 0.0% of the chord	1.7161%	0.0%
<i>E474 (14,09%)-portato al 16</i>	16.2% at 21.5% of the chord	0.0% at 0.0% of the chord	2.2662%	0.0%
<i>E475 (15,01%)</i>	15.0% at 21.7% of the chord	0.0% at 0.0% of the chord	1.8319%	0.0%
<i>E61 (5,64%)</i>	5.66% at 28.1% of the chord	6.69% at 51.0% of the chord	0.4525%	0.0%
<i>E61 (5,64%)</i>	5.66% at 28.1% of the chord	6.69% at 51.0% of the chord	0.2206%	0.0%
<i>E62 (5,62%)</i>	5.63% at 25.3% of the chord	5.37% at 47.2% of the chord	0.4792%	0.0%

Impact Factor:	ISRA (India) = 6.317	SIS (USA) = 0.912	ICV (Poland) = 6.630
	ISI (Dubai, UAE) = 1.582	РИНЦ (Russia) = 3.939	PIF (India) = 1.940
	GIF (Australia) = 0.564	ESJI (KZ) = 9.035	IBI (India) = 4.260
	JIF = 1.500	SJIF (Morocco) = 7.184	OAJI (USA) = 0.350

<i>E63</i> (4,25%)	4.25% at 19.8% of the chord	5.38% at 52.1% of the chord	0.3814%	0.0%
<i>E64</i> (8,45%)	8.44% at 28.0% of the chord	3.32% at 48.9% of the chord	0.6364%	0.0%
<i>E71</i> (5,15%)	5.16% at 25.9% of the chord	4.64% at 53.1% of the chord	0.426%	0.0%
<i>EB</i> 1,5-10	10.0% at 30.0% of the chord	1.65% at 40.0% of the chord	1.6578%	0.0%
<i>EB</i> 380	9.91% at 30.0% of the chord	2.94% at 40.0% of the chord	0.7954%	0.0%
<i>EH</i> 0,0-9,0	9.0% at 28.7% of the chord	0.0% at 0.0% of the chord	0.5263%	0.0%
<i>EH</i> 1,0-9,0	8.99% at 28.7% of the chord	1.0% at 25.9% of the chord	0.5408%	0.0%
<i>EH</i> 1,5-9,0	8.99% at 28.7% of the chord	1.49% at 25.9% of the chord	0.5392%	0.0%
<i>EH</i> 1.07.0 (<i>from EH</i> 1.0/9,0)	7.0% at 31.6% of the chord	1.0% at 25.9% of the chord	0.3821%	0.0%
<i>EH</i> 2,0-10	10.08% at 28.7% of the chord	2.0% at 25.9% of the chord	0.626%	0.0%
<i>EH</i> 2,0-12	11.99% at 28.7% of the chord	1.99% at 25.9% of the chord	0.8956%	0.0%
<i>EH</i> 2,5-10	9.99% at 30.0% of the chord	2.49% at 25.0% of the chord	0.463%	0.0%
<i>EH</i> 3,0-12	11.98% at 30.0% of the chord	3.0% at 25.0% of the chord	0.6929%	0.0%
<i>Eiffel</i> 375	9.92% at 30.0% of the chord	2.49% at 30.0% of the chord	1.4074%	0.0%
<i>Eiffel</i> 400	13.0% at 30.0% of the chord	6.6% at 30.0% of the chord	1.1077%	0.0%
<i>Eiffel</i> 428	8.8% at 40.0% of the chord	5.1% at 40.0% of the chord	0.9129%	0.0%
<i>Eiffel</i> 430	9.69% at 15.0% of the chord	6.4% at 30.0% of the chord	1.7186%	0.0%
<i>Eiffel</i> 431	9.9% at 20.0% of the chord	7.5% at 40.0% of the chord	1.3847%	0.0%
<i>EIFFL</i> 32	5.06% at 20.0% of the chord	5.43% at 30.0% of the chord	1.7603%	0.67%
<i>EIFFL</i> 338	8.04% at 40.0% of the chord	0.0% at 0.0% of the chord	1.6831%	0.0%
<i>EIFFL</i> 359	10.83% at 30.0% of the chord	5.42% at 30.0% of the chord	1.7593%	0.0%
<i>EIFFL</i> 371	14.4% at 30.0% of the chord	7.27% at 30.0% of the chord	1.254%	0.0%
<i>EIFFL</i> 385	13.35% at 20.0% of the chord	7.53% at 40.0% of the chord	1.9339%	0.0%
<i>EIFFL</i> 389	7.93% at 40.0% of the chord	4.54% at 30.0% of the chord	1.6678%	0.0%
<i>EIFFL</i> 437	11.23% at 20.0% of the chord	6.24% at 40.0% of the chord	1.8311%	0.0%
<i>EL</i> 25108	10.78% at 40.0% of the chord	2.5% at 40.0% of the chord	0.7749%	0.0%
<i>ELEK</i>	12.0% at 30.9% of the chord	4.0% at 43.5% of the chord	1.1914%	0.0%
<i>ELINA</i>	9.47% at 29.9% of the chord	2.95% at 40.2% of the chord	0.3471%	0.0%
<i>EMX</i> -07	9.9% at 29.7% of the chord	2.53% at 20.6% of the chord	0.7331%	0.304%
<i>EPB</i> - 1	14.76% at 30.0% of the chord	7.38% at 30.0% of the chord	3.4711%	0.0%
<i>EPPLER</i> 1098	18.95% at 36.9% of the chord	3.7% at 56.7% of the chord	1.0292%	0.0%
<i>EPPLER</i> 1200	16.95% at 37.2% of the chord	3.43% at 47.4% of the chord	1.58%	0.0%
<i>EPPLER</i> 1210	15.81% at 20.4% of the chord	5.18% at 35.5% of the chord	2.9263%	0.0%
<i>EPPLER</i> 1211	18.0% at 20.2% of the chord	4.42% at 40.0% of the chord	3.3009%	0.0%
<i>EPPLER</i> 1213	17.34% at 23.7% of the chord	2.05% at 33.1% of the chord	2.7377%	0.0%
<i>EPPLER</i> 1214	19.82% at 23.9% of the chord	2.11% at 32.9% of the chord	3.0901%	0.0%
<i>EPPLER</i> 1230	17.45% at 29.6% of the chord	3.6% at 26.6% of the chord	2.3131%	0.02%
<i>EPPLER</i> 1233	18.92% at 29.6% of the chord	4.32% at 29.6% of the chord	2.058%	0.0%
<i>Eppler</i> 166	10.44% at 30.0% of the chord	1.32% at 30.0% of the chord	0.9403%	0.0%
<i>Eppler</i> 189	8.22% at 30.0% of the chord	1.17% at 40.0% of the chord	0.9289%	0.0%
<i>Eppler</i> 228	10.2% at 30.0% of the chord	0.3% at 30.0% of the chord	1.0712%	0.0%
<i>EPPLER</i> 266	17.32% at 39.8% of the chord	3.2% at 39.8% of the chord	1.1246%	0.0%
<i>Eppler</i> 270	10.16% at 30.0% of the chord	0.0% at 0.0% of the chord	1.1165%	0.0%
<i>EPPLER</i> 297	11.39% at 37.7% of the chord	0.05% at 0.0% of the chord	0.1034%	0.0%
<i>EPPLER</i> 325	12.62% at 34.3% of the chord	1.75% at 16.3% of the chord	0.7201%	0.0%
<i>EPPLER</i> 326	12.86% at 33.4% of the chord	2.17% at 19.5% of the chord	0.9824%	0.0%
<i>EPPLER</i> 327	13.11% at 32.4% of the chord	2.59% at 23.0% of the chord	1.0816%	0.0%
<i>EPPLER</i> 328	13.33% at 31.5% of the chord	3.03% at 22.1% of the chord	1.3353%	0.0%
<i>EPPLER</i> 329	13.52% at 30.6% of the chord	3.54% at 25.7% of the chord	1.3256%	0.0%
<i>EPPLER</i> 330	11.02% at 29.2% of the chord	2.16% at 16.9% of the chord	0.6991%	0.0%
<i>EPPLER</i> 331	11.25% at 28.3% of the chord	2.59% at 23.6% of the chord	0.4837%	0.0%
<i>EPPLER</i> 332	11.52% at 32.3% of the chord	3.04% at 22.6% of the chord	0.8634%	0.0%
<i>EPPLER</i> 333	11.75% at 31.3% of the chord	3.54% at 26.4% of the chord	1.1851%	0.0%
<i>EPPLER</i> 334	11.93% at 30.3% of the chord	4.04% at 25.4% of the chord	1.2059%	0.0%
<i>EPPLER</i> 335	12.56% at 29.0% of the chord	2.36% at 19.9% of the chord	1.0209%	0.0%
<i>EPPLER</i> 336	12.79% at 28.1% of the chord	2.79% at 23.4% of the chord	1.0164%	0.0%
<i>EPPLER</i> 337	13.1% at 32.0% of the chord	3.25% at 22.4% of the chord	1.3266%	0.0%
<i>EPPLER</i> 338	13.3% at 31.1% of the chord	3.74% at 26.2% of the chord	1.32%	0.0%
<i>EPPLER</i> 339	13.54% at 30.1% of the chord	4.21% at 25.2% of the chord	1.5434%	0.0%
<i>EPPLER</i> 340	13.68% at 28.8% of the chord	2.59% at 19.7% of the chord	1.1378%	0.0%
<i>EPPLER</i> 341	13.94% at 32.8% of the chord	3.04% at 23.2% of the chord	1.3422%	0.0%
<i>EPPLER</i> 342	14.26% at 31.8% of the chord	3.49% at 22.2% of the chord	1.6374%	0.0%
<i>EPPLER</i> 343	14.47% at 30.9% of the chord	3.96% at 26.0% of the chord	1.548%	0.0%
<i>EPPLER</i> 344	14.72% at 29.9% of the chord	4.44% at 25.0% of the chord	1.7864%	0.0%
<i>EPPLER</i> 360	12.23% at 36.9% of the chord	1.54% at 27.2% of the chord	1.0835%	0.0%
<i>EPPLER</i> 361	12.11% at 37.1% of the chord	1.64% at 27.4% of the chord	1.0704%	0.0%
<i>Eppler</i> 375	10.9% at 40.0% of the chord	2.25% at 40.0% of the chord	0.7883%	0.0%
<i>EPPLER</i> 376	2.44% at 3.8% of the chord	8.93% at 32.6% of the chord	0.453%	0.0%
<i>EPPLER</i> 377	3.85% at 6.8% of the chord	8.74% at 37.2% of the chord	0.503%	0.0%

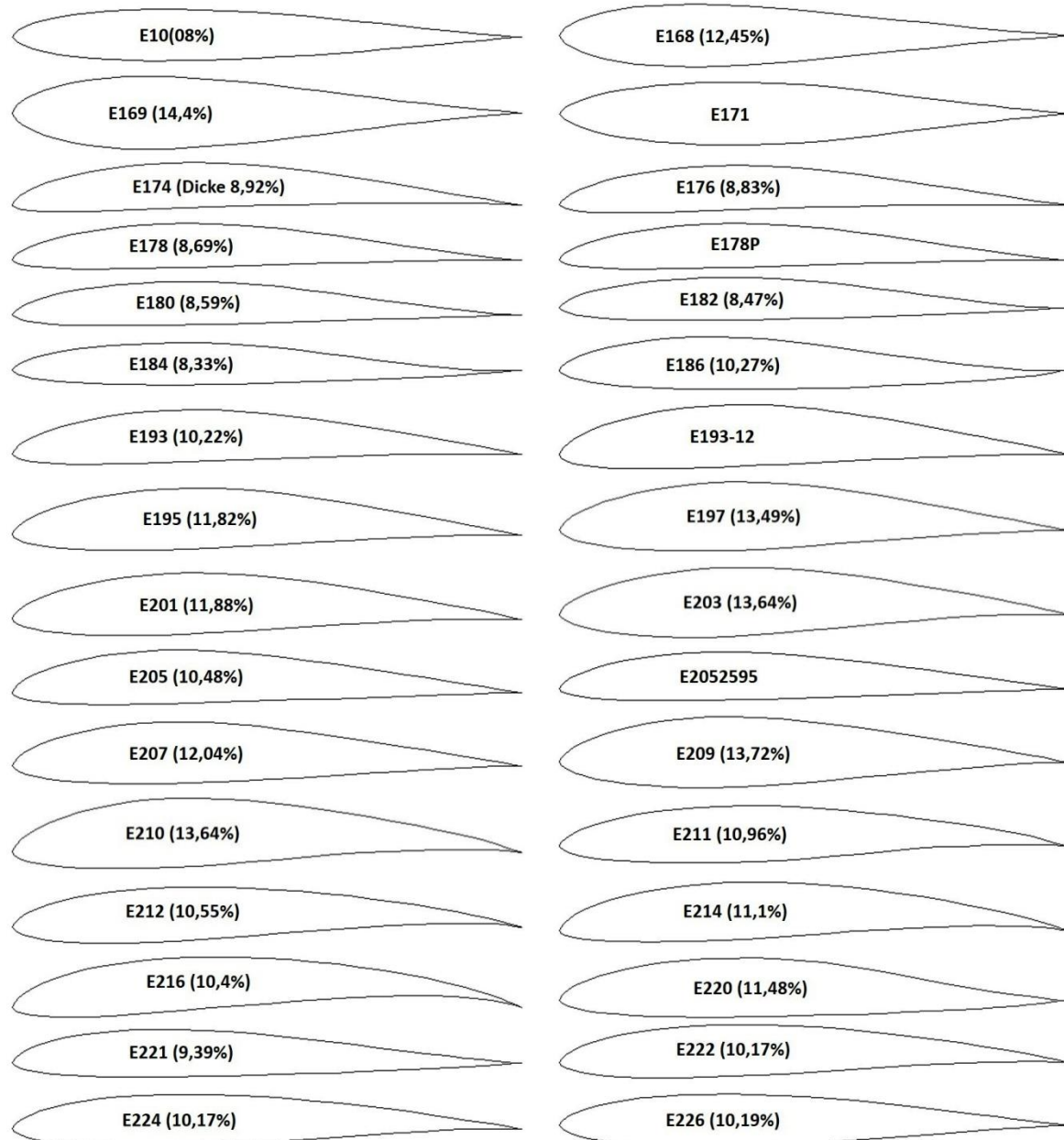
Impact Factor:	ISRA (India) = 6.317	SIS (USA) = 0.912	ICV (Poland) = 6.630
	ISI (Dubai, UAE) = 1.582	РИНЦ (Russia) = 3.939	PIF (India) = 1.940
	GIF (Australia) = 0.564	ESJI (KZ) = 9.035	IBI (India) = 4.260
	JIF = 1.500	SJIF (Morocco) = 7.184	OAJI (USA) = 0.350

EPPLER 377 (MODIFIED)	3.76% at 6.5% of the chord	9.13% at 32.6% of the chord	0.5042%	0.0%
EPPLER 378	4.07% at 7.7% of the chord	7.99% at 38.5% of the chord	0.4654%	0.0%
EPPLER 379	2.21% at 7.9% of the chord	7.99% at 34.2% of the chord	0.4615%	0.0%
Eppler 387	9.1% at 30.0% of the chord	5.8% at 40.0% of the chord	0.7091%	0.0%
EPPLER 393	11.52% at 32.1% of the chord	3.99% at 47.7% of the chord	0.6346%	0.0%
EPPLER 395	12.29% at 29.5% of the chord	5.24% at 51.1% of the chord	0.6173%	0.0%
EPPLER 396	13.06% at 29.5% of the chord	5.44% at 51.1% of the chord	0.6128%	0.0%

Note:

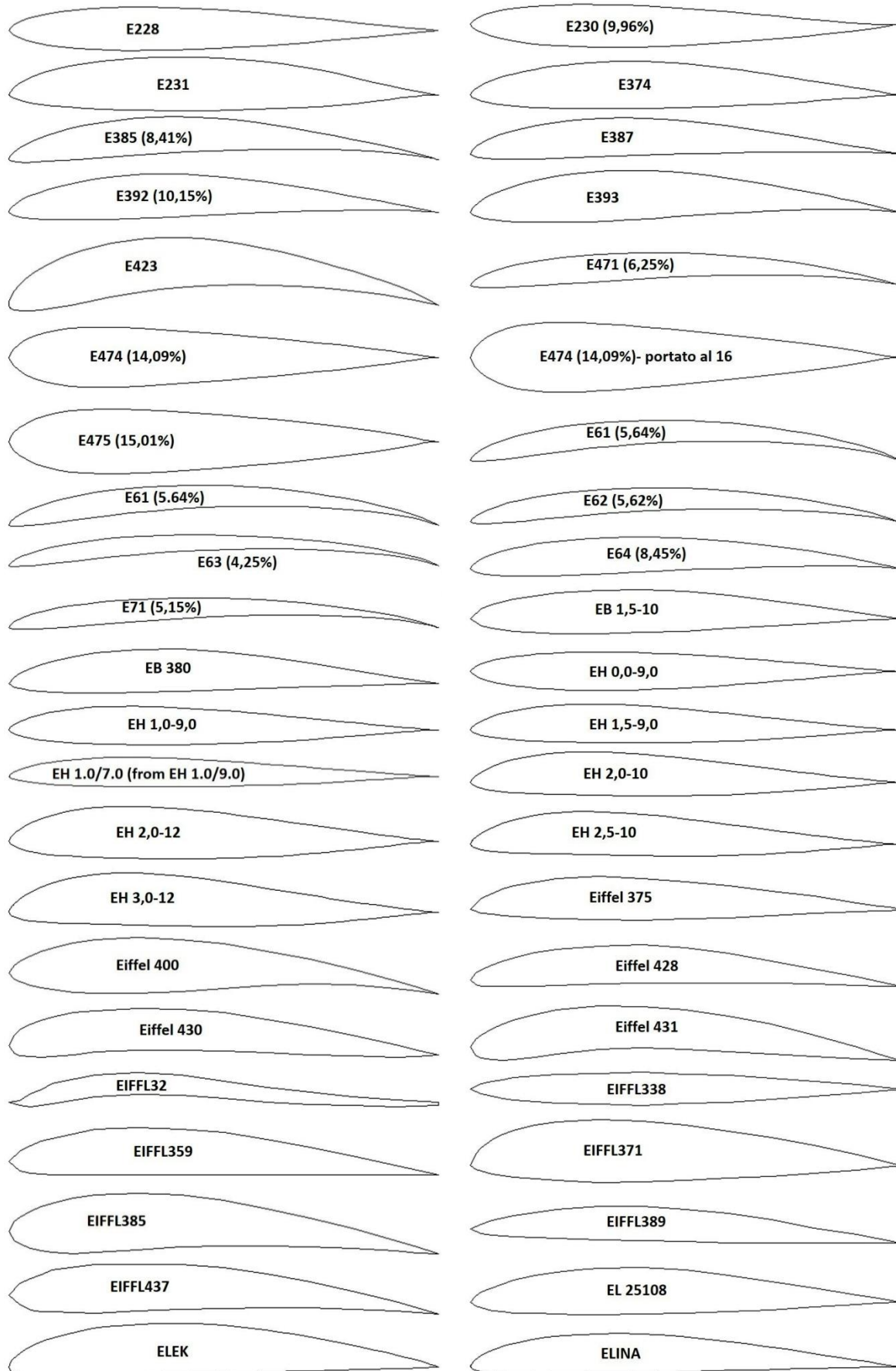
E474 (14,09%)- portato al 16 (Mod.);
 EB 1,5-10 (USA);
 EB 380 (T. Bartovsky (Czechoslovakia));
Eiffel 375, Eiffel 400, Eiffel 428, Eiffel 430, Eiffel 431 (B. Eiffel (France));
 EL 25108 (L. Lister (USA));
 EMX-07 (Designed by Martin Lichte);
 EPB - 1 (USA);
Eppler 166, Eppler 189, Eppler 228, Eppler 270, Eppler 375, Eppler 387 (R. Eppler (Germany)).

Table 2. The geometric shapes of the airfoils (hydrofoils) in the cross section.



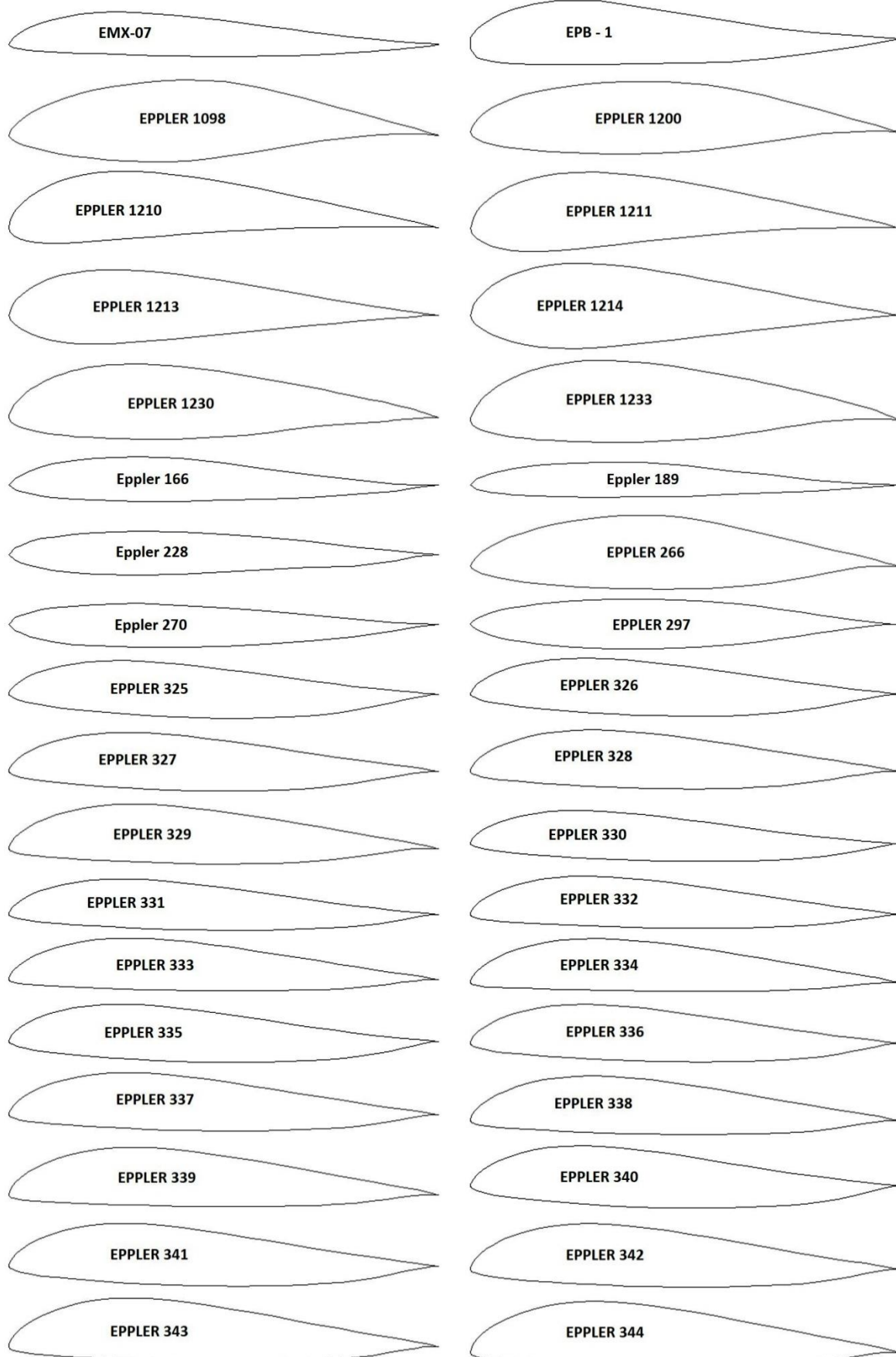
Impact Factor:

ISRA (India) = 6.317	SIS (USA) = 0.912	ICV (Poland) = 6.630
ISI (Dubai, UAE) = 1.582	РИНЦ (Russia) = 3.939	PIF (India) = 1.940
GIF (Australia) = 0.564	ESJI (KZ) = 9.035	IBI (India) = 4.260
JIF = 1.500	SJIF (Morocco) = 7.184	OAJI (USA) = 0.350



Impact Factor:

ISRA (India) = 6.317	SIS (USA) = 0.912	ICV (Poland) = 6.630
ISI (Dubai, UAE) = 1.582	РИНЦ (Russia) = 3.939	PIF (India) = 1.940
GIF (Australia) = 0.564	ESJI (KZ) = 9.035	IBI (India) = 4.260
JIF = 1.500	SJIF (Morocco) = 7.184	OAJI (USA) = 0.350

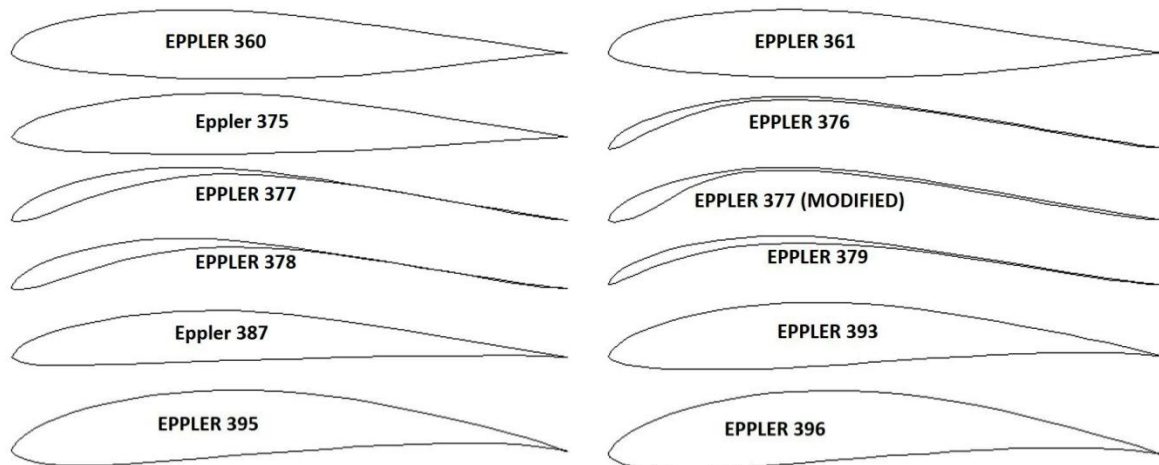


Impact Factor:

ISRA (India) = **6.317**
ISI (Dubai, UAE) = **1.582**
GIF (Australia) = **0.564**
JIF = **1.500**

SIS (USA) = **0.912**
РИНЦ (Russia) = **3.939**
ESJI (KZ) = **9.035**
SJIF (Morocco) = **7.184**

ICV (Poland) = **6.630**
PIF (India) = **1.940**
IBI (India) = **4.260**
OAJI (USA) = **0.350**



Results and discussion

The calculated pressure contours on the surfaces of the airfoils (hydrofoils) at the different angles of attack are presented in the Figs. 1-124. The calculated magnitudes on the scale can be represented as the basic magnitudes when comparing the pressure drop under conditions of changing the angle of attack of the airfoils (hydrofoils).

The leading edge pressure was determined for the E, Eiffel and EPPLER series airfoils and hydrofoils. Other airfoils were also considered.

The range of change in positive pressure at the leading edge of the studied airfoils (hydrofoils) is on average 6.3-6.6 kPa. This is 1.0-1.2 kPa less than pressure at the leading edge of the EPPLER 1200 airfoil. With an increase in the angle of attack by 15 degrees, pressure increases by more than 20 times, for example, during takeoff of the airplane with the asymmetric airfoil of the wing (EPPLER 393).

The EPPLER 379 airfoil is subjected to the least stress at the negative angle of attack.

The maximum increase in pressure at the leading edge occurs at the angle of attack of 15 degrees for the following airfoils (hydrofoils): E168 (12,45%), E169 (14,4%), E171, E174 (Dicke 8,92%), E176 (8,83%), E178 (8,69%), E178P, E180 (8,59%), E182 (8,47%), E184 (8,33%), E193 (10,22%), E2052595, E216 (10,4%), E221 (9,39%), E228, E385 (8,41%), E387, E392 (10,15%), E393, E471 (6,25%), E474 (14,09%), E474 (14,09%)- portato al 16, E475 (15,01%), E61 (5,64%), E61 (5,64%), E62 (5,62%), E63 (4,25%), E64 (8,45%), E71 (5,15%), EB 380, EH 0,0-9,0, EH 1,0-9,0, EH 1,5-9,0, EH 1,0/7,0 (from EH 1,0/9,0), EH 2,5-10, Eiffel 375, Eiffel 400, Eiffel 428, Eiffel 431, EIFFL32, EIFFL359, EIFFL371, EIFFL385, EIFFL389, EIFFL437, ELINA, EMX-07, Eppler 189, EPPLER 330, EPPLER 331, EPPLER 332, EPPLER 333, EPPLER 334, EPPLER 376, EPPLER 377, EPPLER 377 (MODIFIED), EPPLER 378, EPPLER 379, Eppler 387, EPPLER 393. The maximum increase in pressure at the leading edge occurs at the angle of attack of -15 degrees for the remaining airfoils (hydrofoils).

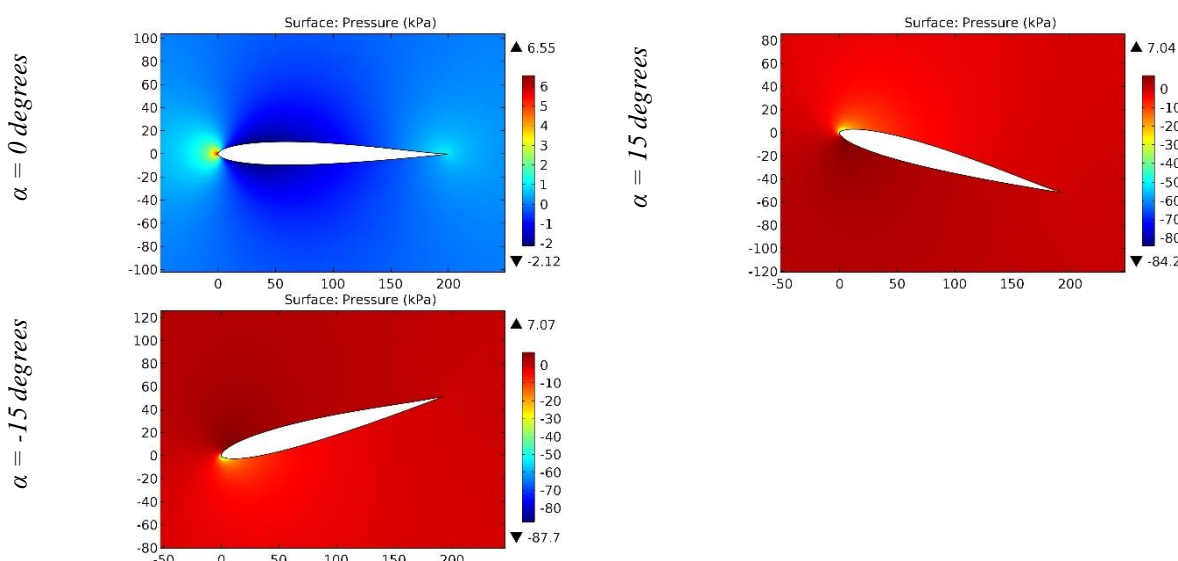


Figure 1. The pressure contours on the surfaces of the E10(08%) airfoil.

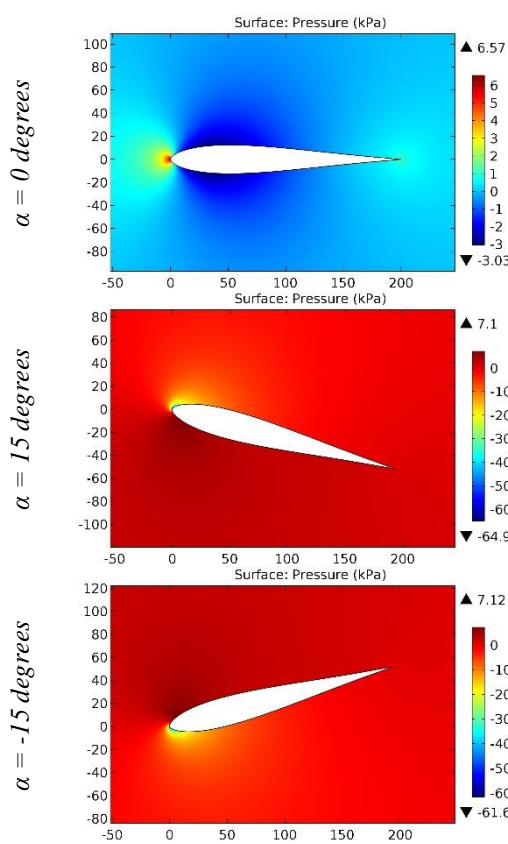


Figure 2. The pressure contours on the surfaces of the E168 (12,45%) airfoil.

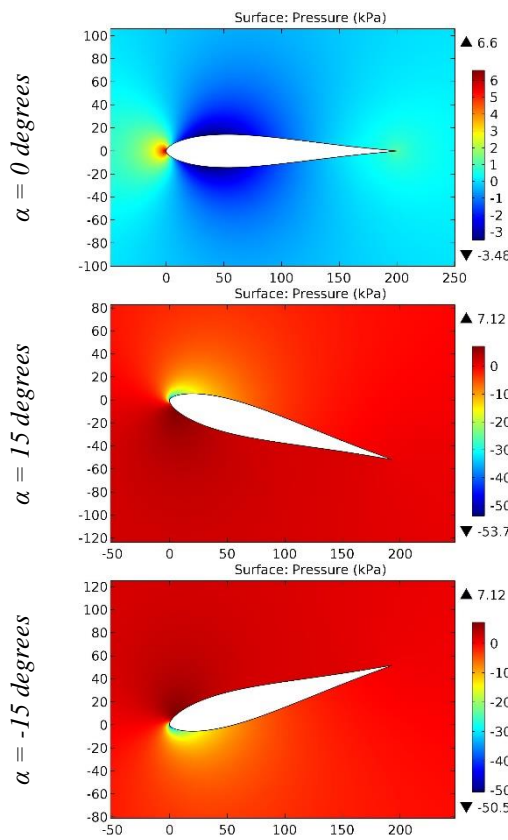


Figure 3. The pressure contours on the surfaces of the E169 (14,4%) airfoil.

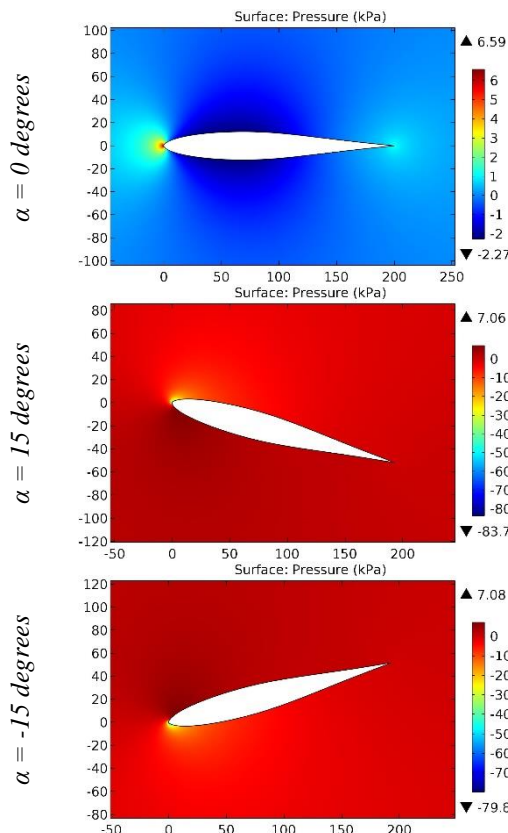


Figure 4. The pressure contours on the surfaces of the E171 airfoil.

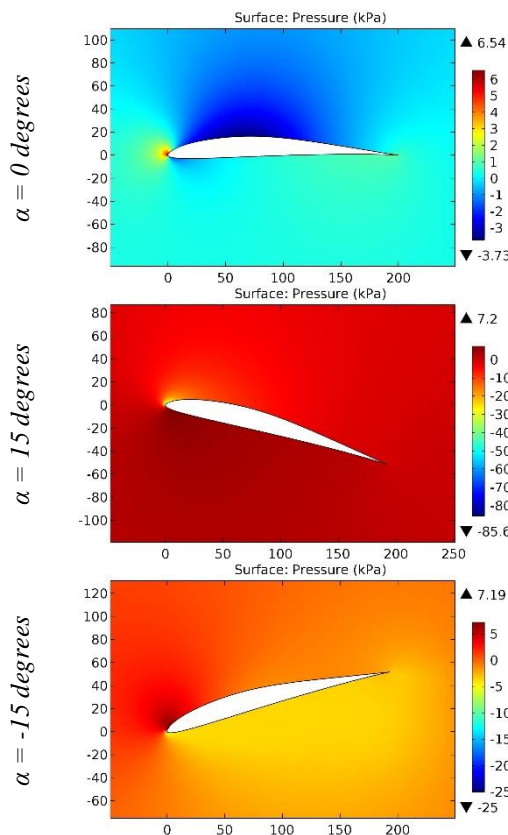


Figure 5. The pressure contours on the surfaces of the E174 (Dicke 8.92%) airfoil.

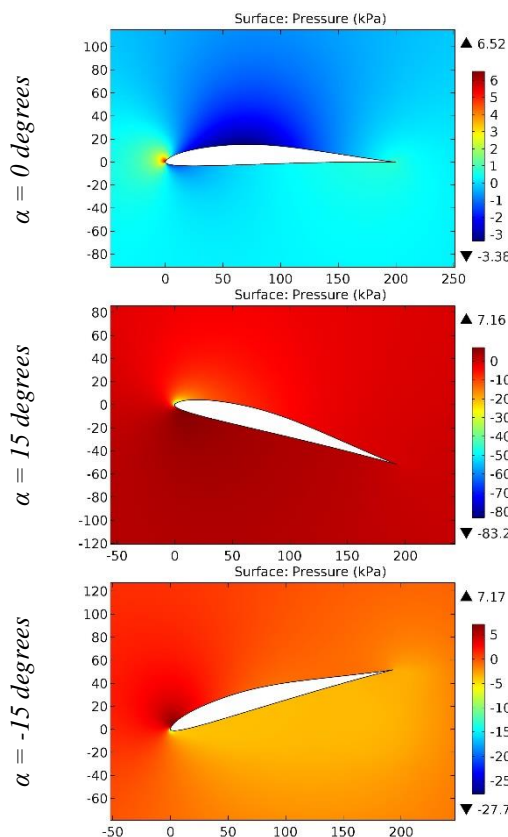


Figure 6. The pressure contours on the surfaces of the E176 (8,83%) airfoil.

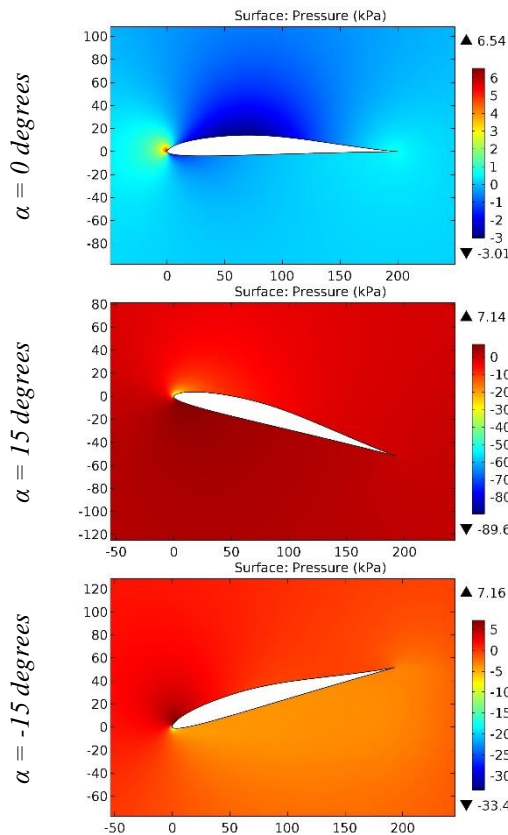


Figure 7. The pressure contours on the surfaces of the E178 (8,69%) airfoil.

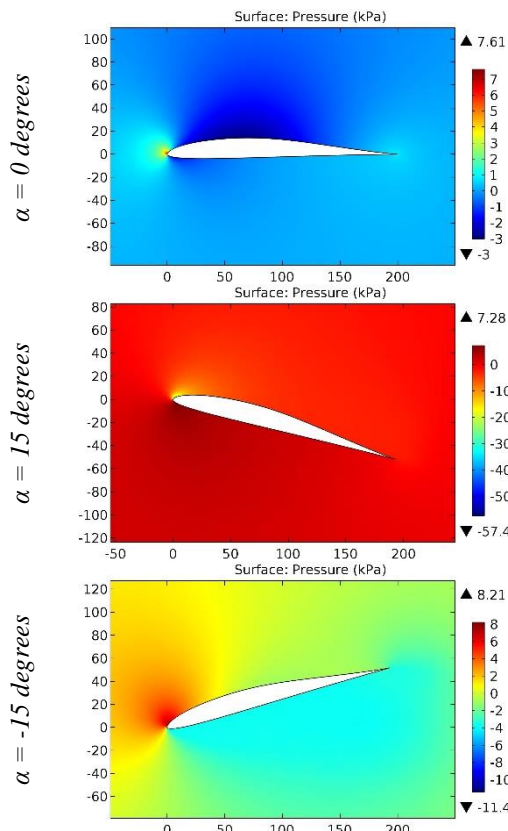


Figure 8. The pressure contours on the surfaces of the E178P airfoil.

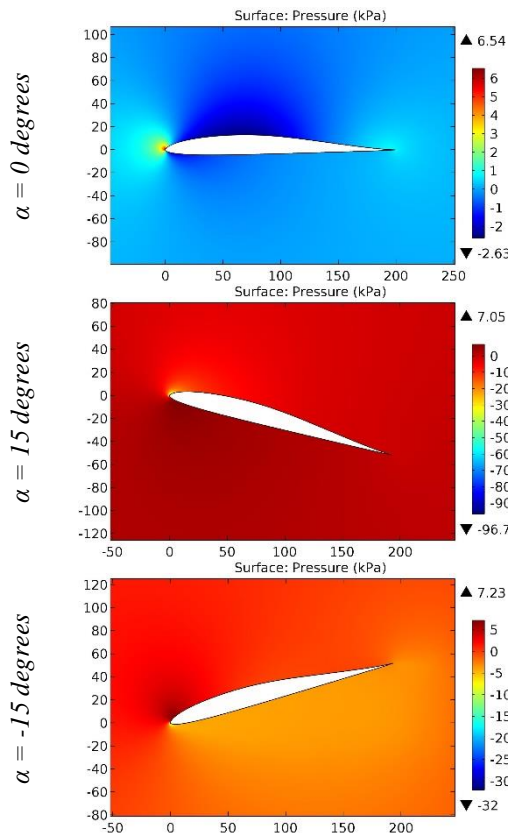


Figure 9. The pressure contours on the surfaces of the E180 (8,59%) airfoil.

ISRA (India) = 6.317	SIS (USA) = 0.912	ICV (Poland) = 6.630
ISI (Dubai, UAE) = 1.582	РИНЦ (Russia) = 3.939	PIF (India) = 1.940
GIF (Australia) = 0.564	ESJI (KZ) = 9.035	IBI (India) = 4.260
JIF = 1.500	SJIF (Morocco) = 7.184	OAJI (USA) = 0.350

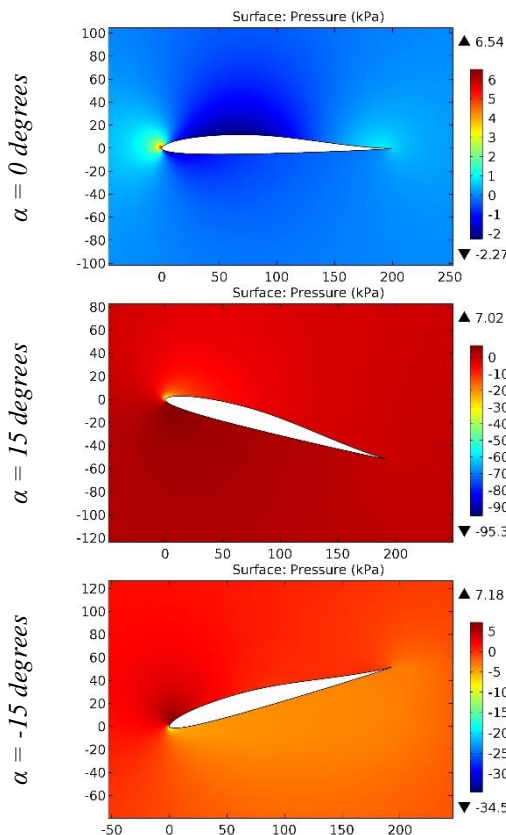


Figure 10. The pressure contours on the surfaces of the E182 (8,47%) airfoil.

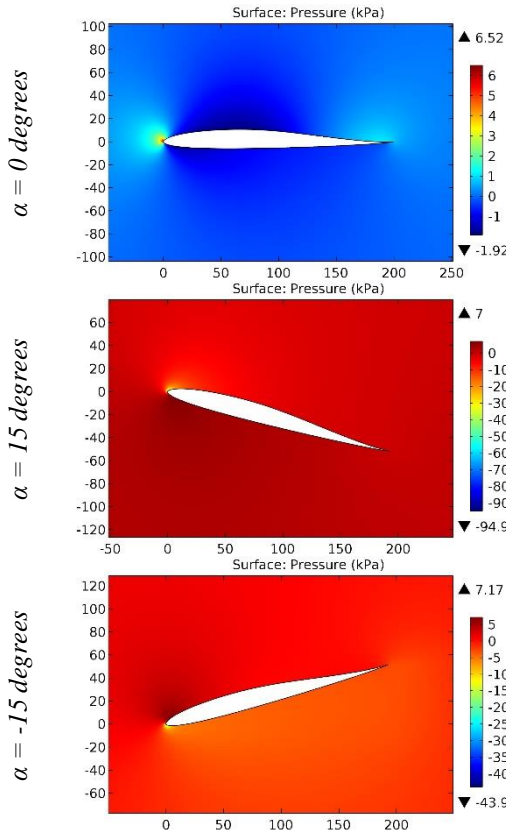


Figure 11. The pressure contours on the surfaces of the E184 (8,33%) airfoil.

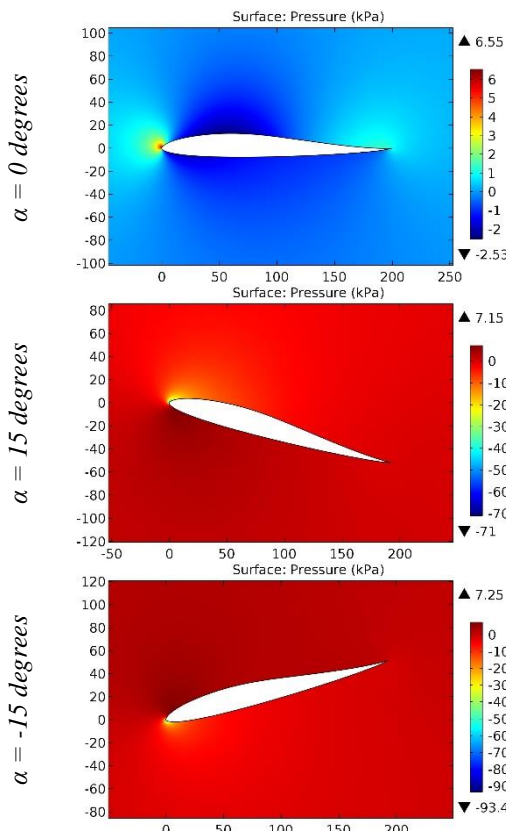


Figure 12. The pressure contours on the surfaces of the E186 (10,27%) airfoil.

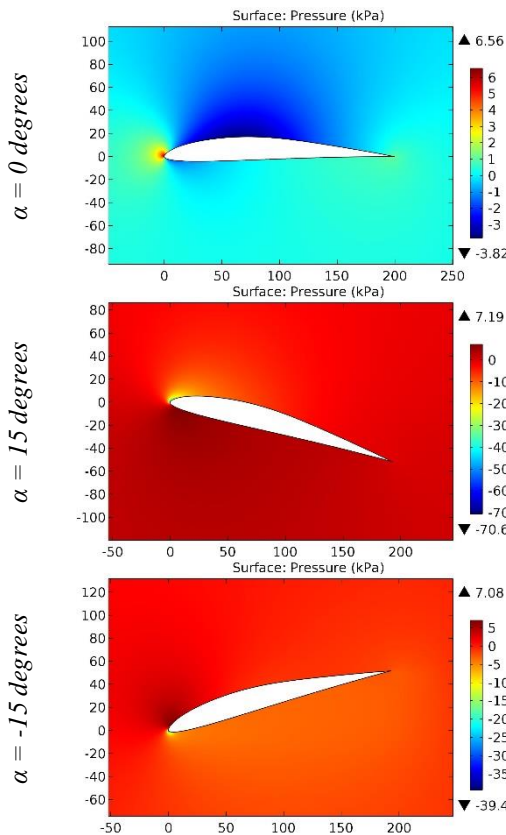


Figure 13. The pressure contours on the surfaces of the E193 (10,22%) airfoil.

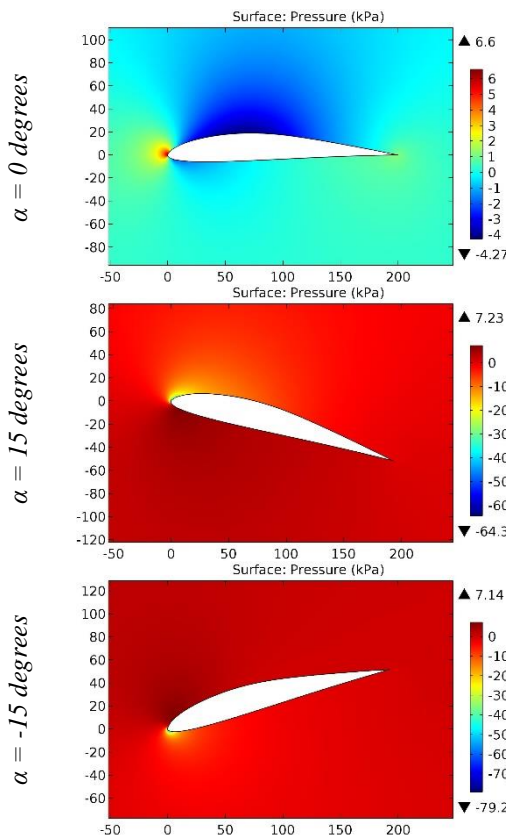


Figure 14. The pressure contours on the surfaces of the E193-12 airfoil.

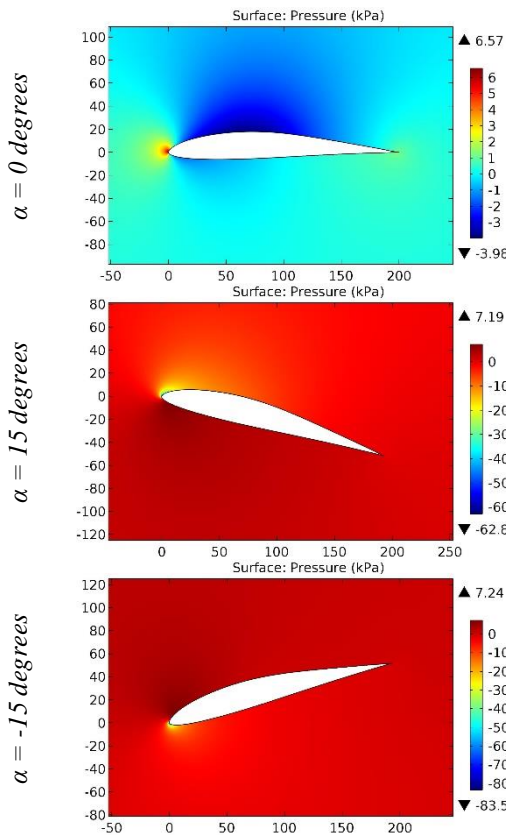


Figure 15. The pressure contours on the surfaces of the E195 (11,82%) airfoil.

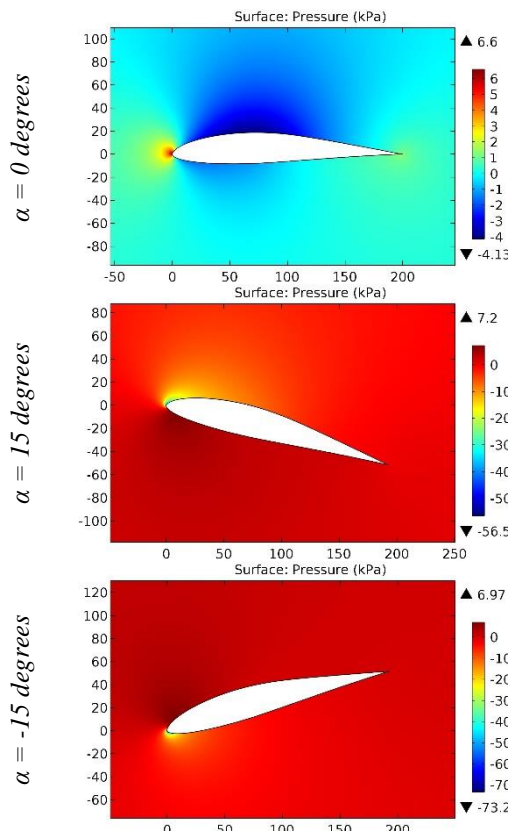


Figure 16. The pressure contours on the surfaces of the E197 (13,49%) airfoil.

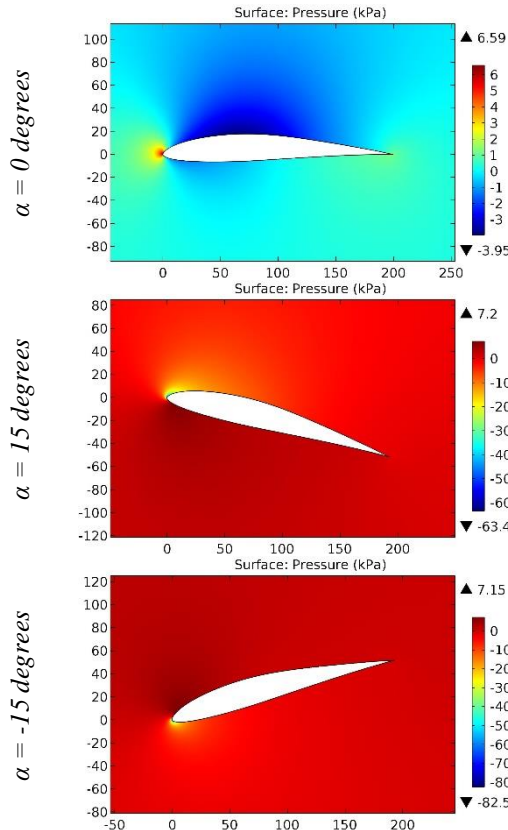


Figure 17. The pressure contours on the surfaces of the E201 (11,88%) airfoil.

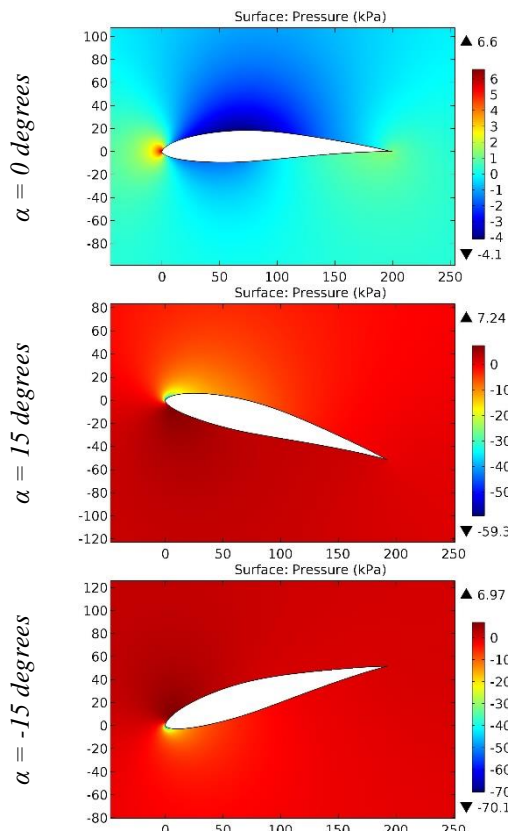


Figure 18. The pressure contours on the surfaces of the E203 (13,64%) airfoil.

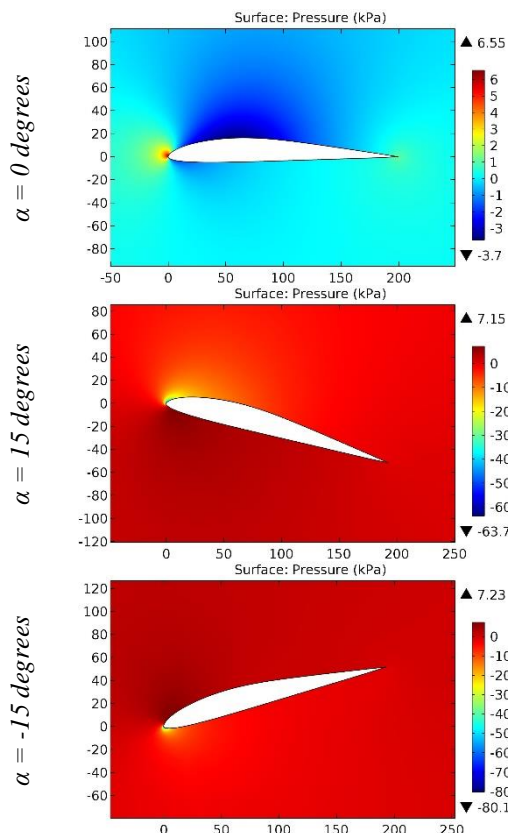


Figure 19. The pressure contours on the surfaces of the E205 (10,48%) airfoil.

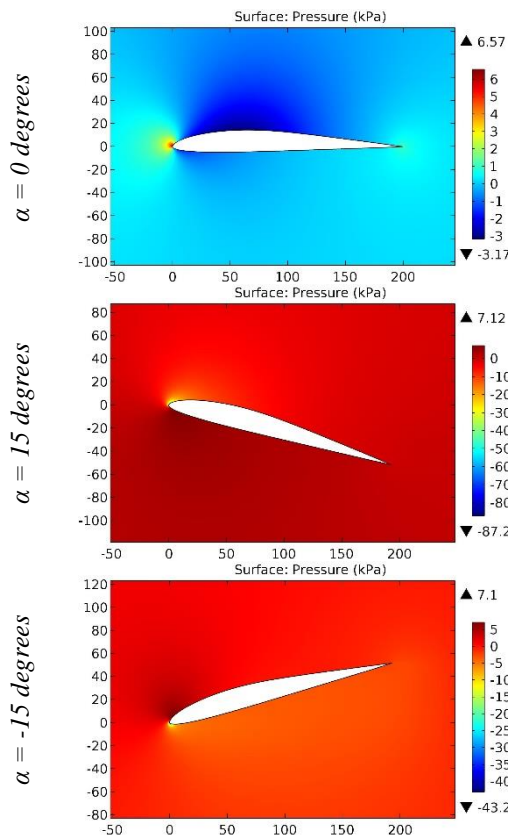


Figure 20. The pressure contours on the surfaces of the E2052595 airfoil.

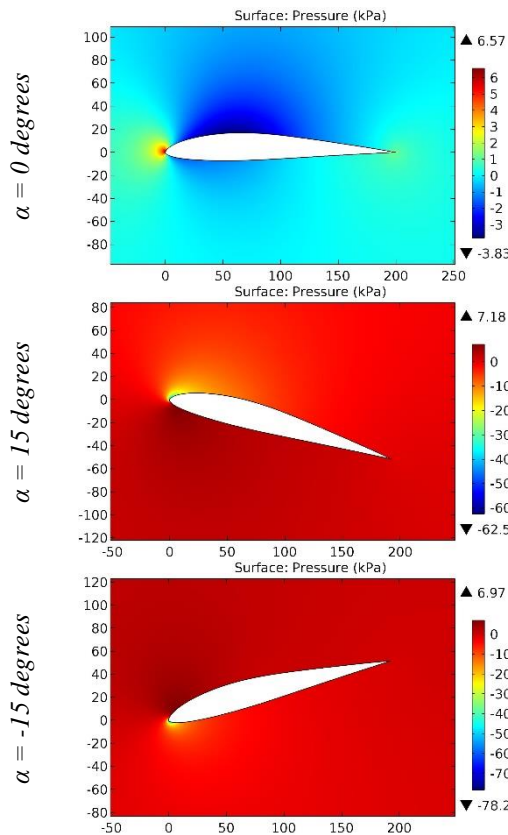


Figure 21. The pressure contours on the surfaces of the E207 (12,04%) airfoil.

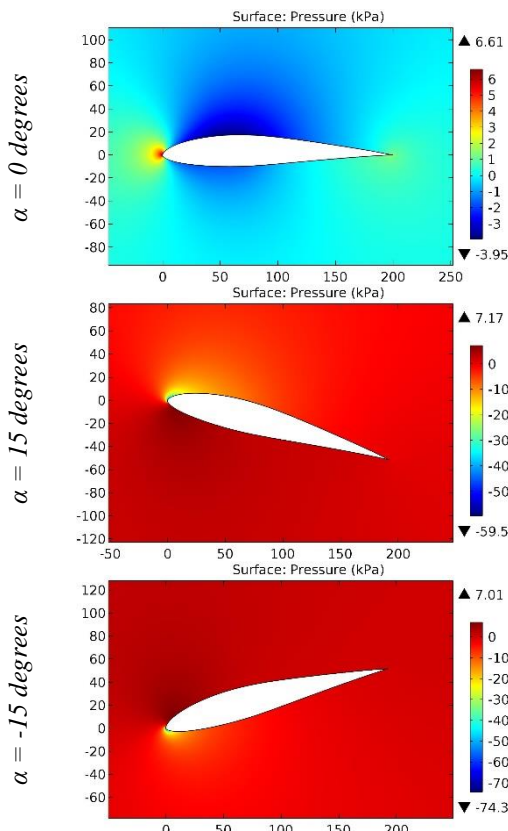


Figure 22. The pressure contours on the surfaces of the E209 (13,72%) airfoil.

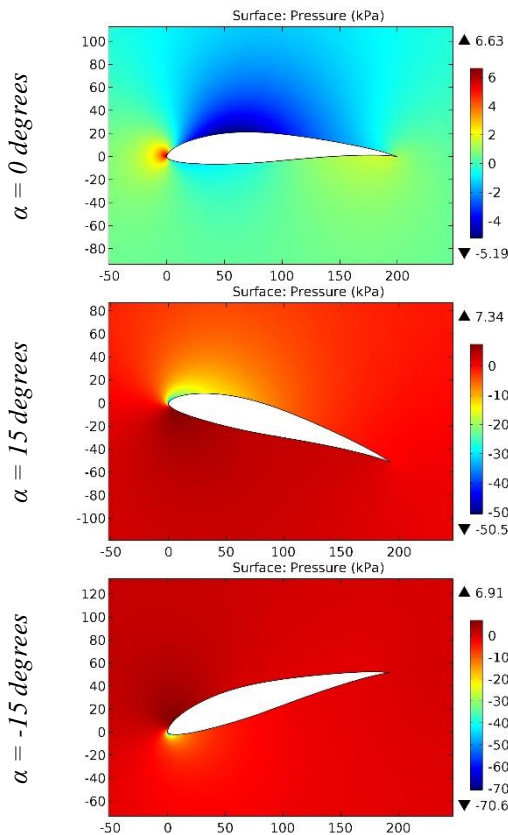


Figure 23. The pressure contours on the surfaces of the E210 (13,64%) airfoil.

ISRA (India)	= 6.317	SIS (USA)	= 0.912	ICV (Poland)	= 6.630
ISI (Dubai, UAE)	= 1.582	РИНЦ (Russia)	= 3.939	PIF (India)	= 1.940
GIF (Australia)	= 0.564	ESJI (KZ)	= 9.035	IBI (India)	= 4.260
JIF	= 1.500	SJIF (Morocco)	= 7.184	OAJI (USA)	= 0.350

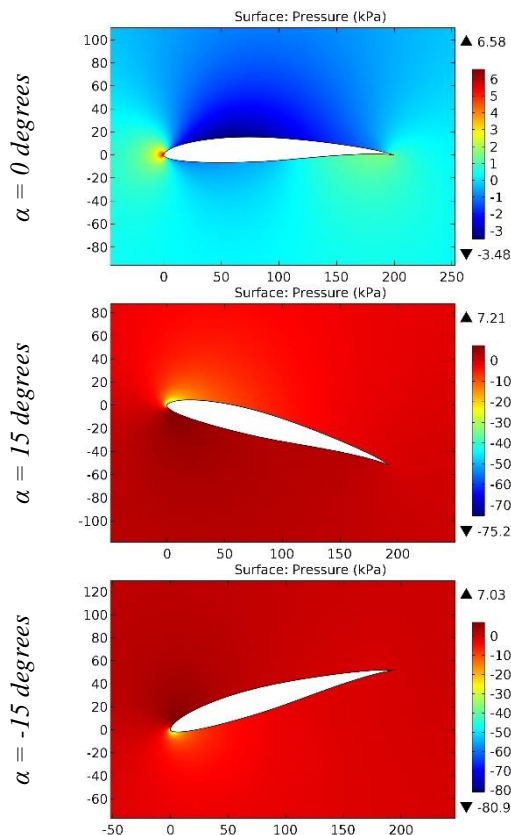


Figure 24. The pressure contours on the surfaces of the E211 (10,96%) airfoil.

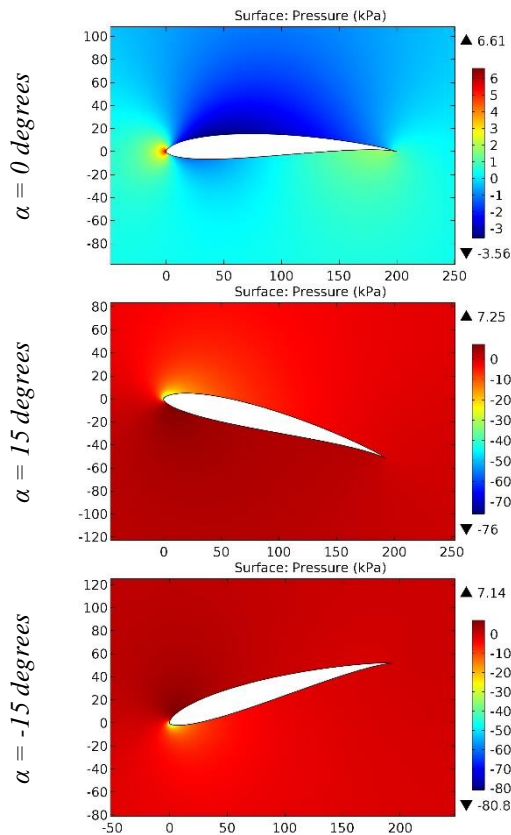


Figure 25. The pressure contours on the surfaces of the E212 (10,55%) airfoil.

ISRA (India) = 6.317	SIS (USA) = 0.912	ICV (Poland) = 6.630
ISI (Dubai, UAE) = 1.582	РИНЦ (Russia) = 3.939	PIF (India) = 1.940
GIF (Australia) = 0.564	ESJI (KZ) = 9.035	IBI (India) = 4.260
JIF = 1.500	SJIF (Morocco) = 7.184	OAJI (USA) = 0.350

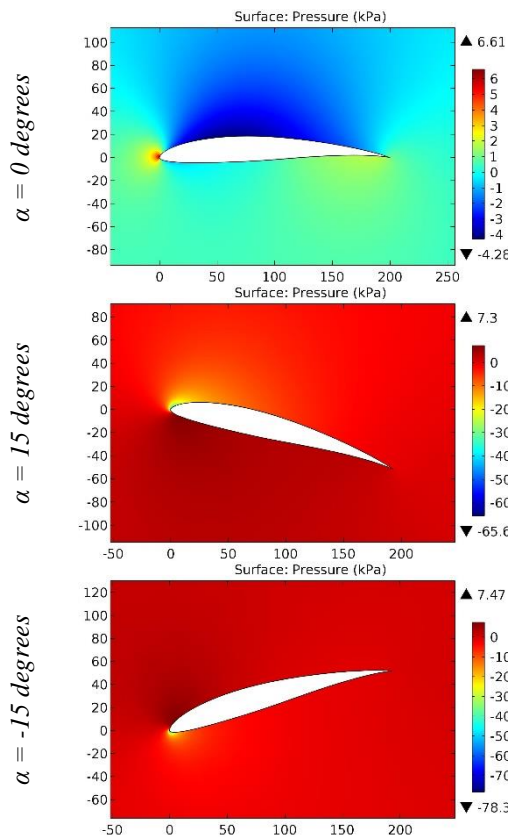


Figure 26. The pressure contours on the surfaces of the E214 (11,1%) airfoil.

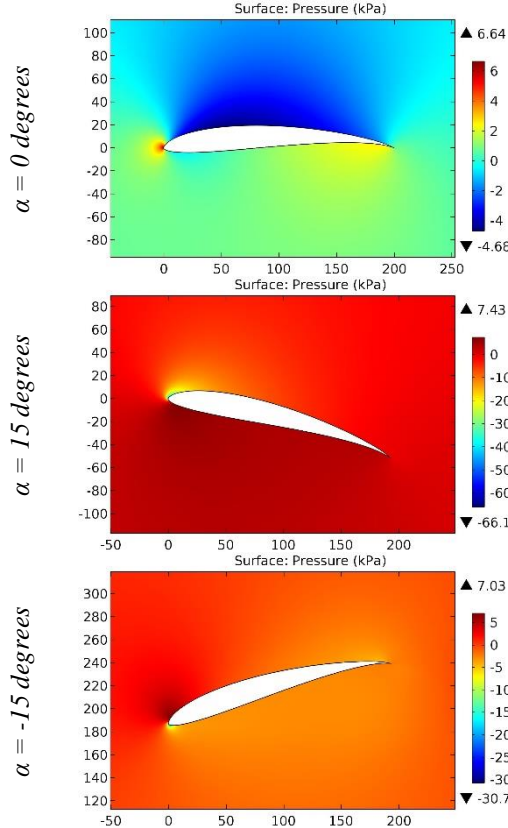


Figure 27. The pressure contours on the surfaces of the E216 (10,4%) airfoil.

ISRA (India)	= 6.317	SIS (USA)	= 0.912	ICV (Poland)	= 6.630
ISI (Dubai, UAE)	= 1.582	РИНЦ (Russia)	= 3.939	PIF (India)	= 1.940
GIF (Australia)	= 0.564	ESJI (KZ)	= 9.035	IBI (India)	= 4.260
JIF	= 1.500	SJIF (Morocco)	= 7.184	OAJI (USA)	= 0.350

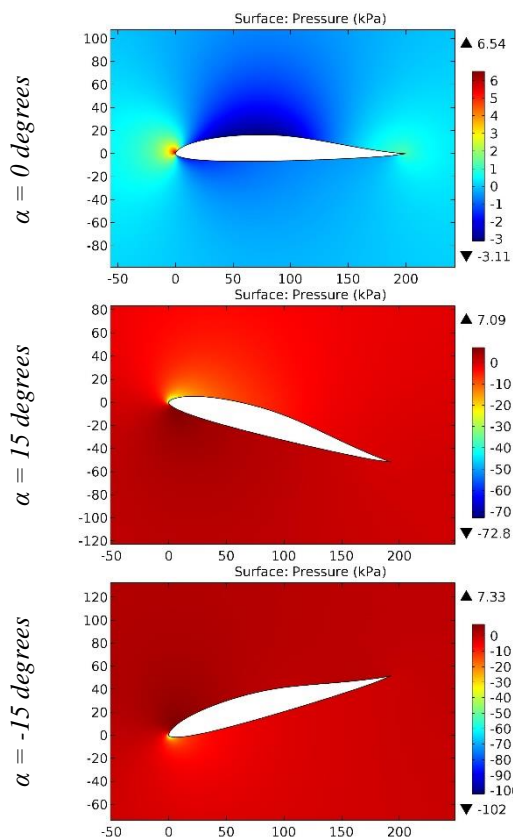


Figure 28. The pressure contours on the surfaces of the E220 (11,48%) airfoil.

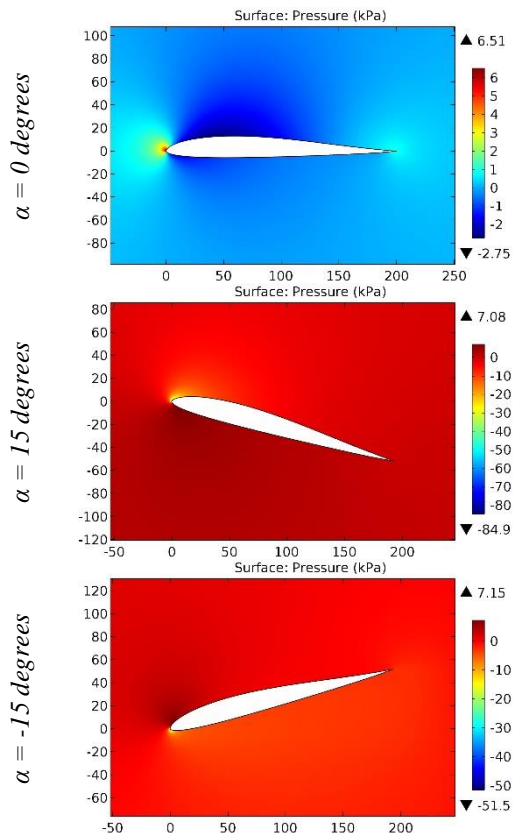


Figure 29. The pressure contours on the surfaces of the E221 (9,39%) airfoil.

ISRA (India)	= 6.317	SIS (USA)	= 0.912	ICV (Poland)	= 6.630
ISI (Dubai, UAE)	= 1.582	РИНЦ (Russia)	= 3.939	PIF (India)	= 1.940
GIF (Australia)	= 0.564	ESJI (KZ)	= 9.035	IBI (India)	= 4.260
JIF	= 1.500	SJIF (Morocco)	= 7.184	OAJI (USA)	= 0.350

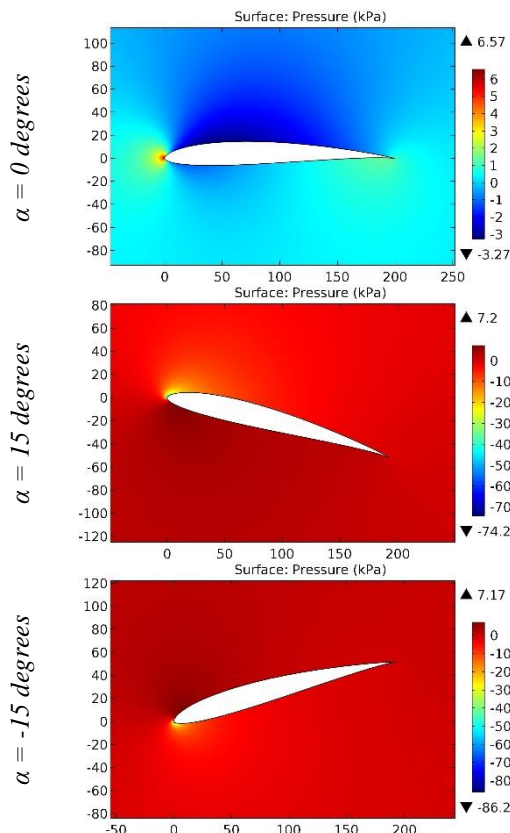


Figure 30. The pressure contours on the surfaces of the E222 (10,17%) airfoil.

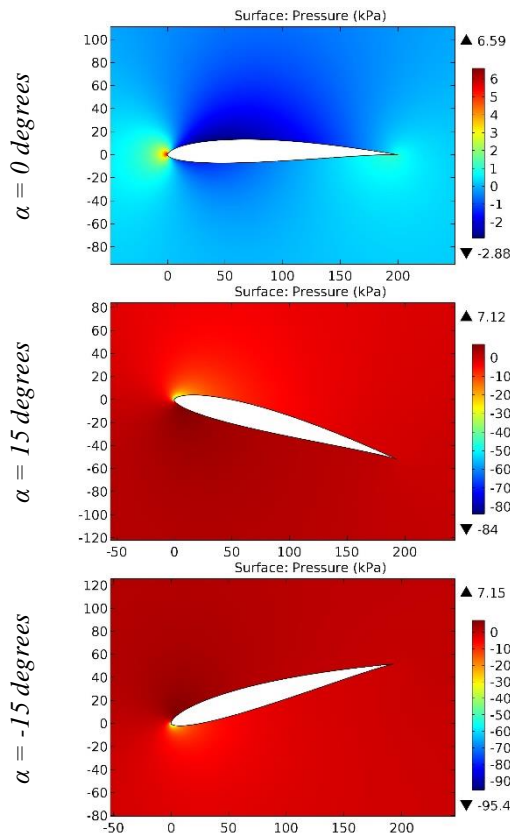


Figure 31. The pressure contours on the surfaces of the E224 (10,17%) airfoil.

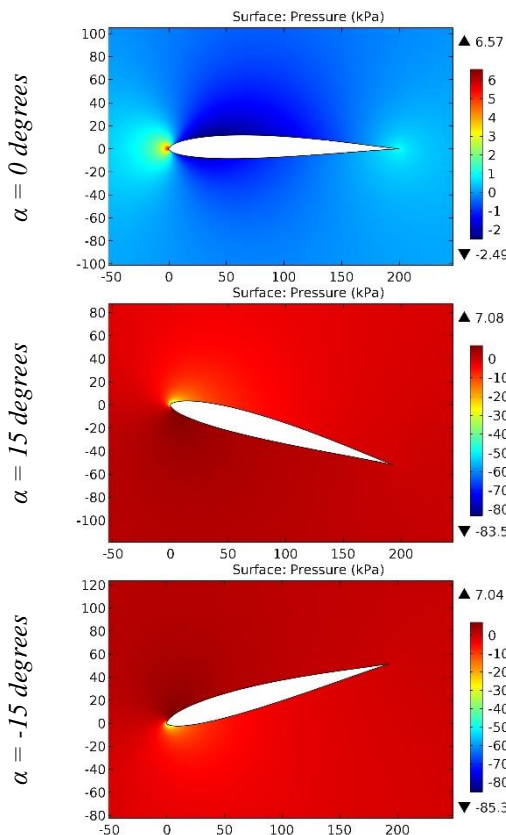


Figure 32. The pressure contours on the surfaces of the E226 (10,19%) airfoil.

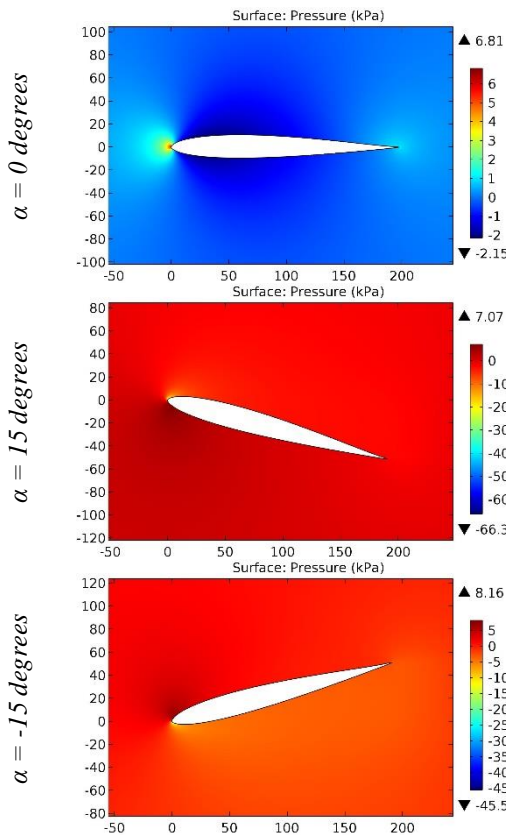


Figure 33. The pressure contours on the surfaces of the E228 airfoil.

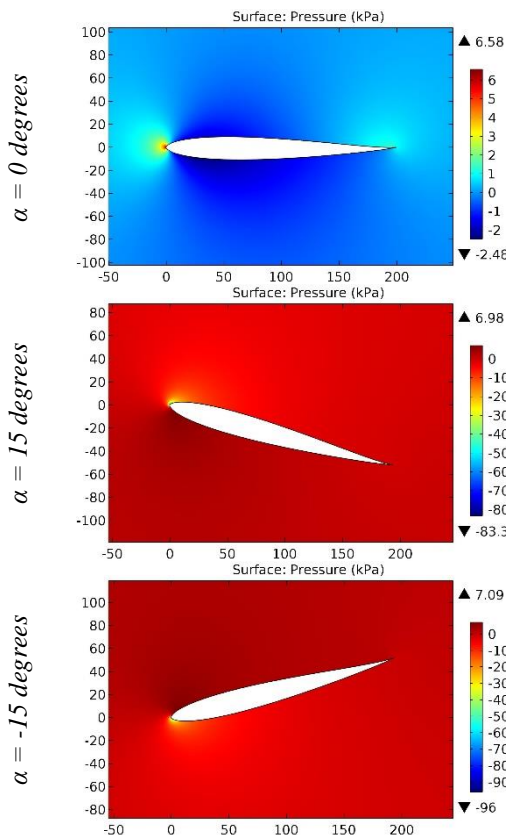


Figure 34. The pressure contours on the surfaces of the E230 (9,96%) airfoil.

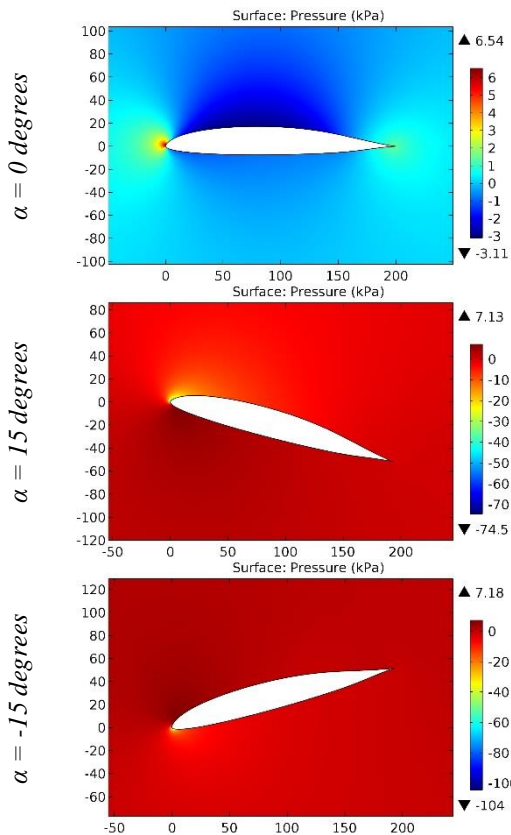


Figure 35. The pressure contours on the surfaces of the E231 airfoil.

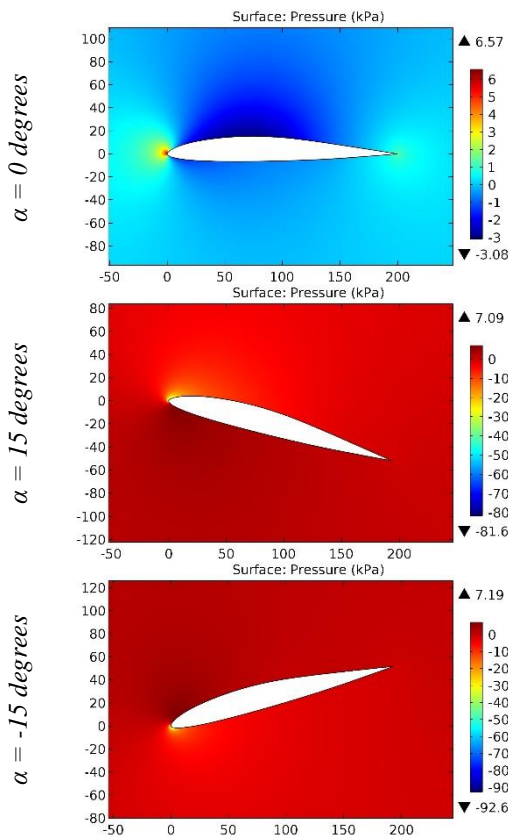


Figure 36. The pressure contours on the surfaces of the E374 airfoil.

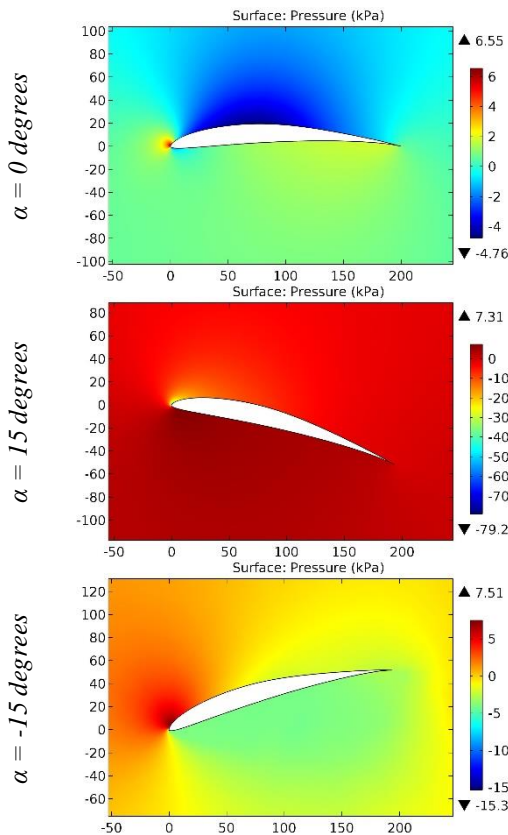


Figure 37. The pressure contours on the surfaces of the E385 (8.41%) airfoil.

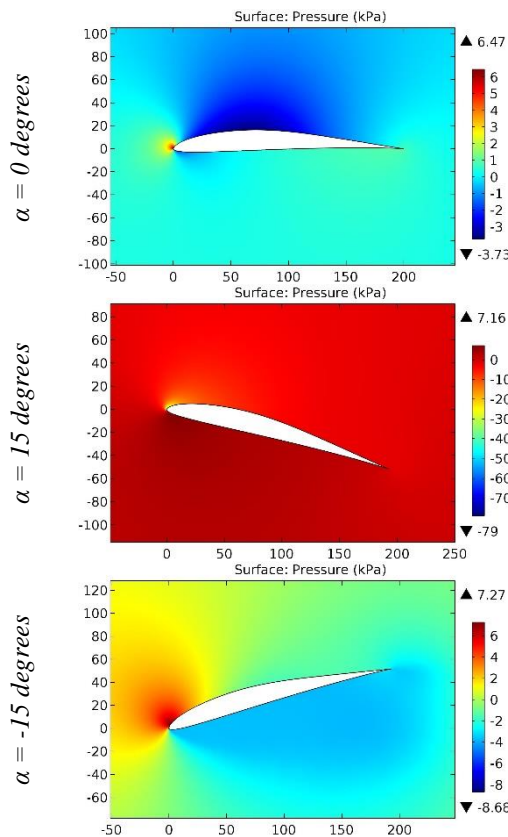


Figure 38. The pressure contours on the surfaces of the E387 airfoil.

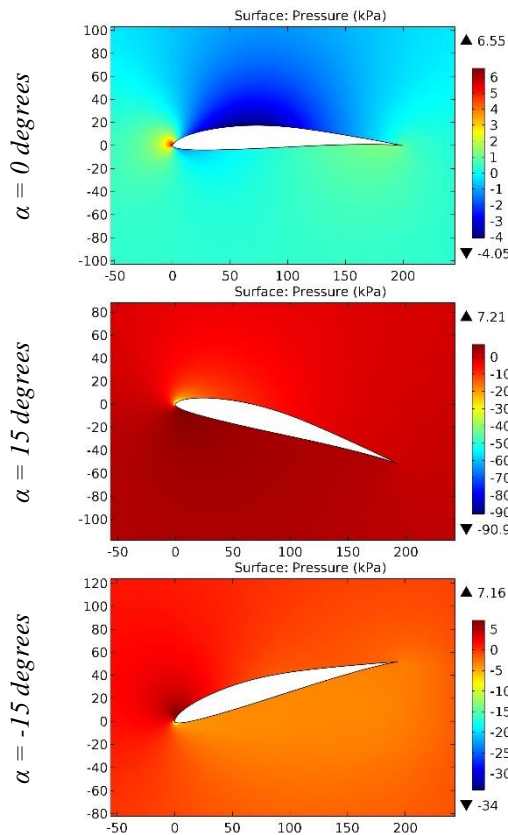


Figure 39. The pressure contours on the surfaces of the E392 (10,15%) airfoil.

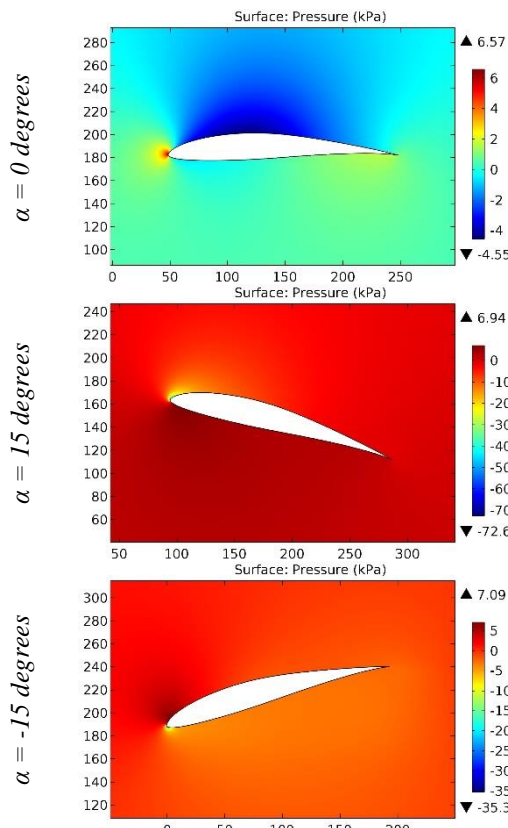


Figure 40. The pressure contours on the surfaces of the E393 airfoil.

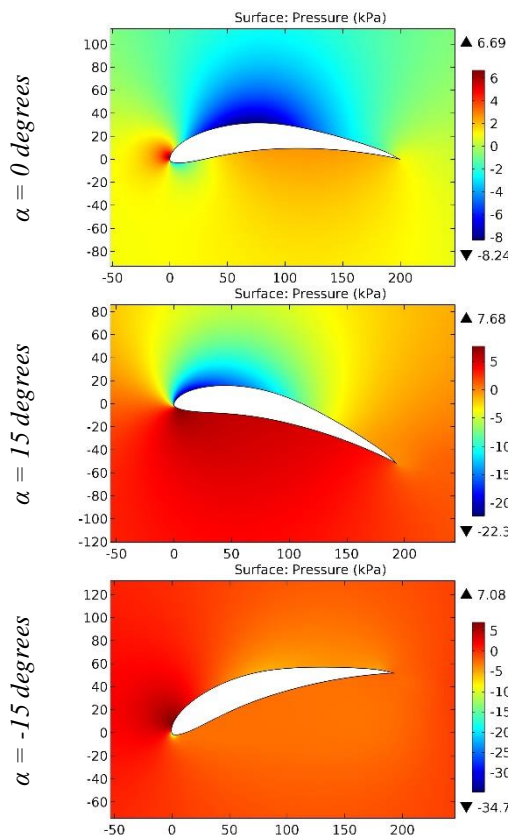


Figure 41. The pressure contours on the surfaces of the E423 airfoil.

ISRA (India) = 6.317	SIS (USA) = 0.912	ICV (Poland) = 6.630
ISI (Dubai, UAE) = 1.582	РИНЦ (Russia) = 3.939	PIF (India) = 1.940
GIF (Australia) = 0.564	ESJI (KZ) = 9.035	IBI (India) = 4.260
JIF = 1.500	SJIF (Morocco) = 7.184	OAJI (USA) = 0.350

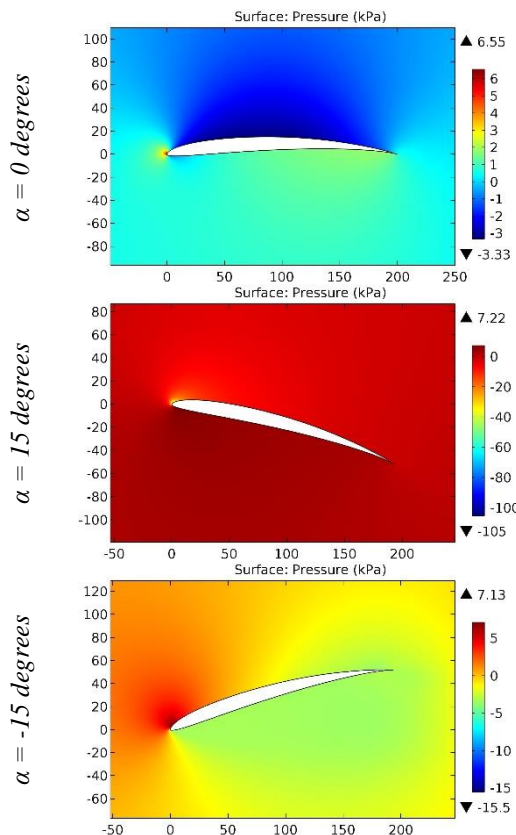


Figure 42. The pressure contours on the surfaces of the E471 (6,25%) airfoil.

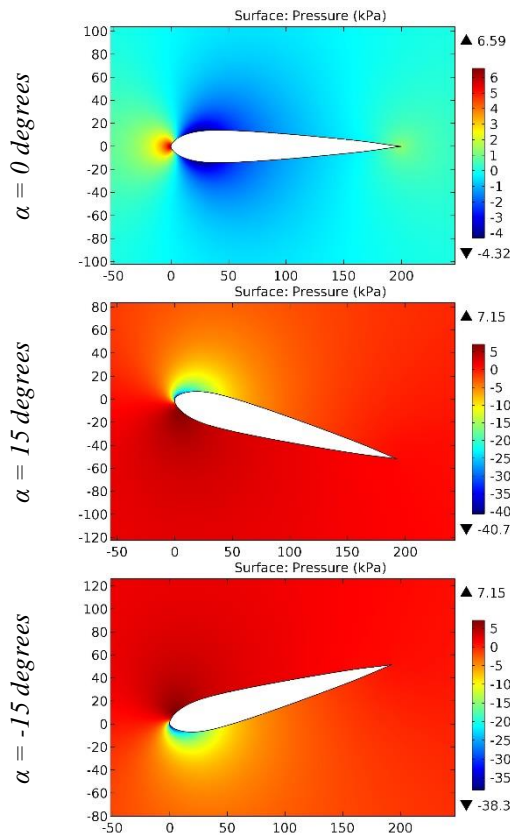


Figure 43. The pressure contours on the surfaces of the E474 (14,09%) airfoil.

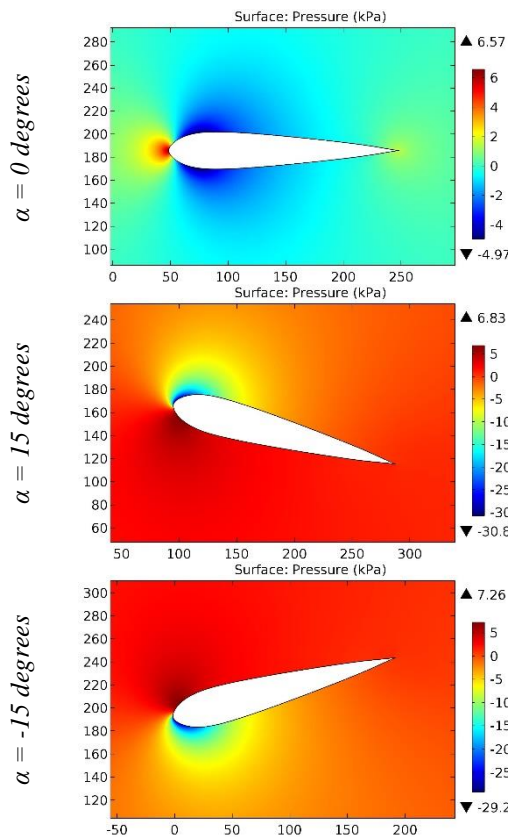


Figure 44. The pressure contours on the surfaces of the E474 (14,09%)- portato al 16 airfoil.

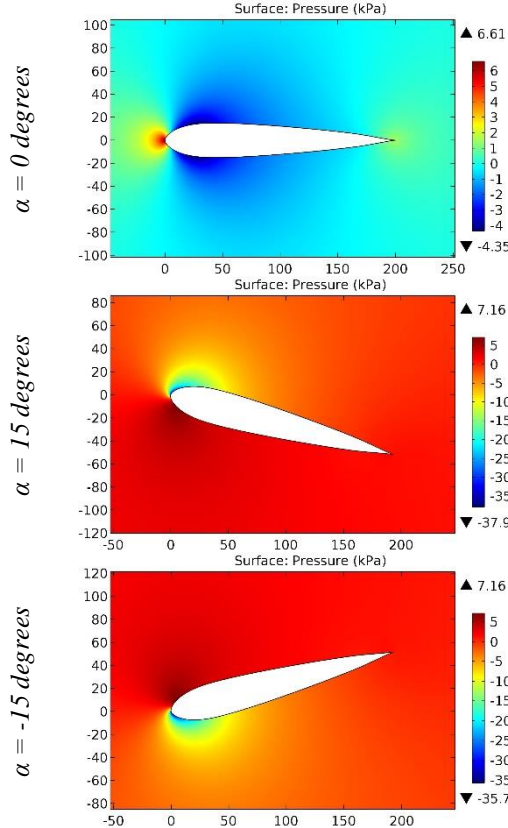


Figure 45. The pressure contours on the surfaces of the E475 (15,01%) airfoil.

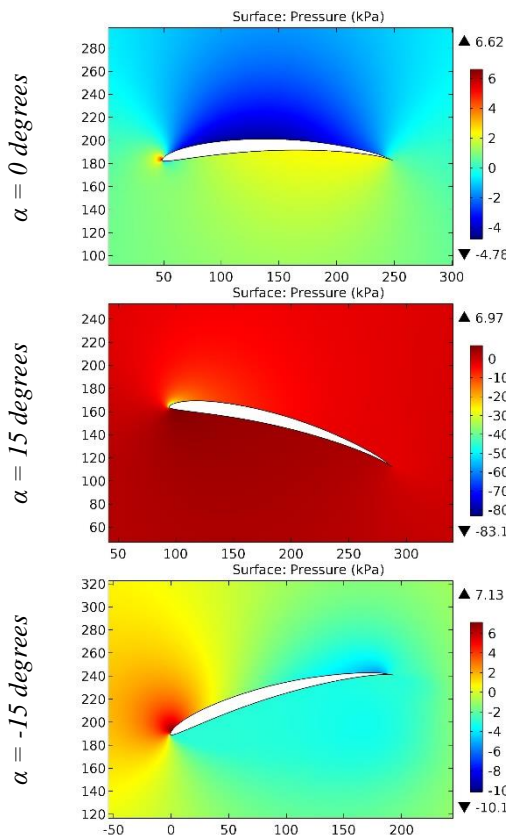


Figure 46. The pressure contours on the surfaces of the E61 (5,64%) airfoil.

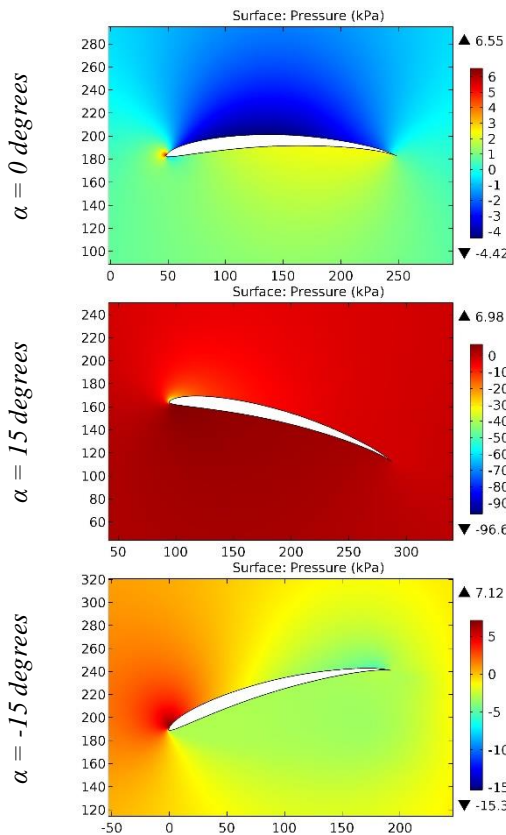


Figure 47. The pressure contours on the surfaces of the E61 (5.64%) airfoil.

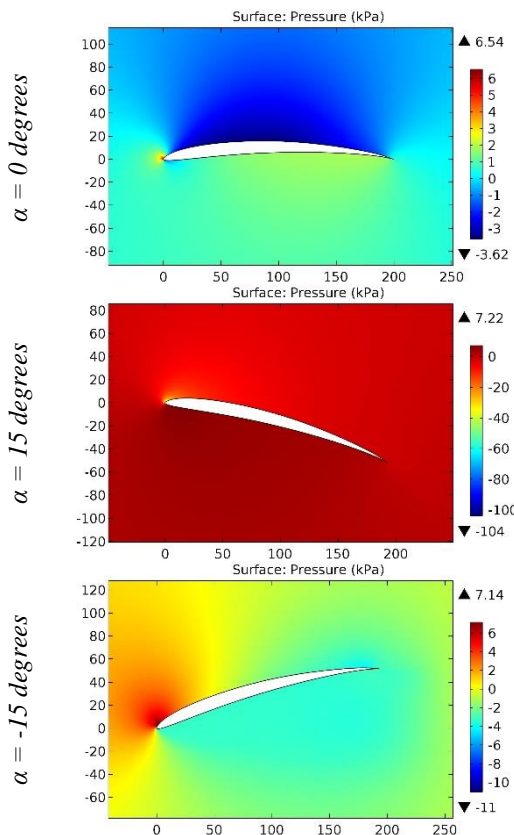


Figure 48. The pressure contours on the surfaces of the E62 (5,62%) airfoil.

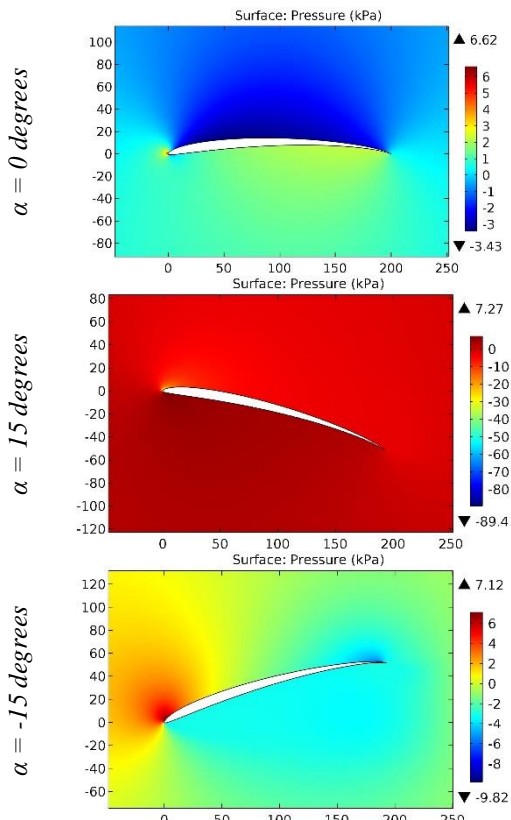


Figure 49. The pressure contours on the surfaces of the E63 (4,25%) airfoil.

ISRA (India) = 6.317	SIS (USA) = 0.912	ICV (Poland) = 6.630
ISI (Dubai, UAE) = 1.582	РИНЦ (Russia) = 3.939	PIF (India) = 1.940
GIF (Australia) = 0.564	ESJI (KZ) = 9.035	IBI (India) = 4.260
JIF = 1.500	SJIF (Morocco) = 7.184	OAJI (USA) = 0.350

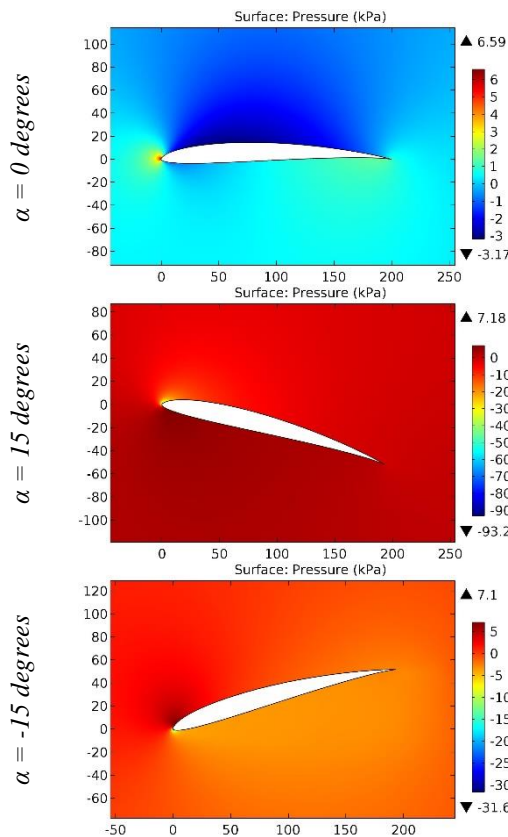


Figure 50. The pressure contours on the surfaces of the E64 (8,45%) airfoil.

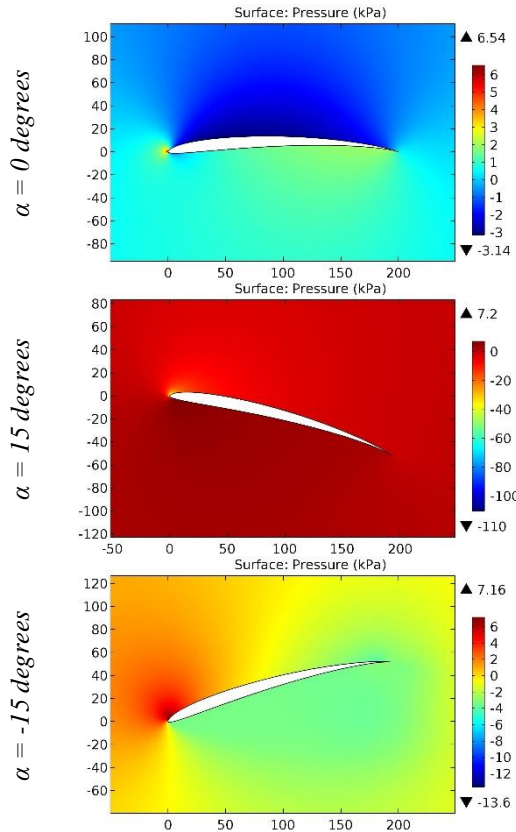


Figure 51. The pressure contours on the surfaces of the E71 (5,15%) airfoil.

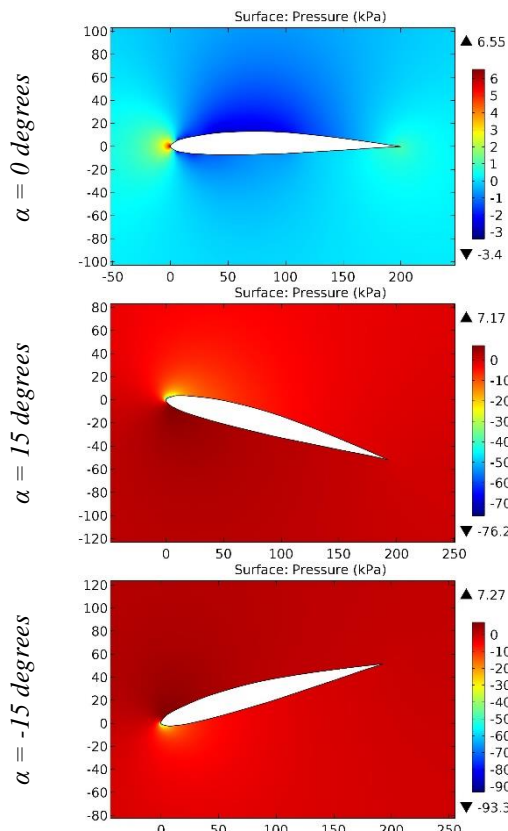


Figure 52. The pressure contours on the surfaces of the EB 1,5-10 airfoil.

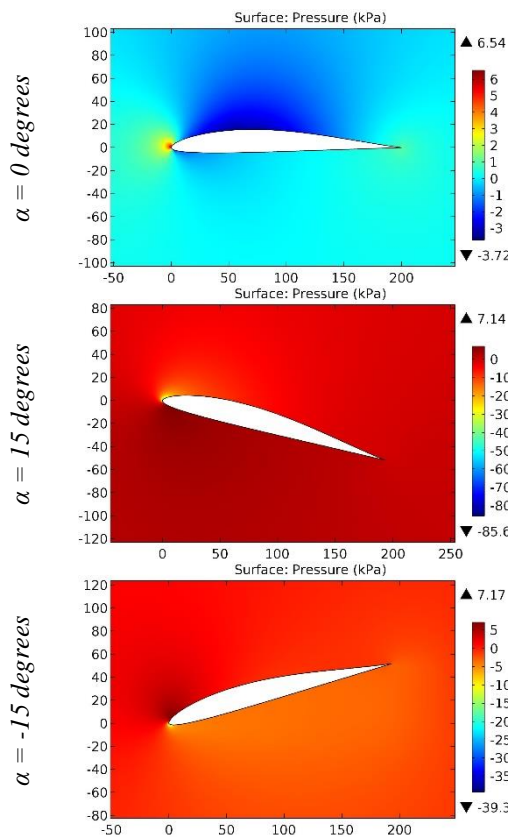


Figure 53. The pressure contours on the surfaces of the EB 380 airfoil.

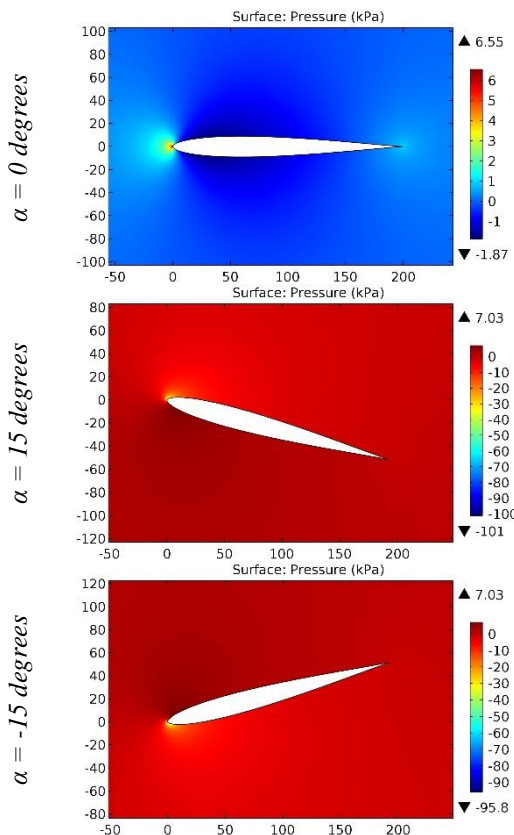


Figure 54. The pressure contours on the surfaces of the EH 0,0-9,0 airfoil.

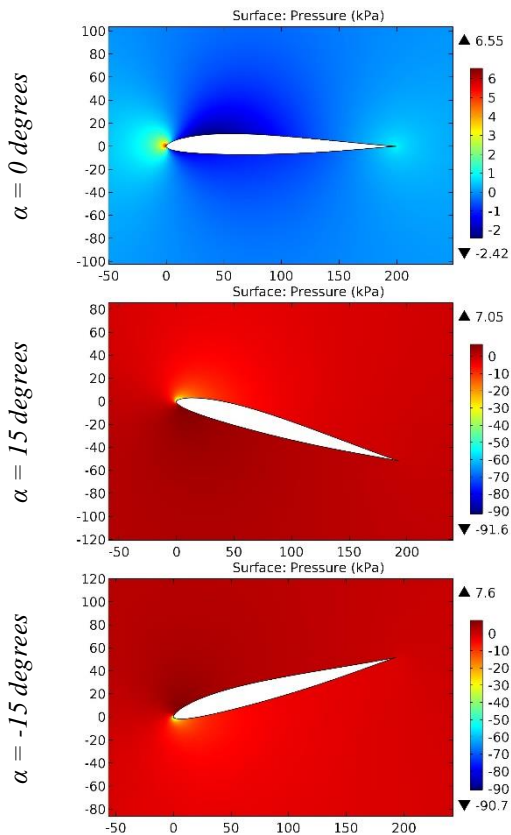


Figure 55. The pressure contours on the surfaces of the EH 1,0-9,0 airfoil.

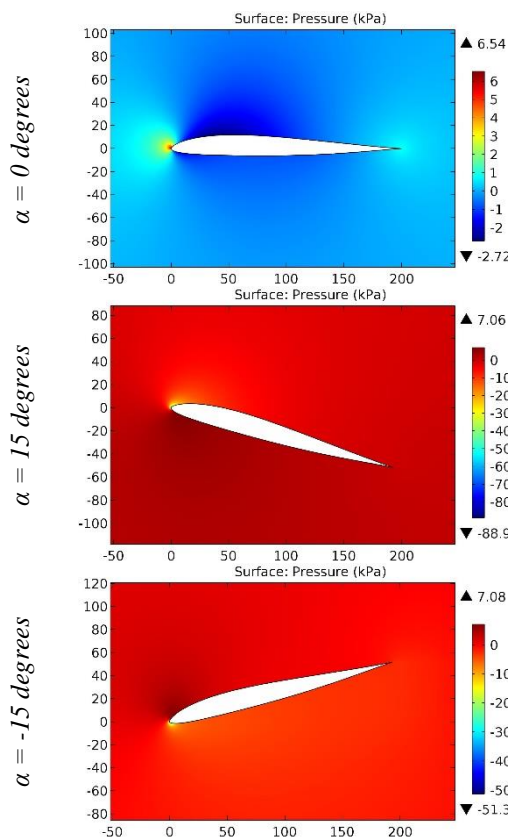


Figure 56. The pressure contours on the surfaces of the EH 1,5-9,0 airfoil.

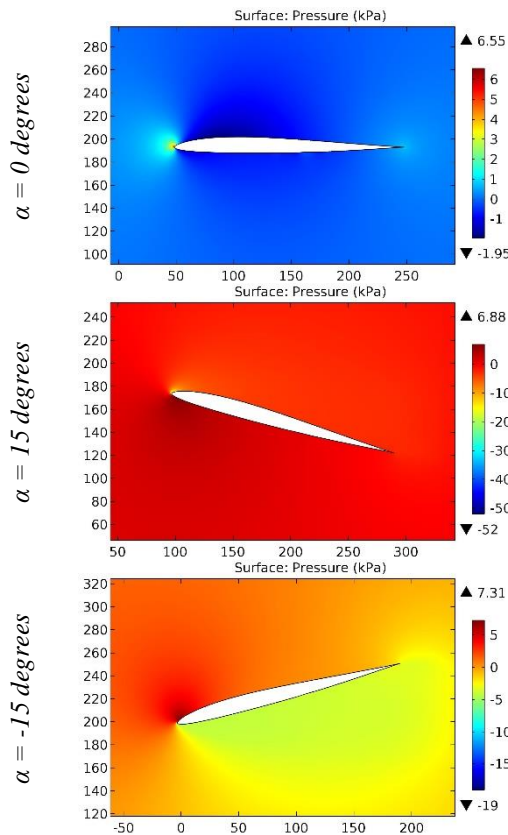


Figure 57. The pressure contours on the surfaces of the EH 1.0/7.0 (from EH 1.0/9.0) airfoil.

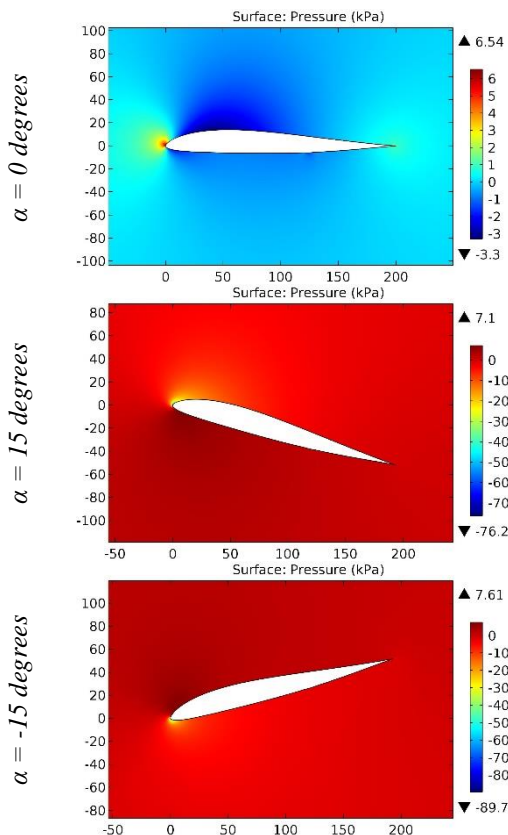


Figure 58. The pressure contours on the surfaces of the EH 2,0-10 airfoil.

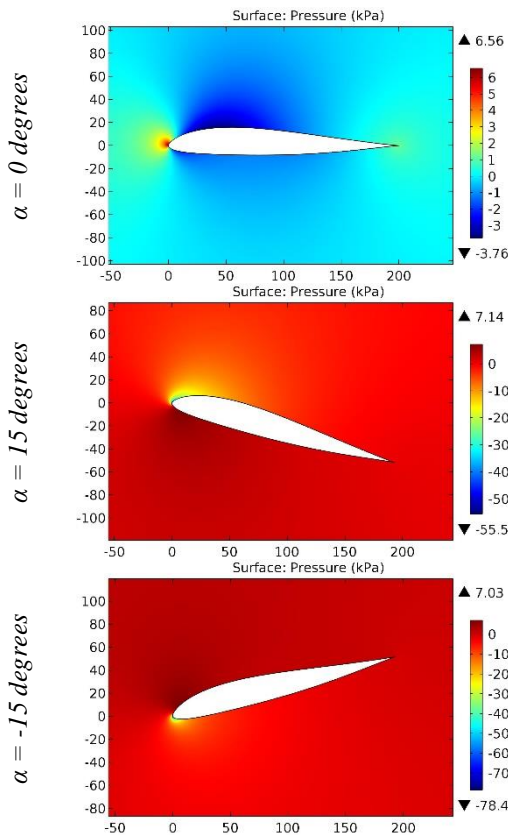


Figure 59. The pressure contours on the surfaces of the EH 2,0-12 airfoil.

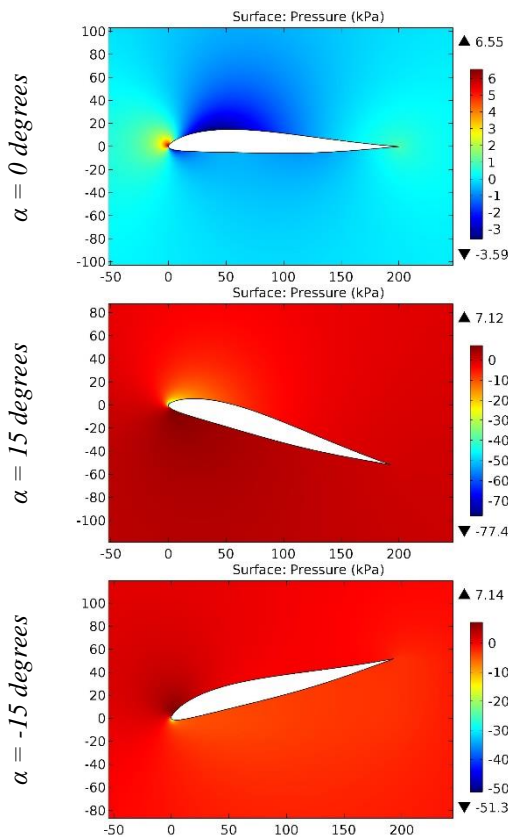


Figure 60. The pressure contours on the surfaces of the EH 2,5-10 airfoil.

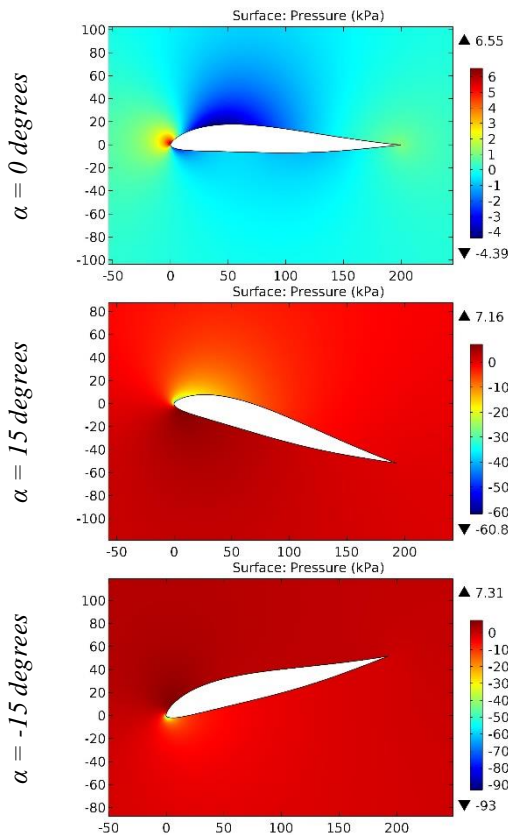


Figure 61. The pressure contours on the surfaces of the EH 3,0-12 airfoil.

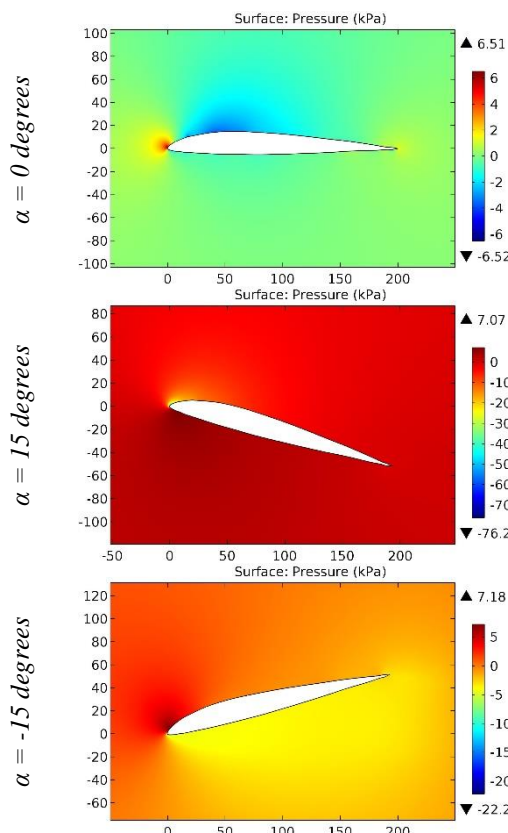


Figure 62. The pressure contours on the surfaces of the Eiffel 375 airfoil.

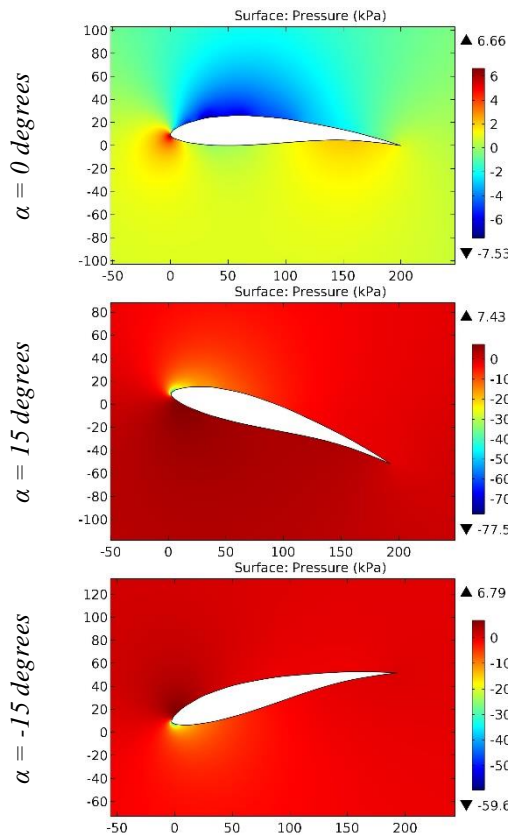


Figure 63. The pressure contours on the surfaces of the Eiffel 400 airfoil.

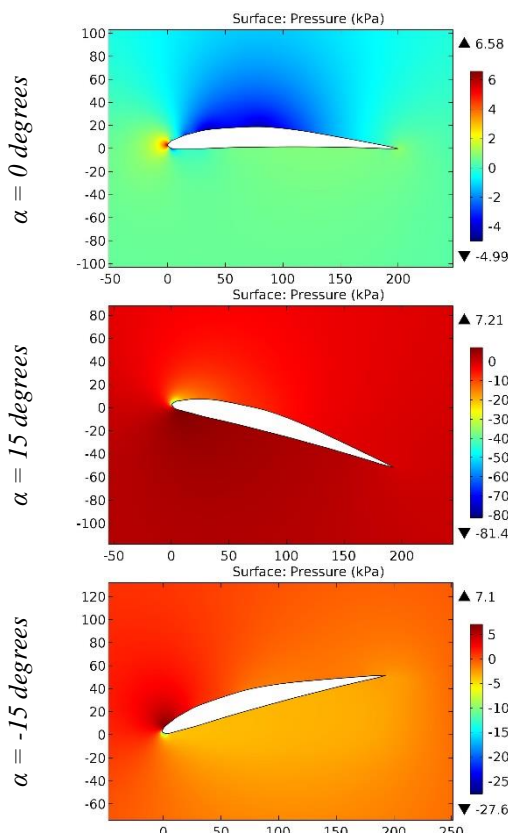


Figure 64. The pressure contours on the surfaces of the Eiffel 428 airfoil.

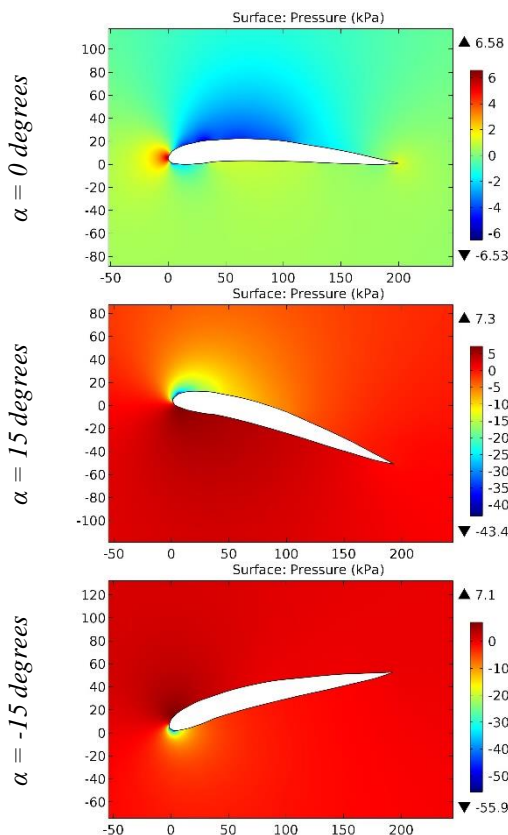


Figure 65. The pressure contours on the surfaces of the Eiffel 430 airfoil.

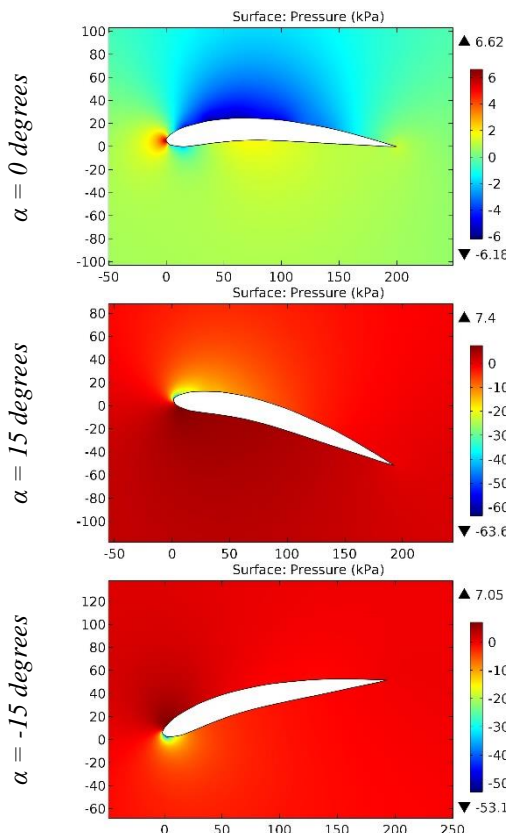


Figure 66. The pressure contours on the surfaces of the Eiffel 431 airfoil.

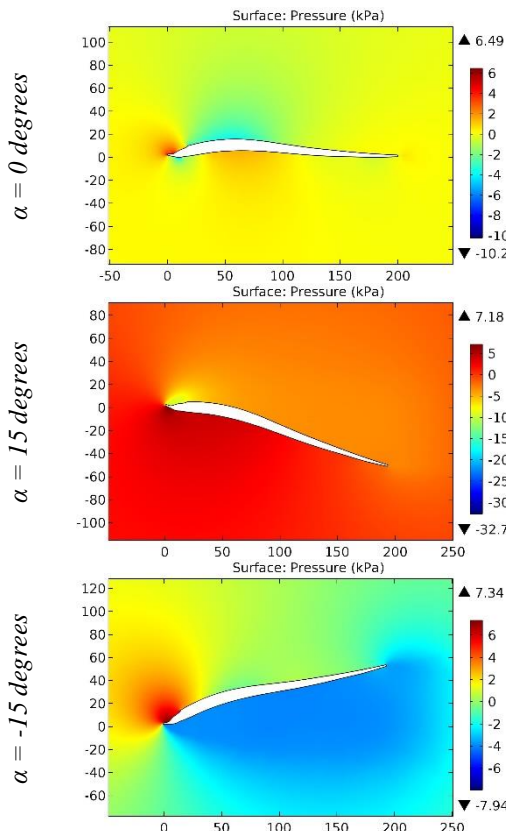


Figure 67. The pressure contours on the surfaces of the EIFFL32 airfoil.

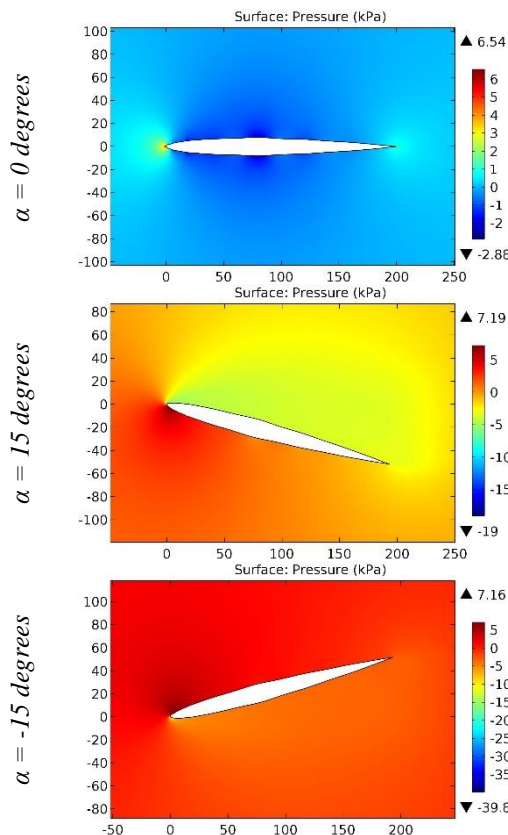


Figure 68. The pressure contours on the surfaces of the EIFFL338 airfoil.

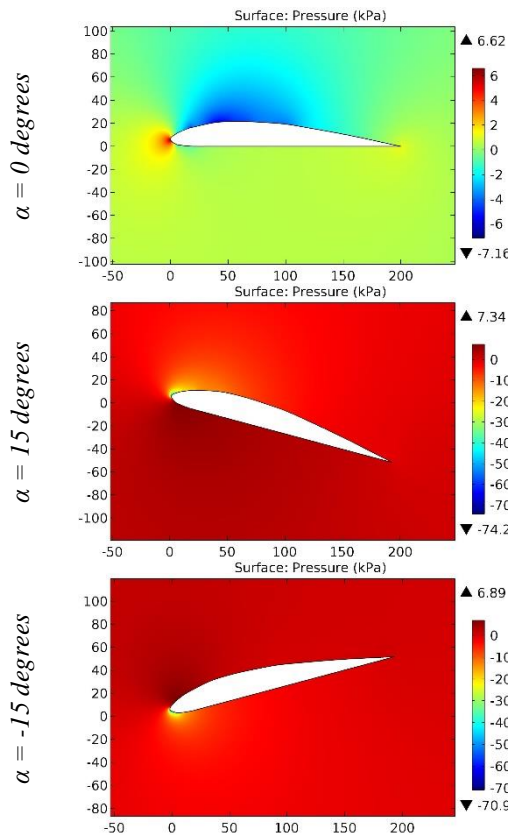


Figure 69. The pressure contours on the surfaces of the EIFFL359 airfoil.

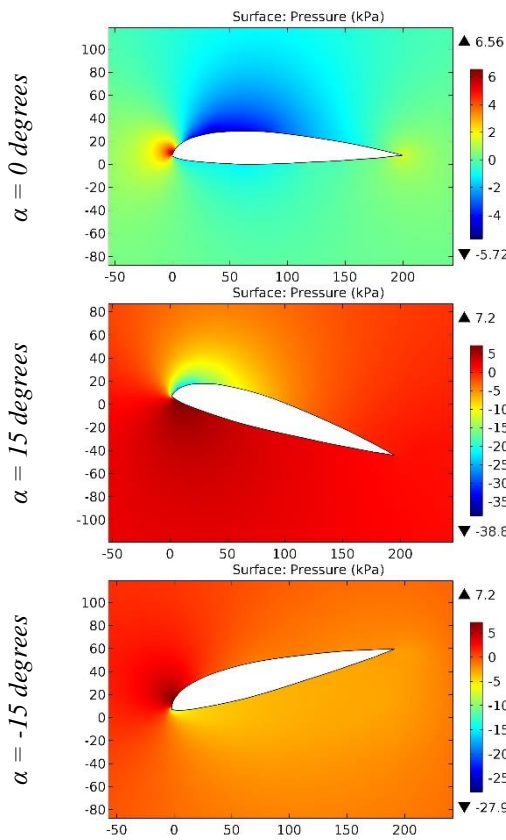


Figure 70. The pressure contours on the surfaces of the EIFFL371 airfoil.

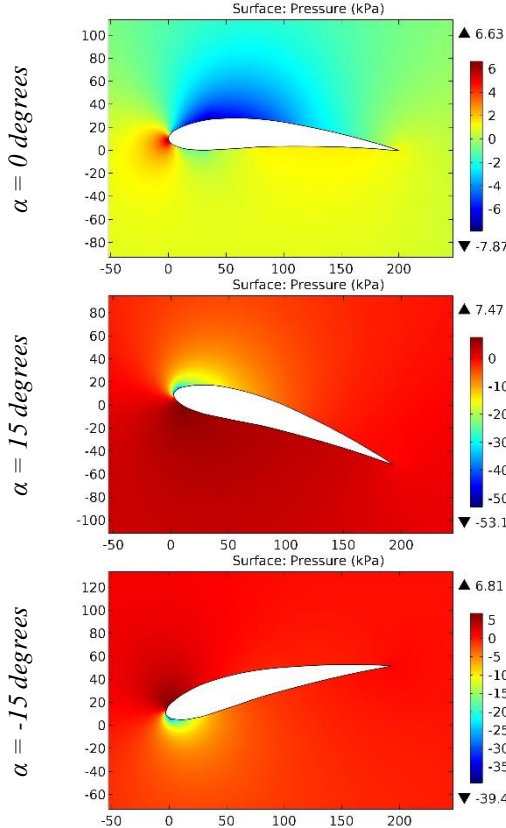


Figure 71. The pressure contours on the surfaces of the EIFFL385 airfoil.

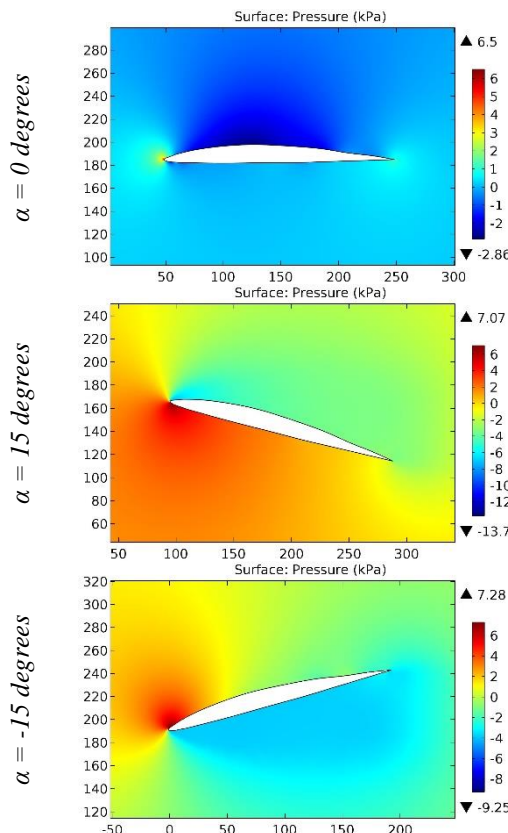


Figure 72. The pressure contours on the surfaces of the EIFFL389 airfoil.

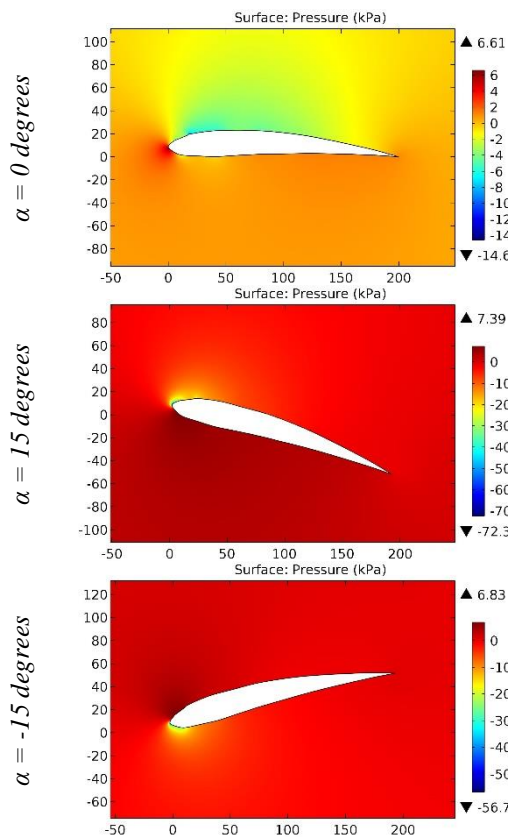


Figure 73. The pressure contours on the surfaces of the EIFFL437 airfoil.

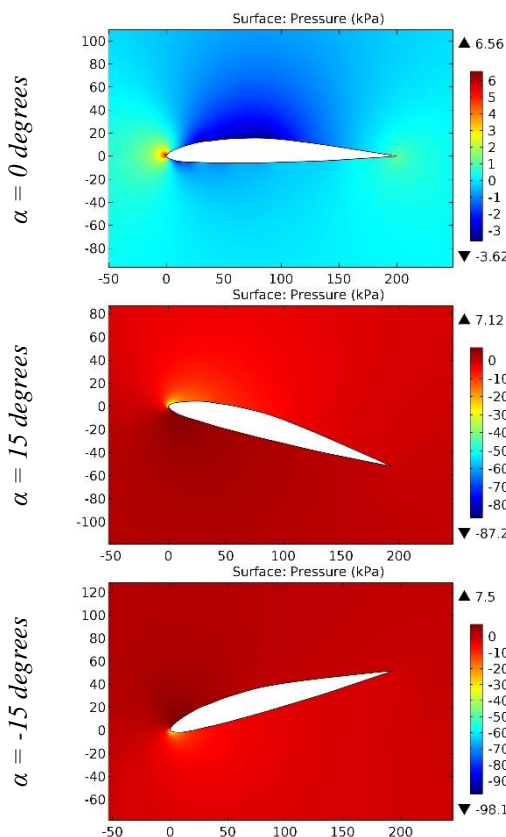


Figure 74. The pressure contours on the surfaces of the EL 25108 airfoil.

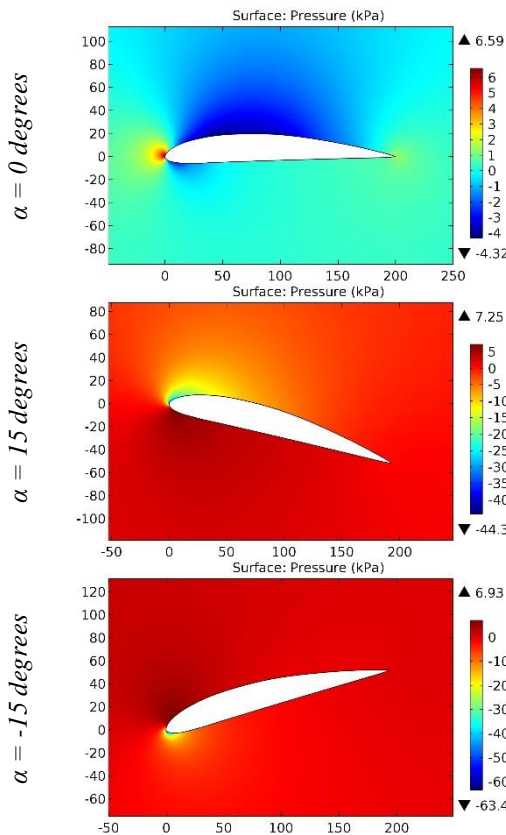


Figure 75. The pressure contours on the surfaces of the ELEK airfoil.

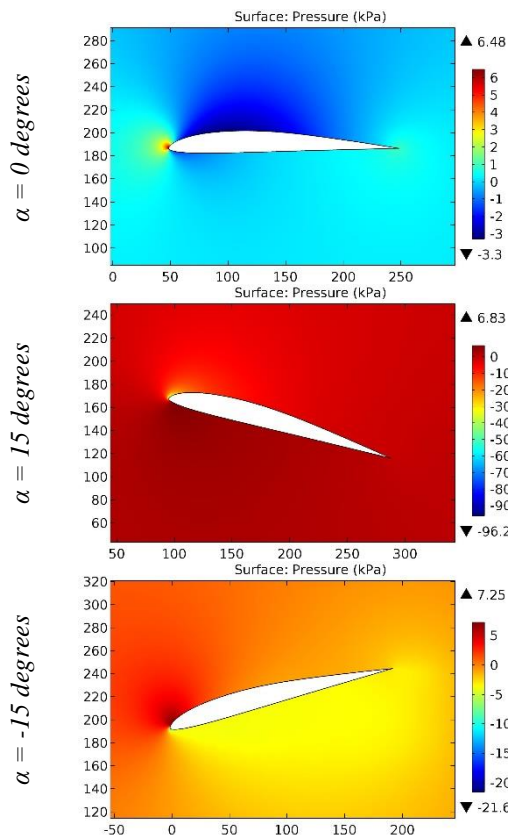


Figure 76. The pressure contours on the surfaces of the ELINA airfoil.

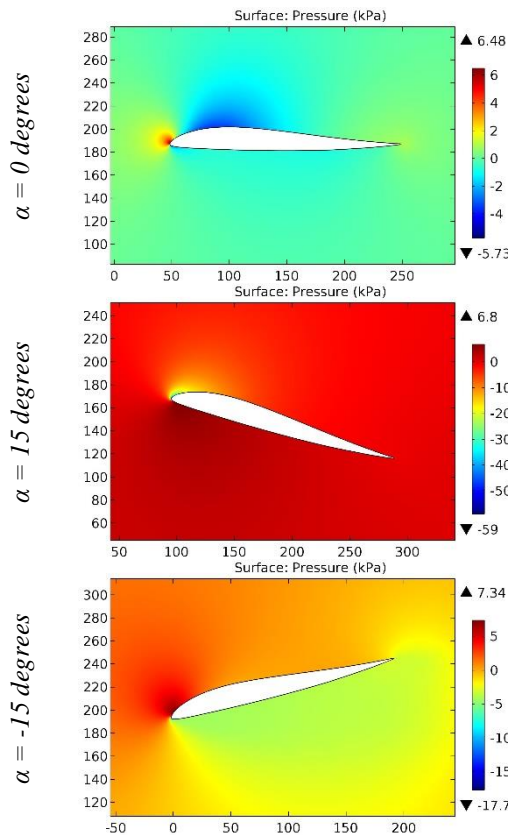


Figure 77. The pressure contours on the surfaces of the EMX-07 airfoil.

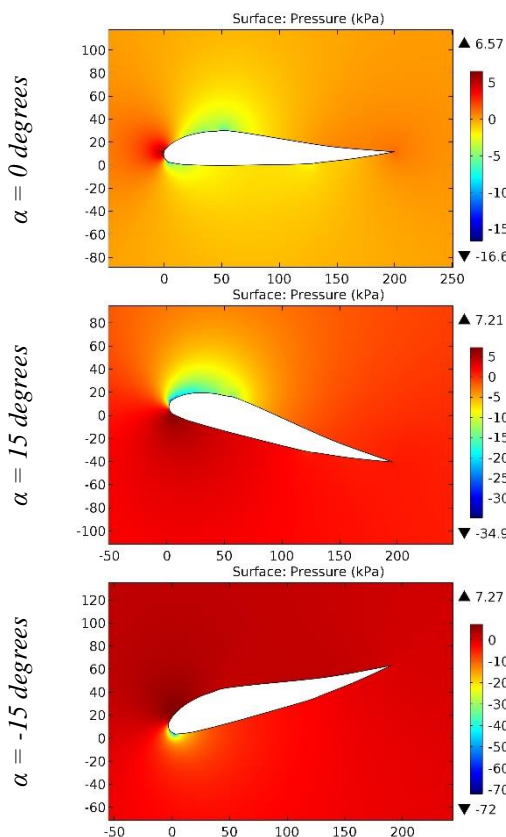


Figure 78. The pressure contours on the surfaces of the EPB - 1 airfoil.

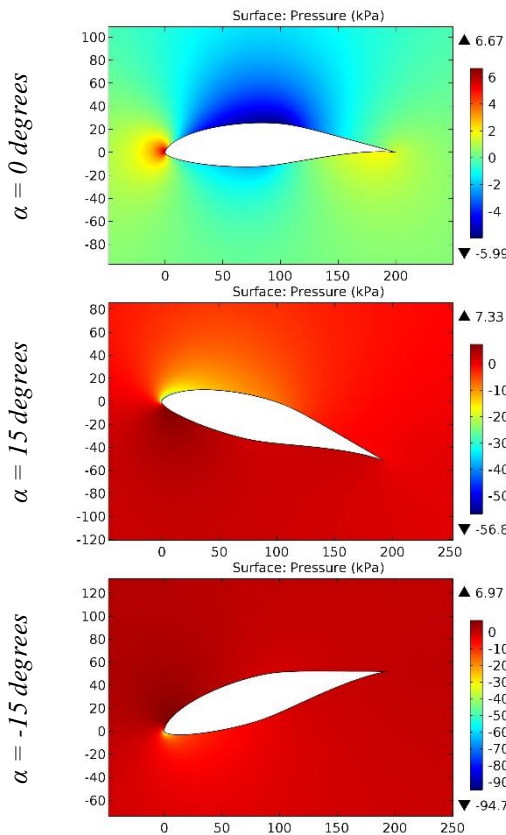


Figure 79. The pressure contours on the surfaces of the EPPLER 1098 airfoil.

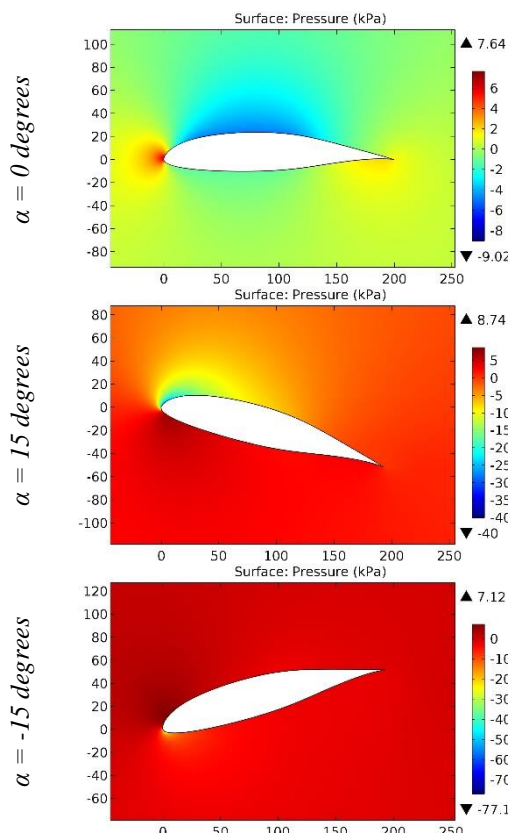


Figure 80. The pressure contours on the surfaces of the EPPLER 1200 airfoil.

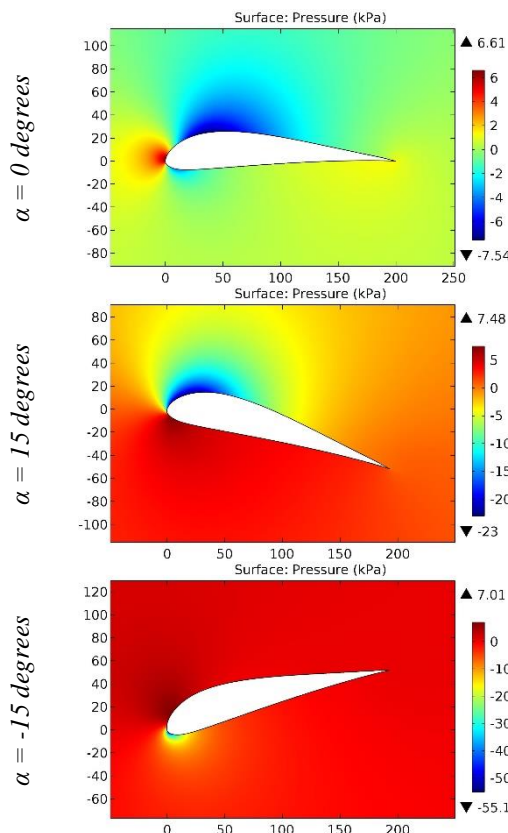


Figure 81. The pressure contours on the surfaces of the EPPLER 1210 airfoil.

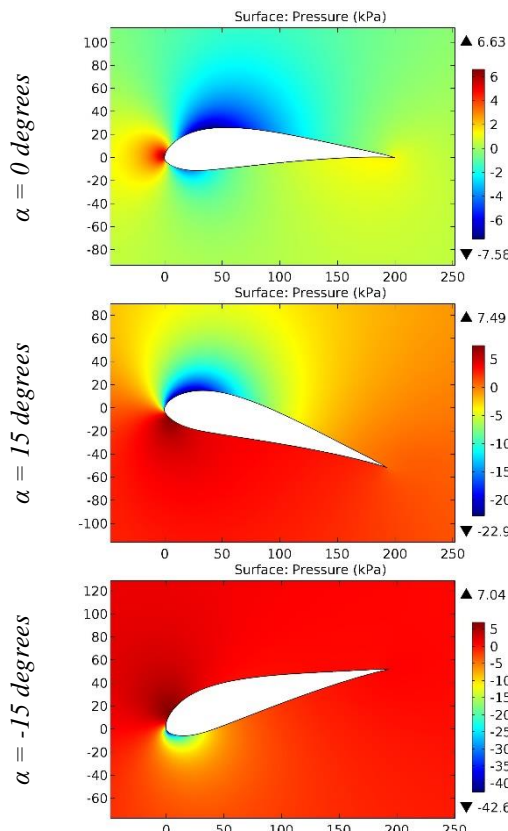


Figure 82. The pressure contours on the surfaces of the EPPLER 1211 airfoil.

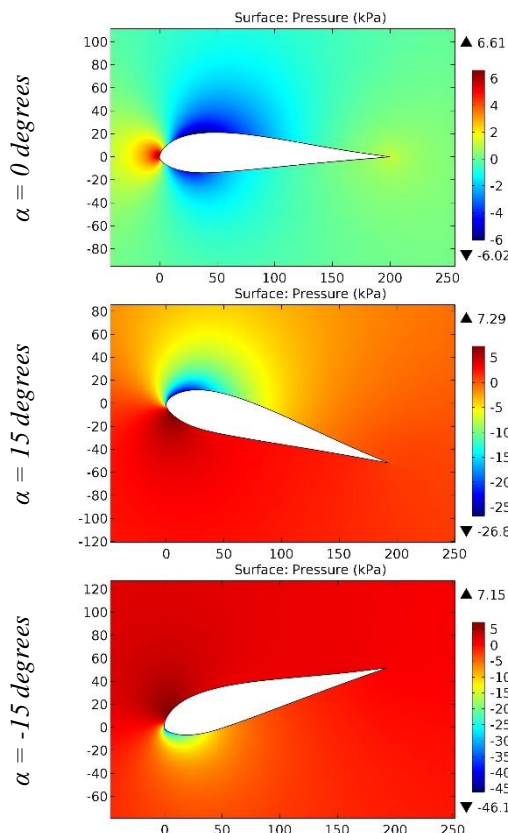


Figure 83. The pressure contours on the surfaces of the EPPLER 1213 airfoil.

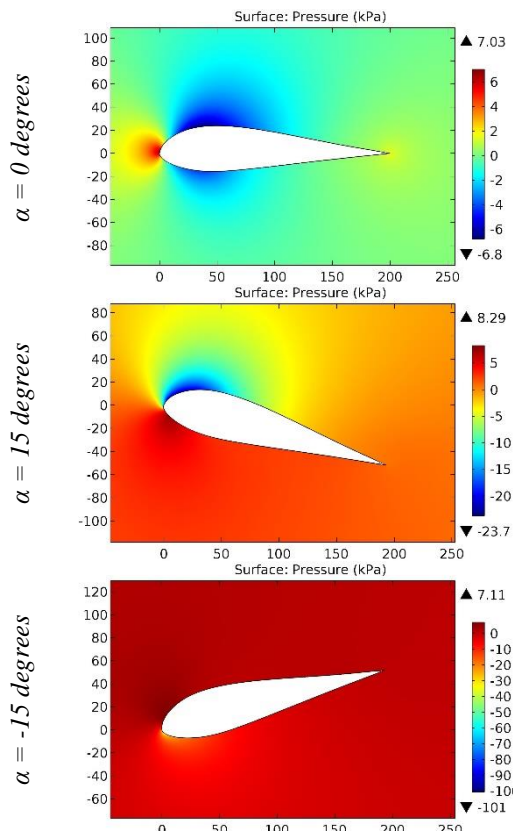


Figure 84. The pressure contours on the surfaces of the EPPLER 1214 airfoil.

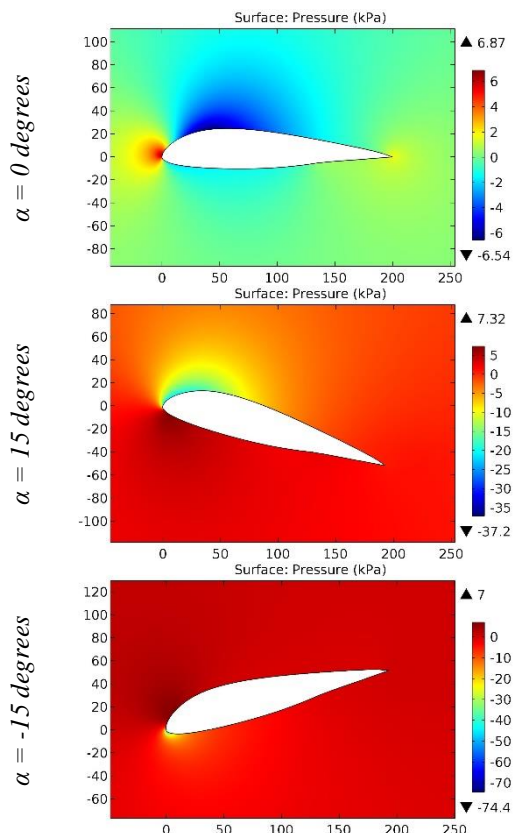


Figure 85. The pressure contours on the surfaces of the EPPLER 1230 airfoil.

ISRA (India) = 6.317	SIS (USA) = 0.912	ICV (Poland) = 6.630
ISI (Dubai, UAE) = 1.582	РИНЦ (Russia) = 3.939	PIF (India) = 1.940
GIF (Australia) = 0.564	ESJI (KZ) = 9.035	IBI (India) = 4.260
JIF = 1.500	SJIF (Morocco) = 7.184	OAJI (USA) = 0.350

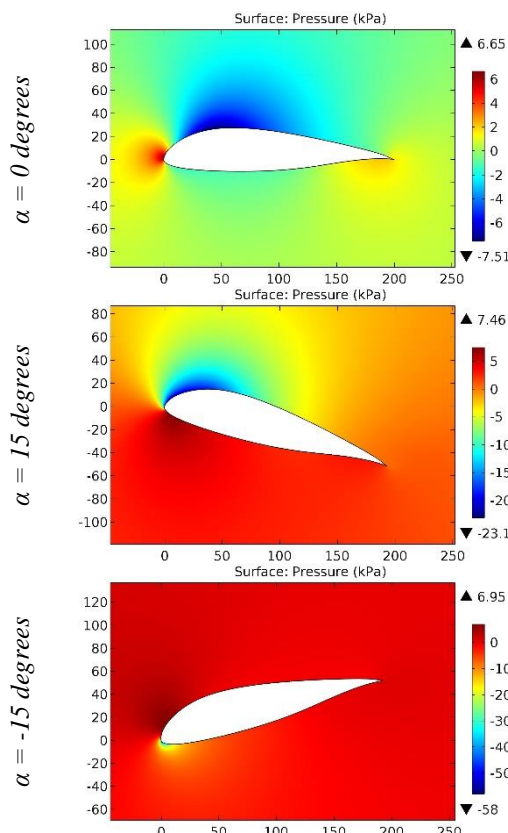


Figure 86. The pressure contours on the surfaces of the EPPLER 1233 airfoil.

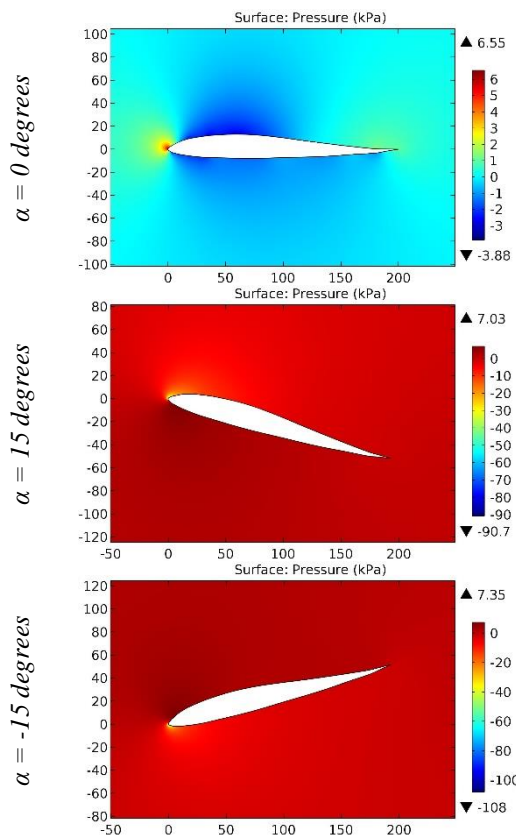


Figure 87. The pressure contours on the surfaces of the Eppler 166 airfoil.

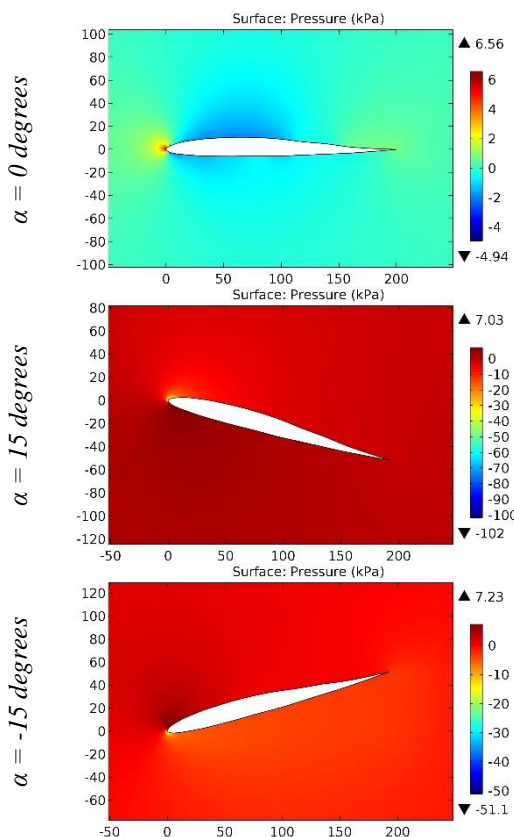


Figure 88. The pressure contours on the surfaces of the Eppler 189 airfoil.

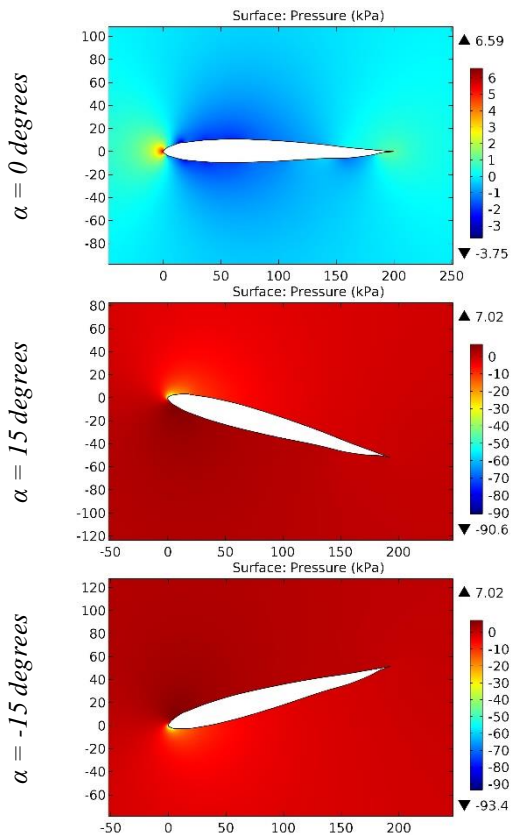


Figure 89. The pressure contours on the surfaces of the Eppler 228 airfoil.

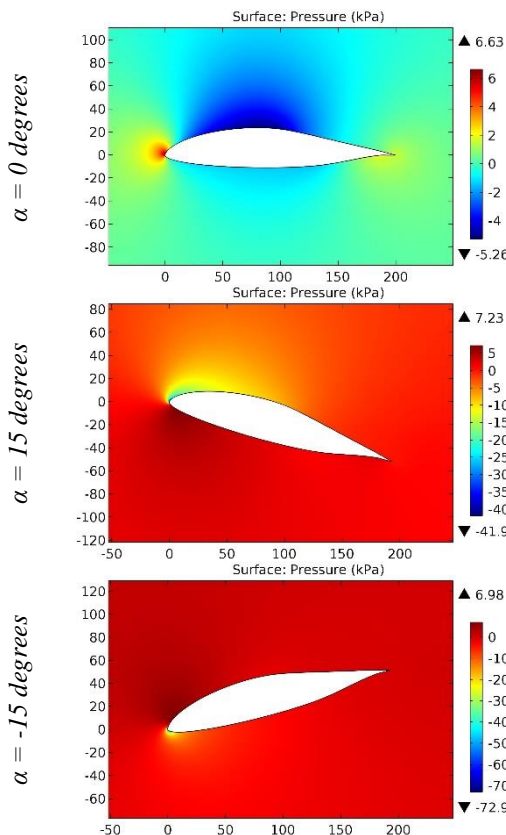


Figure 90. The pressure contours on the surfaces of the EPPLER 266 airfoil.

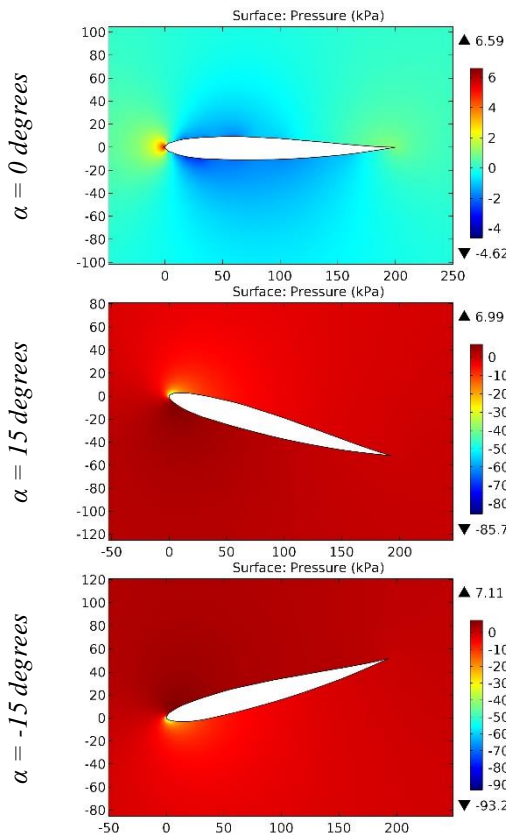


Figure 91. The pressure contours on the surfaces of the Eppler 270 airfoil.

ISRA (India) = 6.317	SIS (USA) = 0.912	ICV (Poland) = 6.630
ISI (Dubai, UAE) = 1.582	РИНЦ (Russia) = 3.939	PIF (India) = 1.940
GIF (Australia) = 0.564	ESJI (KZ) = 9.035	IBI (India) = 4.260
JIF = 1.500	SJIF (Morocco) = 7.184	OAJI (USA) = 0.350

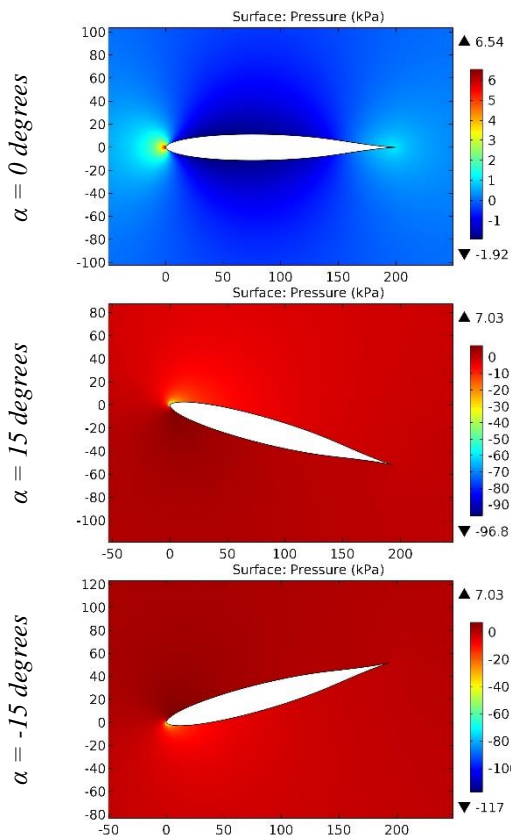


Figure 92. The pressure contours on the surfaces of the EPPLER 297 airfoil.

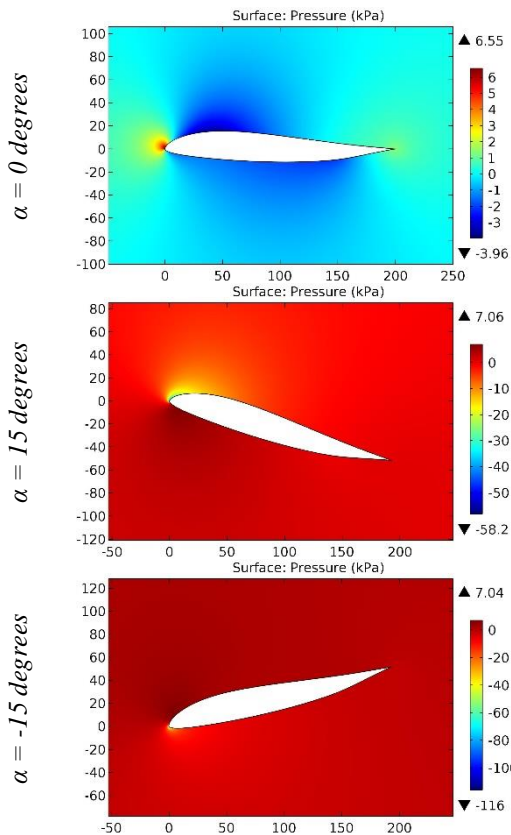


Figure 93. The pressure contours on the surfaces of the EPPLER 325 airfoil.

ISRA (India) = 6.317	SIS (USA) = 0.912	ICV (Poland) = 6.630
ISI (Dubai, UAE) = 1.582	РИНЦ (Russia) = 3.939	PIF (India) = 1.940
GIF (Australia) = 0.564	ESJI (KZ) = 9.035	IBI (India) = 4.260
JIF = 1.500	SJIF (Morocco) = 7.184	OAJI (USA) = 0.350

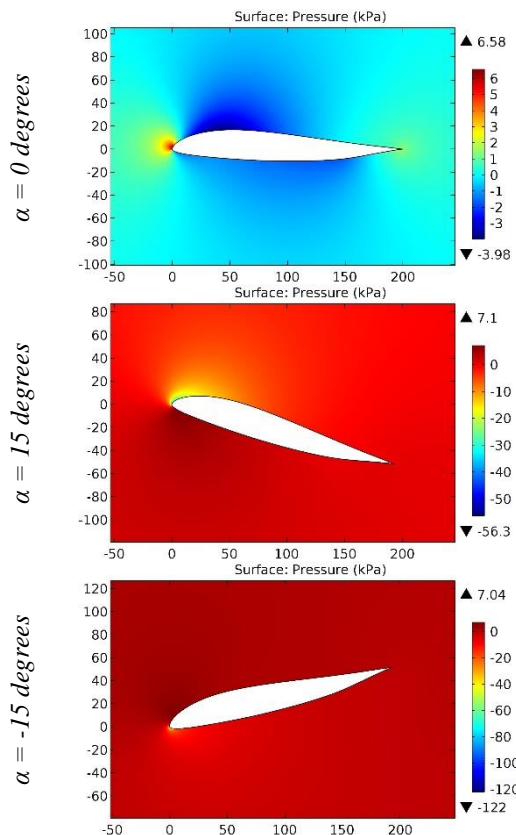


Figure 94. The pressure contours on the surfaces of the EPPLER 326 airfoil.

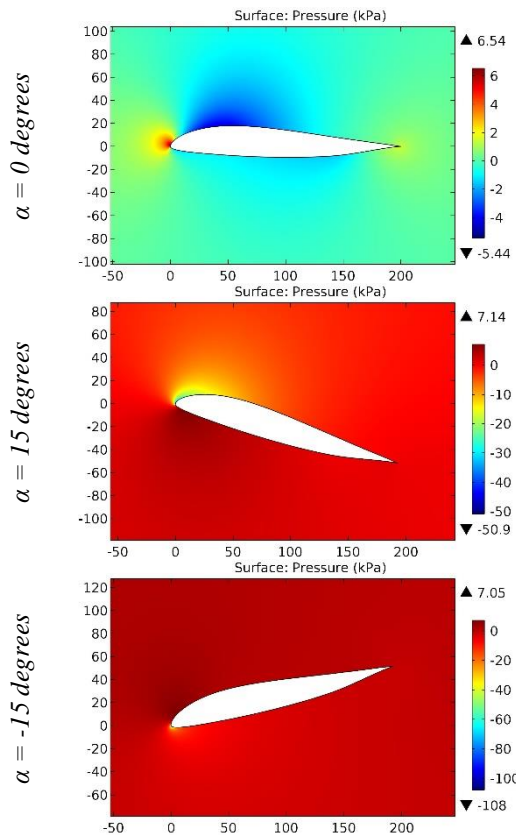


Figure 95. The pressure contours on the surfaces of the EPPLER 327 airfoil.

ISRA (India) = 6.317	SIS (USA) = 0.912	ICV (Poland) = 6.630
ISI (Dubai, UAE) = 1.582	РИНЦ (Russia) = 3.939	PIF (India) = 1.940
GIF (Australia) = 0.564	ESJI (KZ) = 9.035	IBI (India) = 4.260
JIF = 1.500	SJIF (Morocco) = 7.184	OAJI (USA) = 0.350

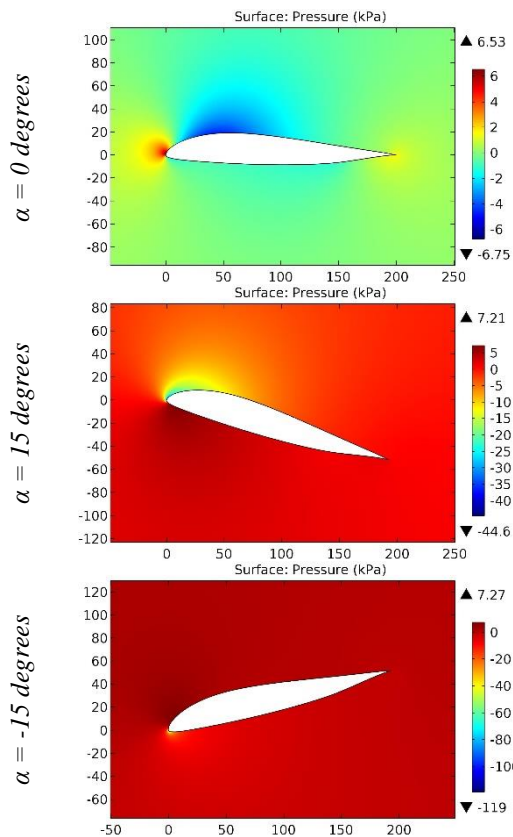


Figure 96. The pressure contours on the surfaces of the EPPLER 328 airfoil.

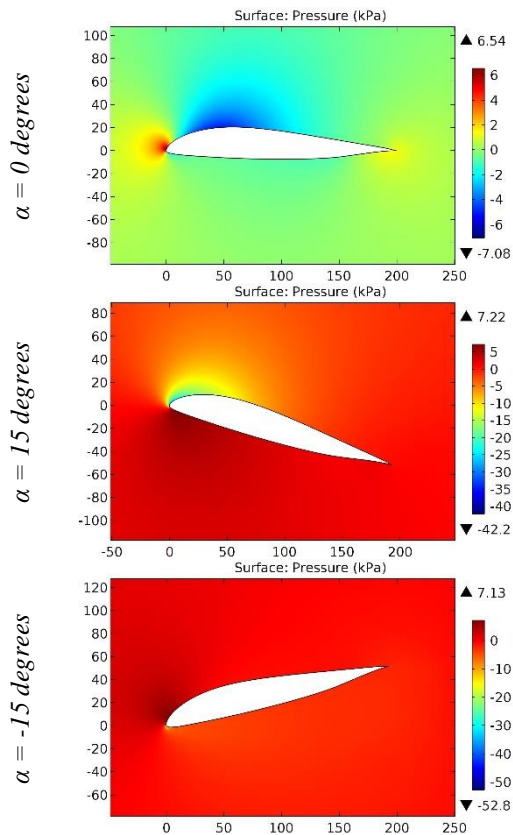


Figure 97. The pressure contours on the surfaces of the EPPLER 329 airfoil.

ISRA (India) = 6.317	SIS (USA) = 0.912	ICV (Poland) = 6.630
ISI (Dubai, UAE) = 1.582	РИНЦ (Russia) = 3.939	PIF (India) = 1.940
GIF (Australia) = 0.564	ESJI (KZ) = 9.035	IBI (India) = 4.260
JIF = 1.500	SJIF (Morocco) = 7.184	OAJI (USA) = 0.350

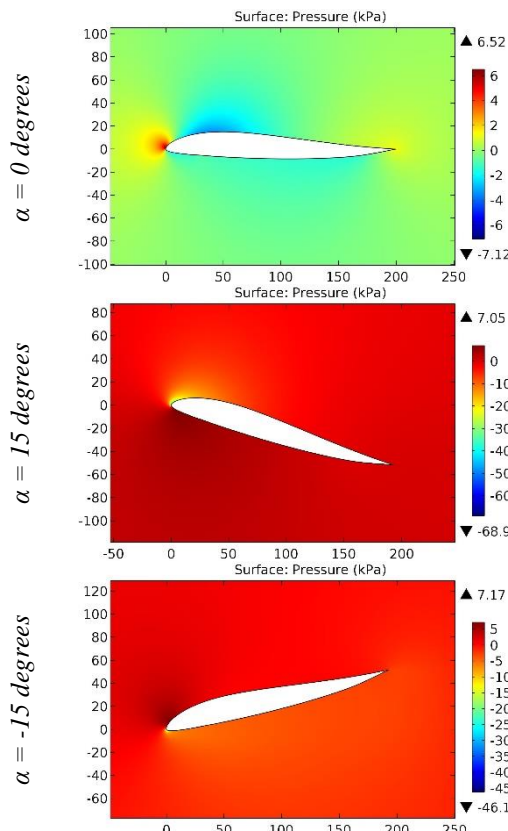


Figure 98. The pressure contours on the surfaces of the EPPLER 330 airfoil.

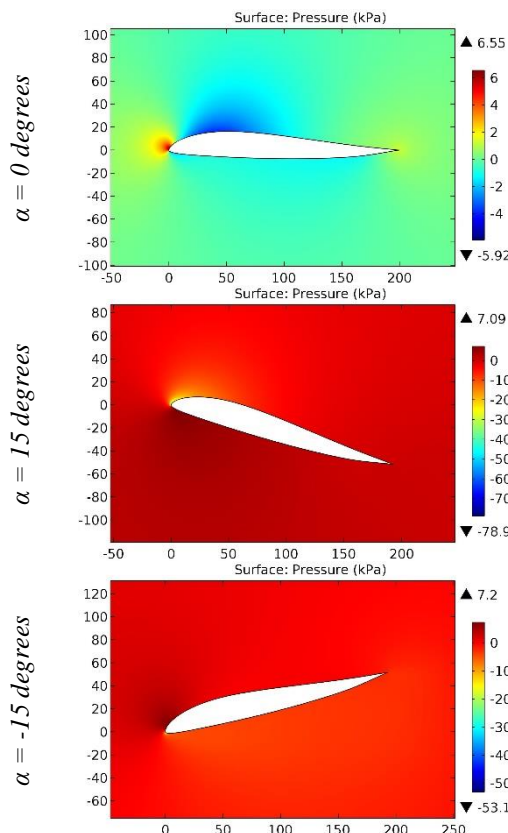


Figure 99. The pressure contours on the surfaces of the EPPLER 331 airfoil.

ISRA (India) = 6.317	SIS (USA) = 0.912	ICV (Poland) = 6.630
ISI (Dubai, UAE) = 1.582	РИНЦ (Russia) = 3.939	PIF (India) = 1.940
GIF (Australia) = 0.564	ESJI (KZ) = 9.035	IBI (India) = 4.260
JIF = 1.500	SJIF (Morocco) = 7.184	OAJI (USA) = 0.350

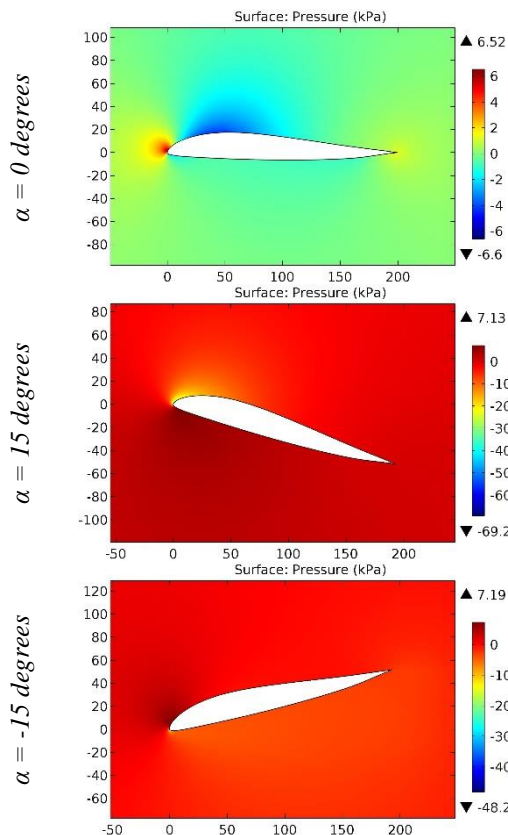


Figure 100. The pressure contours on the surfaces of the EPPLER 332 airfoil.

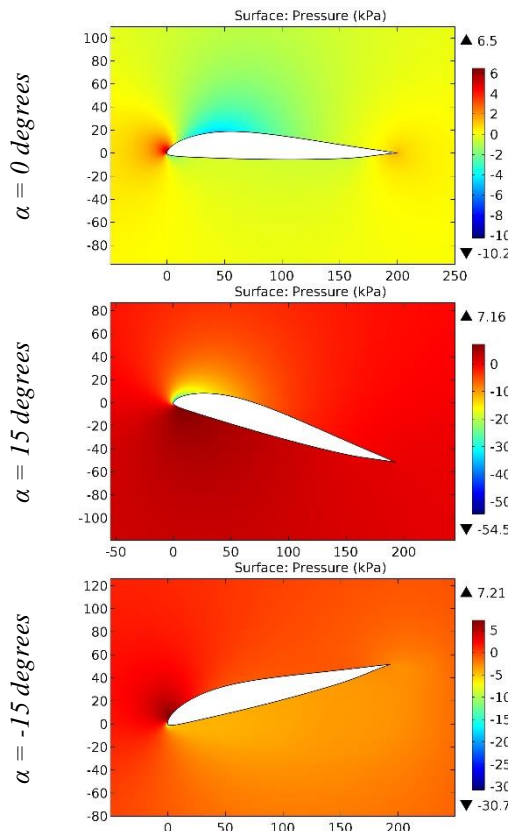


Figure 101. The pressure contours on the surfaces of the EPPLER 333 airfoil.

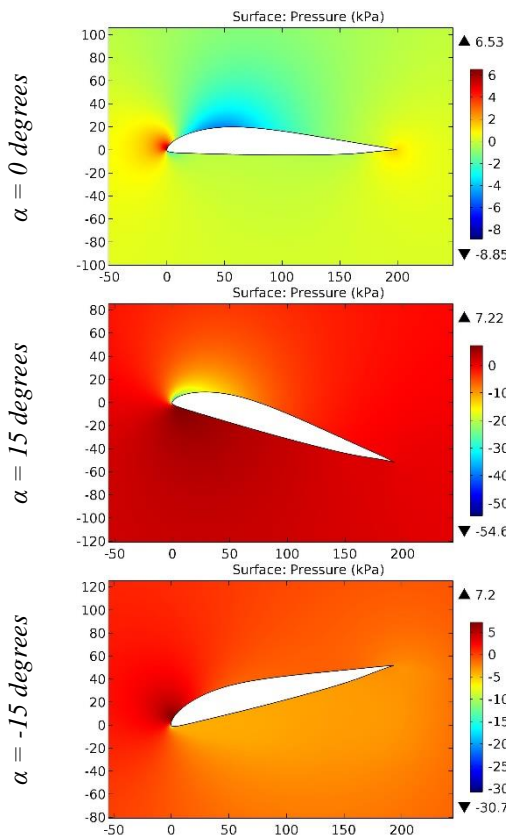


Figure 102. The pressure contours on the surfaces of the EPPLER 334 airfoil.

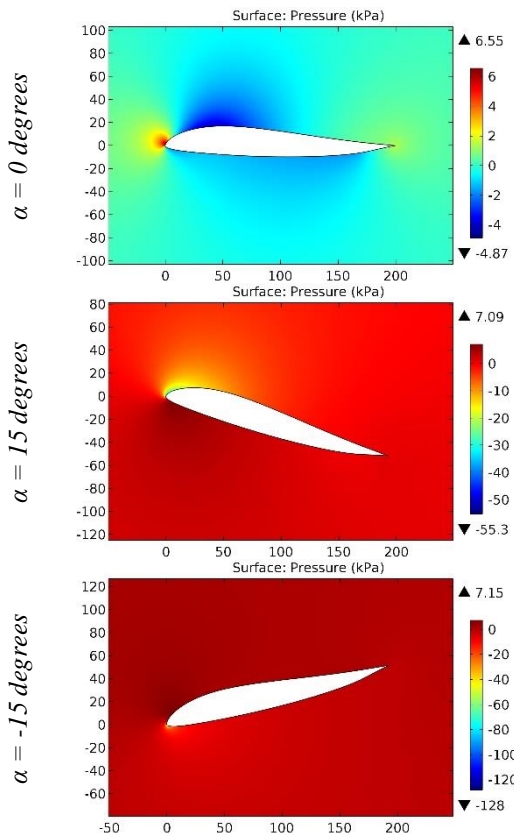


Figure 103. The pressure contours on the surfaces of the EPPLER 335 airfoil.

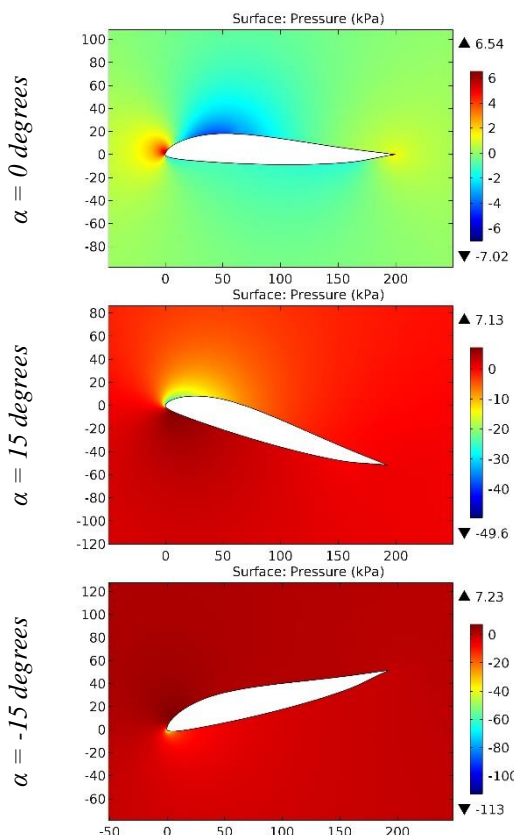


Figure 104. The pressure contours on the surfaces of the EPPLER 336 airfoil.

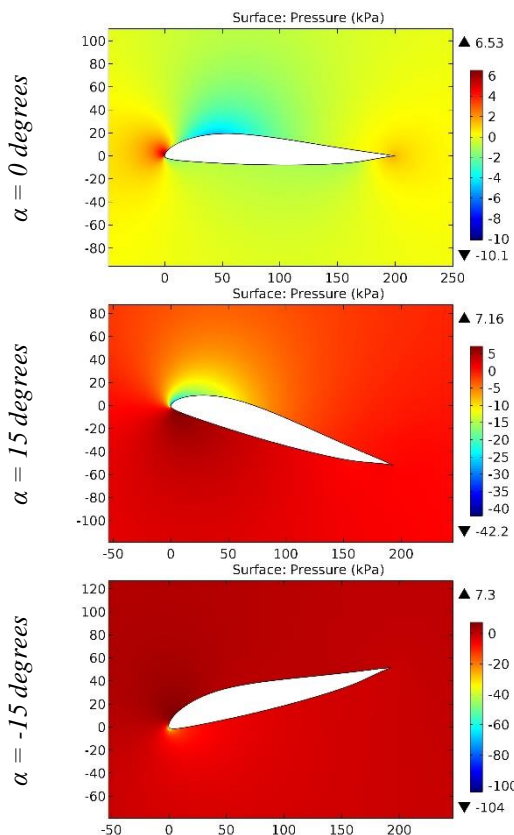


Figure 105. The pressure contours on the surfaces of the EPPLER 337 airfoil.

ISRA (India)	= 6.317	SIS (USA)	= 0.912	ICV (Poland)	= 6.630
ISI (Dubai, UAE)	= 1.582	РИНЦ (Russia)	= 3.939	PIF (India)	= 1.940
GIF (Australia)	= 0.564	ESJI (KZ)	= 9.035	IBI (India)	= 4.260
JIF	= 1.500	SJIF (Morocco)	= 7.184	OAJI (USA)	= 0.350

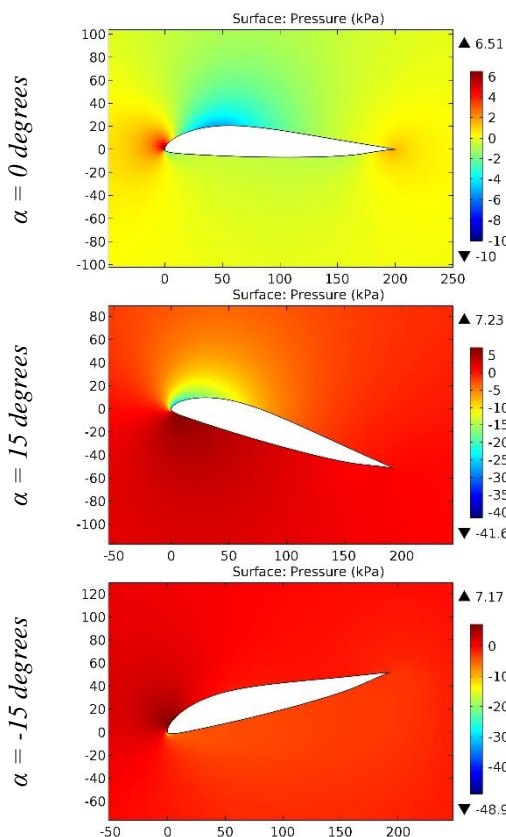


Figure 106. The pressure contours on the surfaces of the EPPLER 338 airfoil.

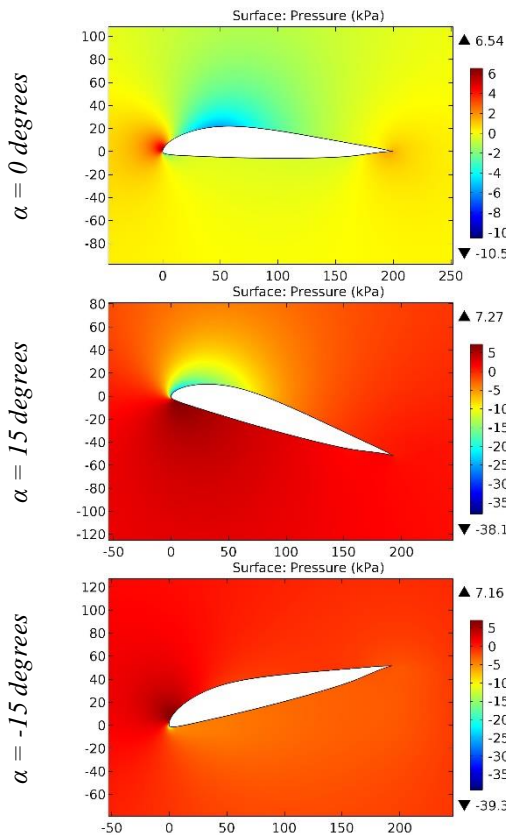


Figure 107. The pressure contours on the surfaces of the EPPLER 339 airfoil.

ISRA (India)	= 6.317	SIS (USA)	= 0.912	ICV (Poland)	= 6.630
ISI (Dubai, UAE)	= 1.582	РИНЦ (Russia)	= 3.939	PIF (India)	= 1.940
GIF (Australia)	= 0.564	ESJI (KZ)	= 9.035	IBI (India)	= 4.260
JIF	= 1.500	SJIF (Morocco)	= 7.184	OAJI (USA)	= 0.350

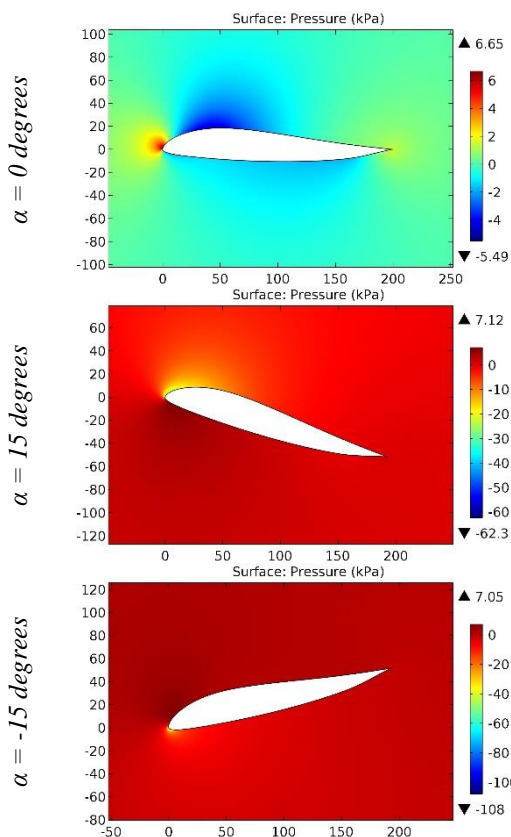


Figure 108. The pressure contours on the surfaces of the EPPLER 340 airfoil.

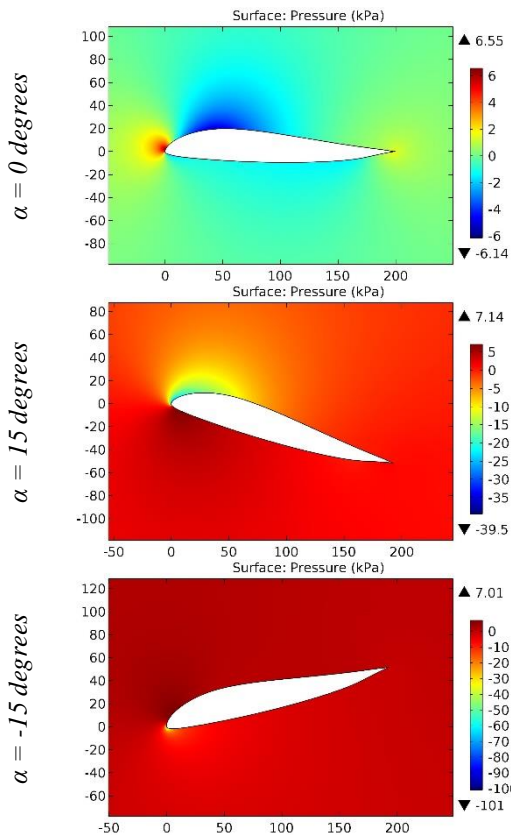


Figure 109. The pressure contours on the surfaces of the EPPLER 341 airfoil.

ISRA (India) = 6.317	SIS (USA) = 0.912	ICV (Poland) = 6.630
ISI (Dubai, UAE) = 1.582	РИНЦ (Russia) = 3.939	PIF (India) = 1.940
GIF (Australia) = 0.564	ESJI (KZ) = 9.035	IBI (India) = 4.260
JIF = 1.500	SJIF (Morocco) = 7.184	OAJI (USA) = 0.350

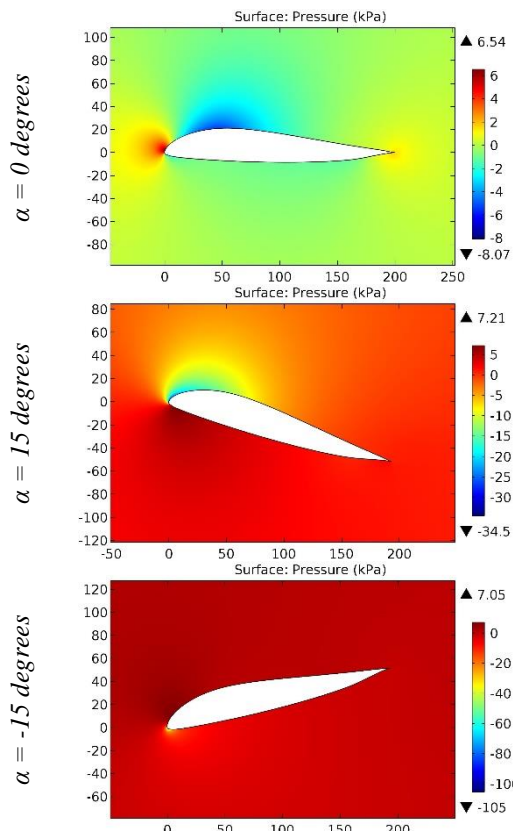


Figure 110. The pressure contours on the surfaces of the EPPLER 342 airfoil.

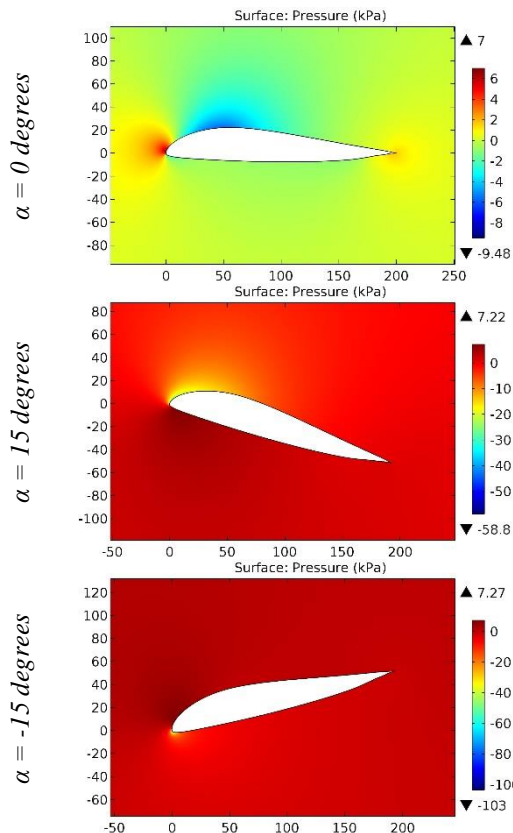


Figure 111. The pressure contours on the surfaces of the EPPLER 343 airfoil.

ISRA (India) = 6.317	SIS (USA) = 0.912	ICV (Poland) = 6.630
ISI (Dubai, UAE) = 1.582	РИНЦ (Russia) = 3.939	PIF (India) = 1.940
GIF (Australia) = 0.564	ESJI (KZ) = 9.035	IBI (India) = 4.260
JIF = 1.500	SJIF (Morocco) = 7.184	OAJI (USA) = 0.350

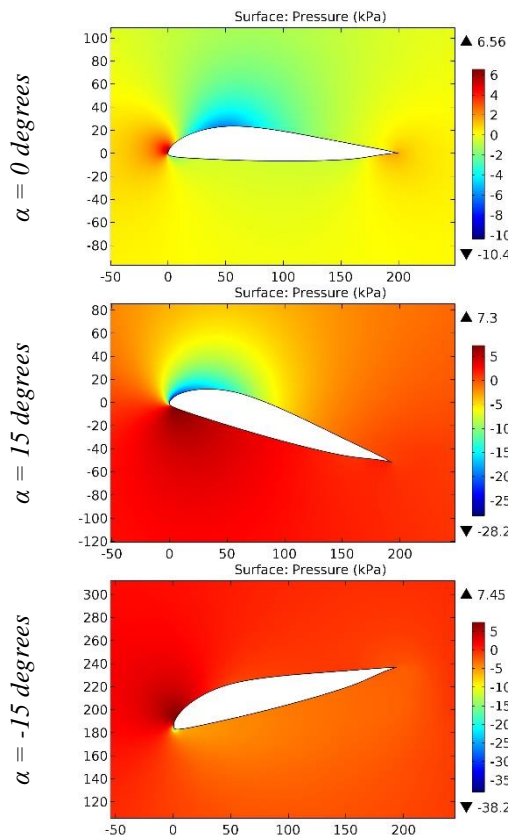


Figure 112. The pressure contours on the surfaces of the EPPLER 344 airfoil.

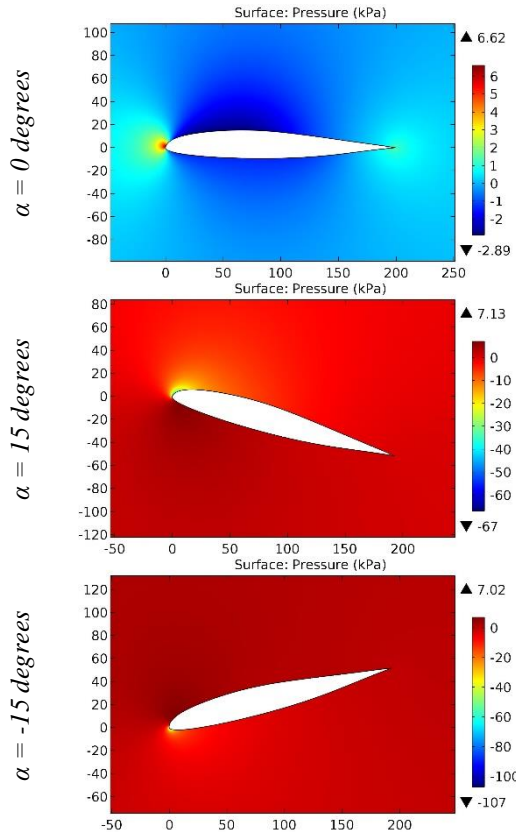


Figure 113. The pressure contours on the surfaces of the EPPLER 360 airfoil.

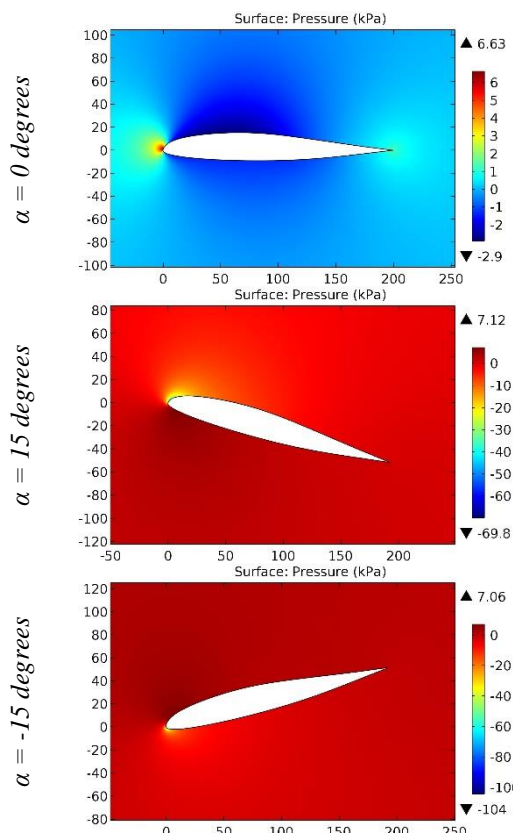


Figure 114. The pressure contours on the surfaces of the EPPLER 361 airfoil.

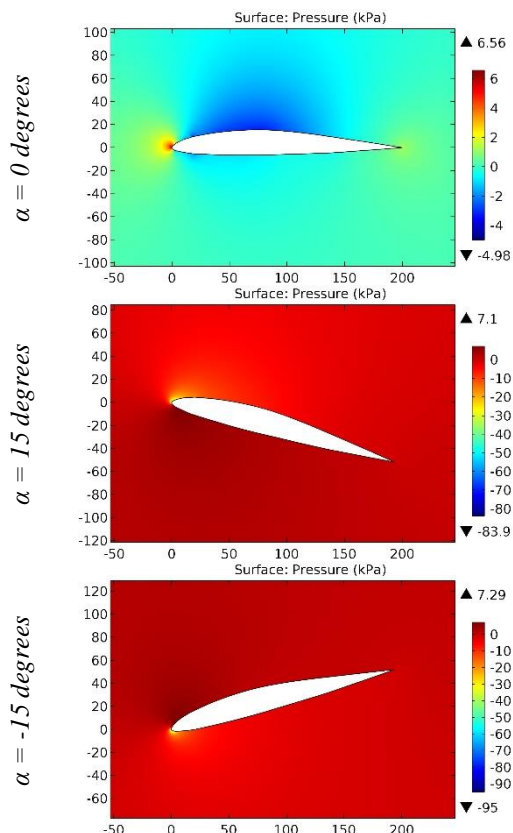


Figure 115. The pressure contours on the surfaces of the Eppler 375 airfoil.

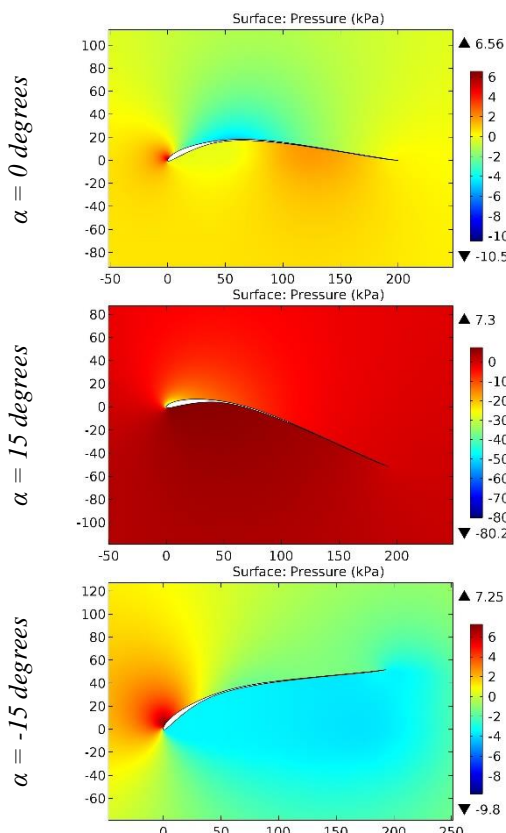


Figure 116. The pressure contours on the surfaces of the EPPLER 376 airfoil.

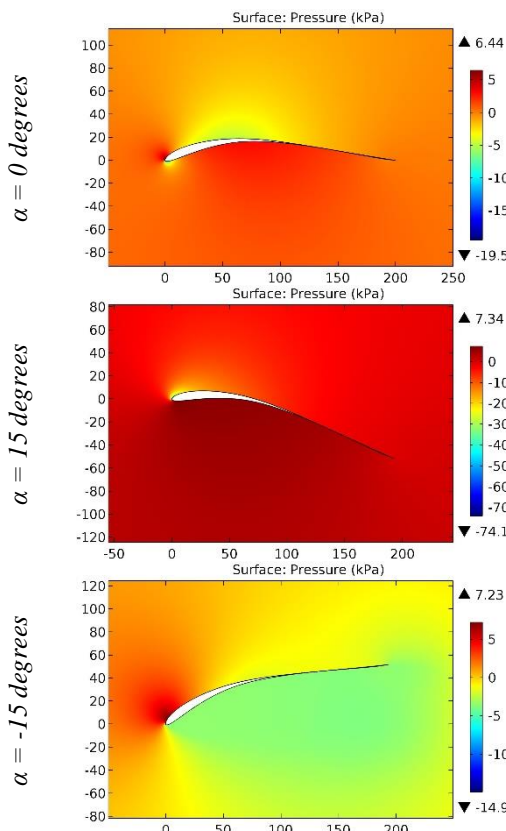


Figure 117. The pressure contours on the surfaces of the EPPLER 377 airfoil.

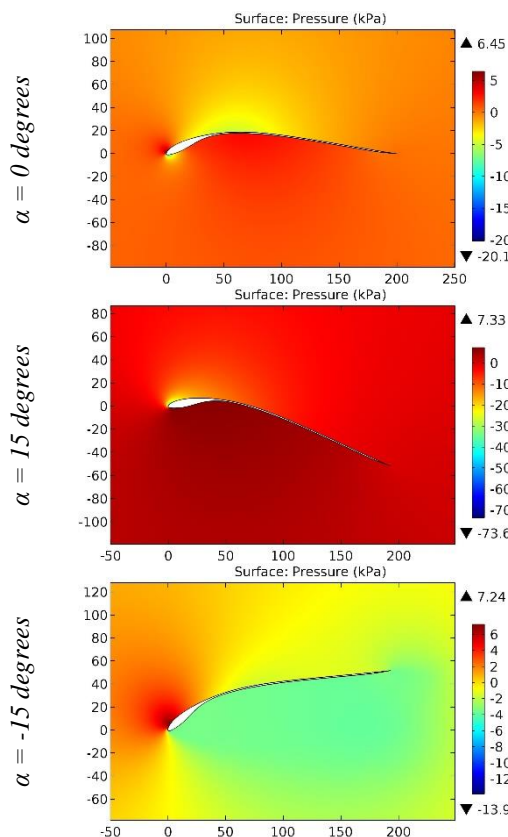


Figure 118. The pressure contours on the surfaces of the EPPLER 377 (MODIFIED) airfoil.

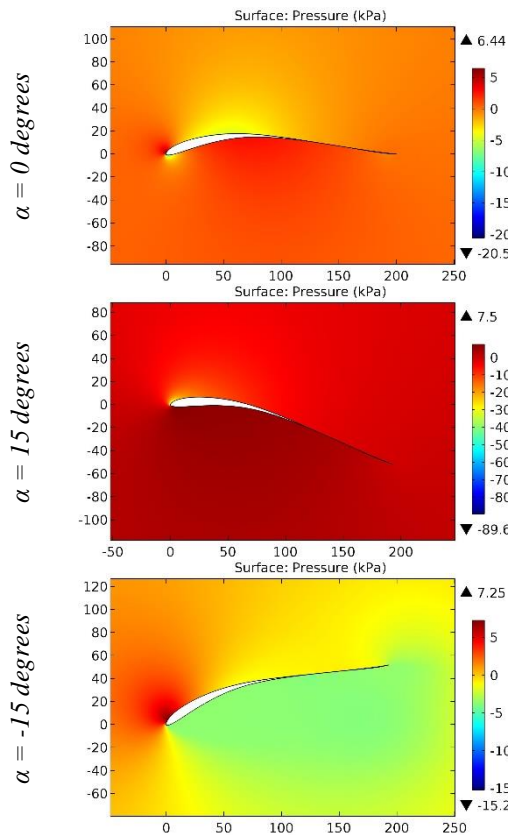


Figure 119. The pressure contours on the surfaces of the EPPLER 378 airfoil.

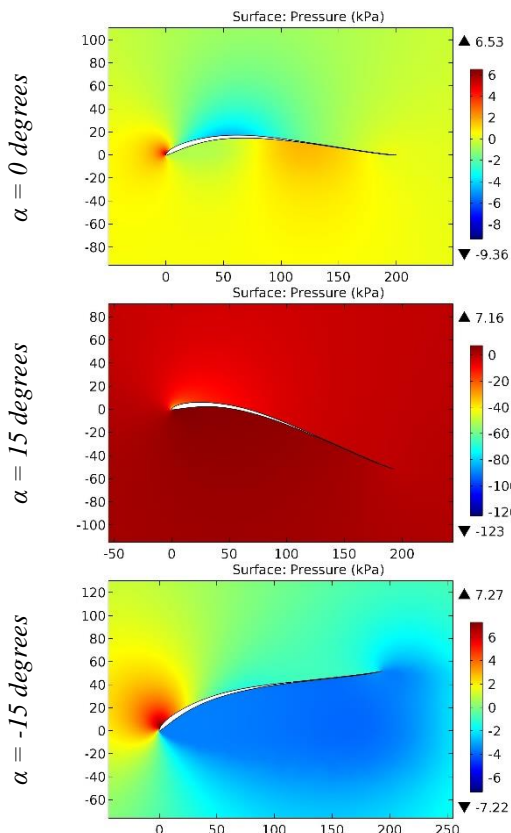


Figure 120. The pressure contours on the surfaces of the EPPLER 379 airfoil.

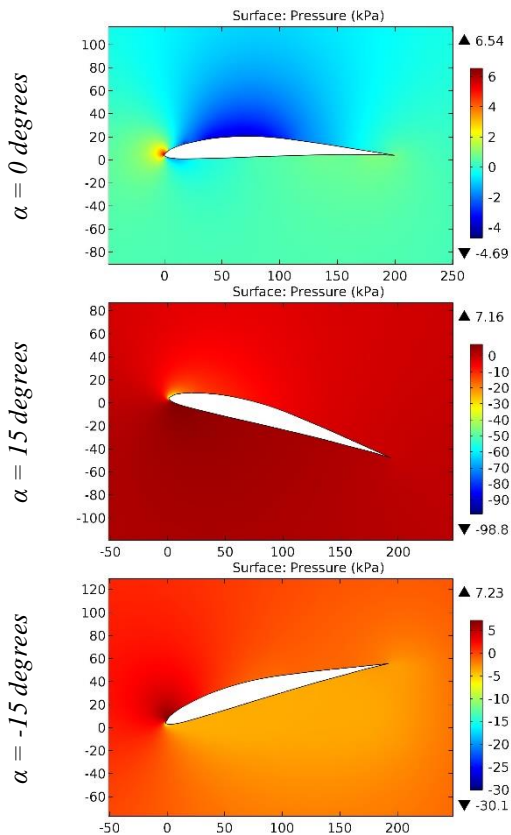


Figure 121. The pressure contours on the surfaces of the Eppler 387 airfoil.

ISRA (India) = 6.317	SIS (USA) = 0.912	ICV (Poland) = 6.630
ISI (Dubai, UAE) = 1.582	РИНЦ (Russia) = 3.939	PIF (India) = 1.940
GIF (Australia) = 0.564	ESJI (KZ) = 9.035	IBI (India) = 4.260
JIF = 1.500	SJIF (Morocco) = 7.184	OAJI (USA) = 0.350

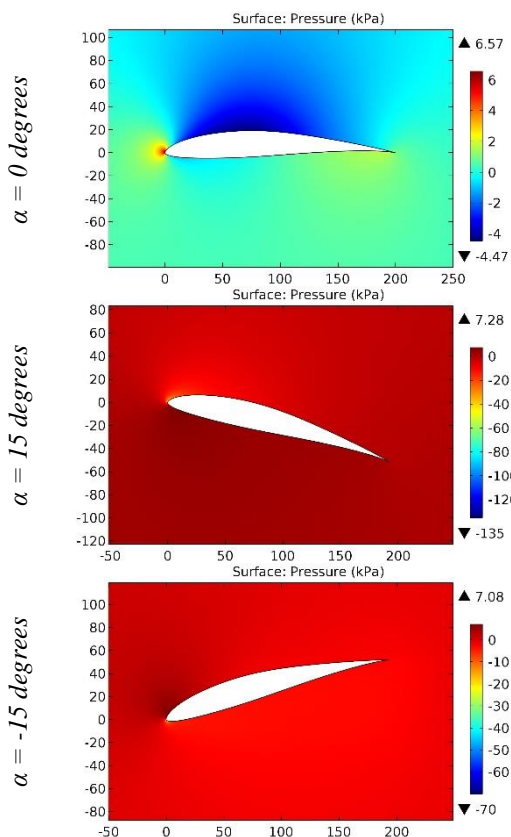


Figure 122. The pressure contours on the surfaces of the EPPLER 393 airfoil.

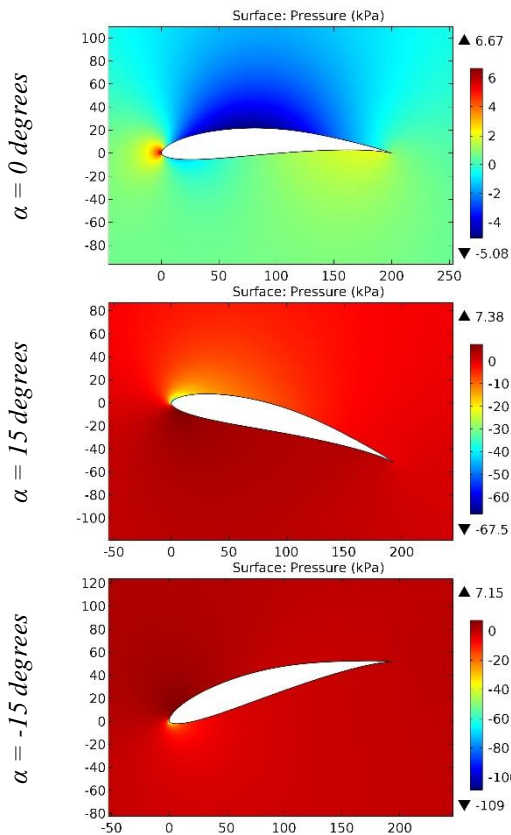


Figure 123. The pressure contours on the surfaces of the EPPLER 395 airfoil.

Impact Factor:

ISRA (India) = **6.317**
ISI (Dubai, UAE) = **1.582**
GIF (Australia) = **0.564**
JIF = **1.500**

SIS (USA) = **0.912**
РИНЦ (Russia) = **3.939**
ESJI (KZ) = **9.035**
SJIF (Morocco) = **7.184**

ICV (Poland) = **6.630**
PIF (India) = **1.940**
IBI (India) = **4.260**
OAJI (USA) = **0.350**

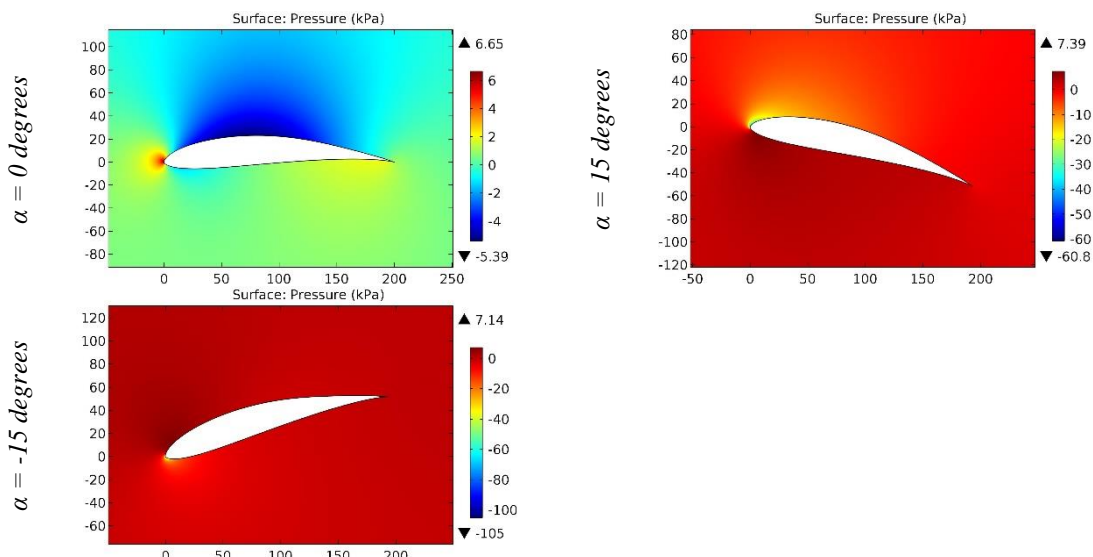


Figure 124. The pressure contours on the surfaces of the EPPLER 396 airfoil.

Conclusion

High pressure occurs on a small area of the leading edge of the airfoil of the airplane wing with the angle of attack greater than 0 degrees. The drag at the leading edge of the E series airfoils is generally

less in magnitude than the drag at the leading edge of the EPPLER series airfoils. The convex-concave airfoils at the negative angle of attack are subjected to less stress during the airplane flight.

References:

- Anderson, J. D. (2010). Fundamentals of Aerodynamics. *McGraw-Hill, Fifth edition*.
- Shevell, R. S. (1989). Fundamentals of Flight. *Prentice Hall, Second edition*.
- Houghton, E. L., & Carpenter, P. W. (2003). Aerodynamics for Engineering Students. *Fifth edition, Elsevier*.
- Lan, E. C. T., & Roskam, J. (2003). Airplane Aerodynamics and Performance. *DAR Corp*.
- Sadraey, M. (2009). Aircraft Performance Analysis. *VDM Verlag Dr. Müller*.
- Anderson, J. D. (1999). Aircraft Performance and Design. *McGraw-Hill*.
- Roskam, J. (2007). Airplane Flight Dynamics and Automatic Flight Control, Part I. *DAR Corp*.
- Etkin, B., & Reid, L. D. (1996). Dynamics of Flight, Stability and Control. *Third Edition, Wiley*.
- Stevens, B. L., & Lewis, F. L. (2003). Aircraft Control and Simulation. *Second Edition, Wiley*.
- Chemezov, D., et al. (2021). Pressure distribution on the surfaces of the NACA 0012 airfoil under conditions of changing the angle of attack. *ISJ Theoretical & Applied Science*, 09 (101), 601-606.
- Chemezov, D., et al. (2021). Stressed state of surfaces of the NACA 0012 airfoil at high angles of attack. *ISJ Theoretical & Applied Science*, 10 (102), 601-604.
- Chemezov, D., et al. (2021). Reference data of pressure distribution on the surfaces of airfoils having the names beginning with the letter A (the first part). *ISJ Theoretical & Applied Science*, 10 (102), 943-958.
- Chemezov, D., et al. (2021). Reference data of pressure distribution on the surfaces of airfoils having the names beginning with the letter A (the second part). *ISJ Theoretical & Applied Science*, 11 (103), 656-675.
- Chemezov, D., et al. (2021). Reference data of pressure distribution on the surfaces of airfoils having the names beginning with the letter B. *ISJ Theoretical & Applied Science*, 11 (103), 1001-1076.
- Chemezov, D., et al. (2021). Reference data of pressure distribution on the surfaces of airfoils having the names beginning with the letter C. *ISJ Theoretical & Applied Science*, 12 (104), 814-844.
- Chemezov, D., et al. (2021). Reference data of pressure distribution on the surfaces of airfoils having the names beginning with the letter D. *ISJ Theoretical & Applied Science*, 12 (104), 1244-1274.